

CTA concept (G.Pérez, IAC)

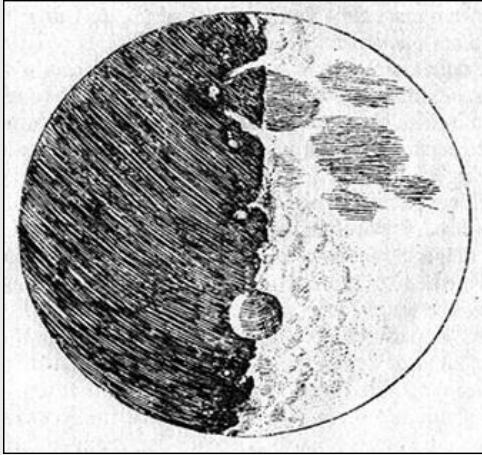
INTENSITY INTERFEROMETRY

FROM ASTRONOMY TO PARTICLE PHYSICS, AND BACK

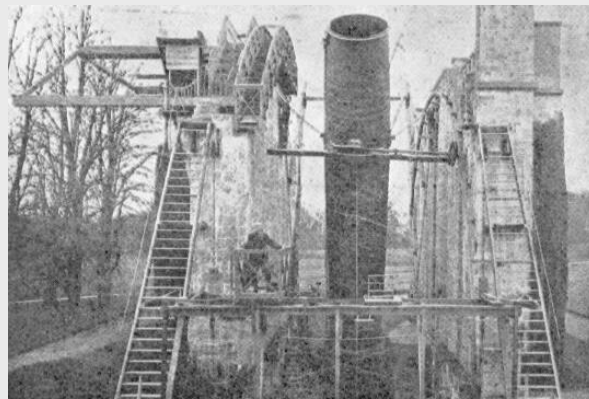
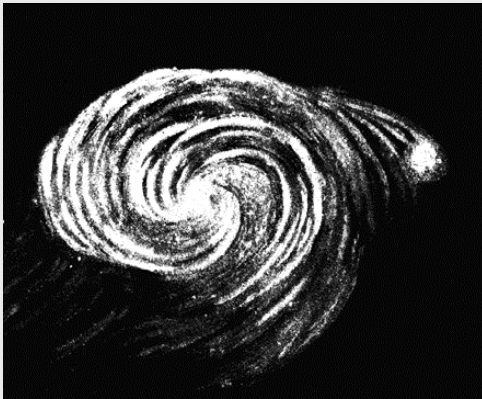
Dainis Dravins — Lund Observatory

www.astro.lu.se/~dainis

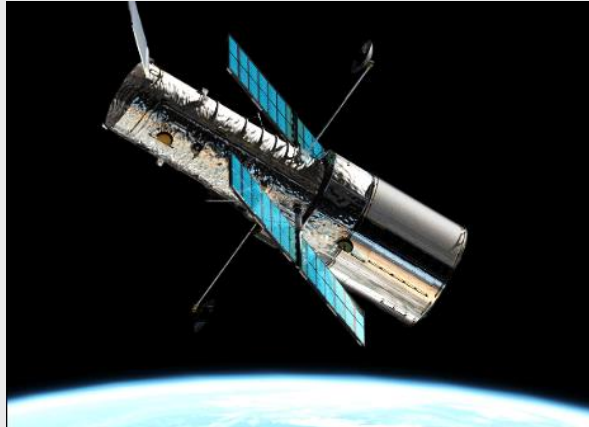
Quest for highest-resolution imaging in astronomy



Galileo Galilei (1609)

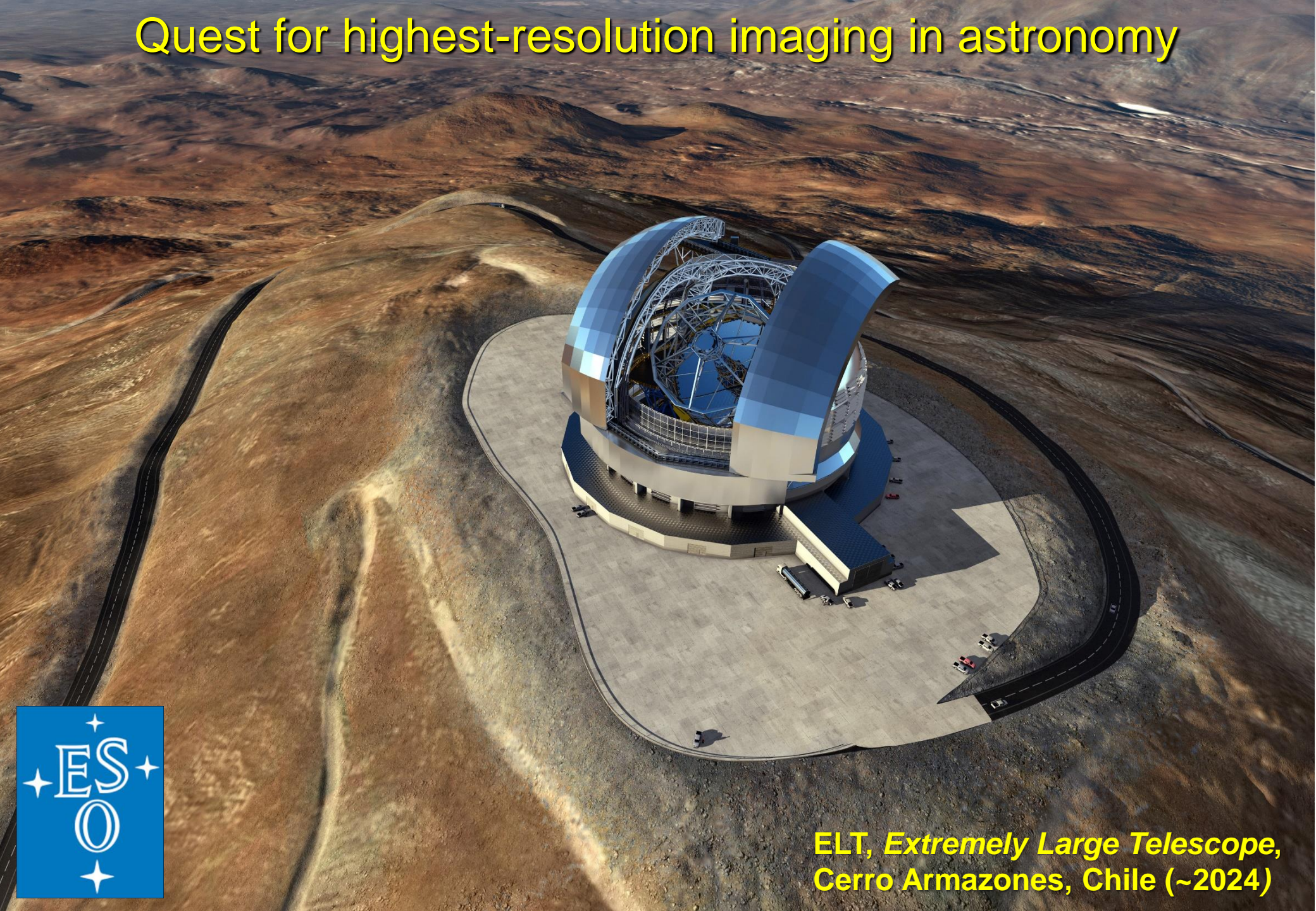


Lord Rosse (1845)



Hubble Space Telescope (1990)

Quest for highest-resolution imaging in astronomy



**ELT, Extremely Large Telescope,
Cerro Armazones, Chile (~2024)**

Quest for highest-resolution imaging in astronomy

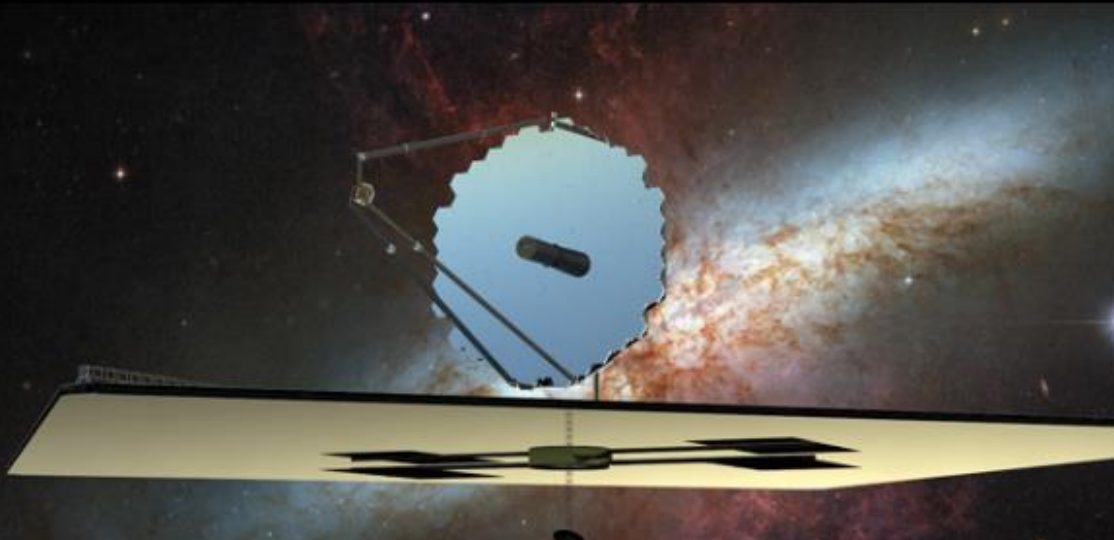
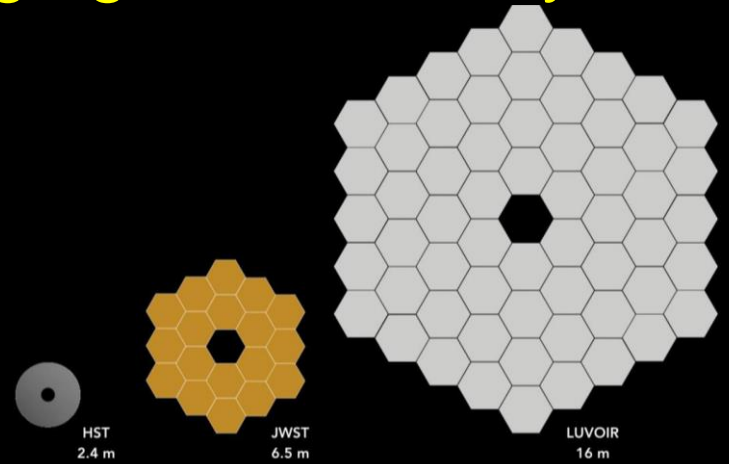
Goddard Space Flight Center
asd.gsfc.nasa.gov/luvoir/

National Aeronautics and
Space Administration



LUVOIR

Large Ultraviolet / Optical / Infrared Surveyor



Outer Bodies

15-m LUVOIR can
image 3.5 km bodies
at 40 AU in 75 sec.



Pluto with HST



15-m LUVOIR

NASA / New Horizons

Ocean Moons

LUVOIR can provide
spectral imaging of
water jets from icy
moons.

Roth et al. (2014)



Europa jets with
HST

G. Ballester (LPL)



15-m LUVOIR

To be evaluated in the U.S. 2020-2030
Astronomy and Astrophysics Decadal Survey

Highest-resolution imaging in astronomy

THE ASTROPHYSICAL JOURNAL, 817:96 (14pp), 2016 February 1

doi:10.3847/0004-637X/817/2/96

© 2016. The American Astronomical Society. All rights reserved.



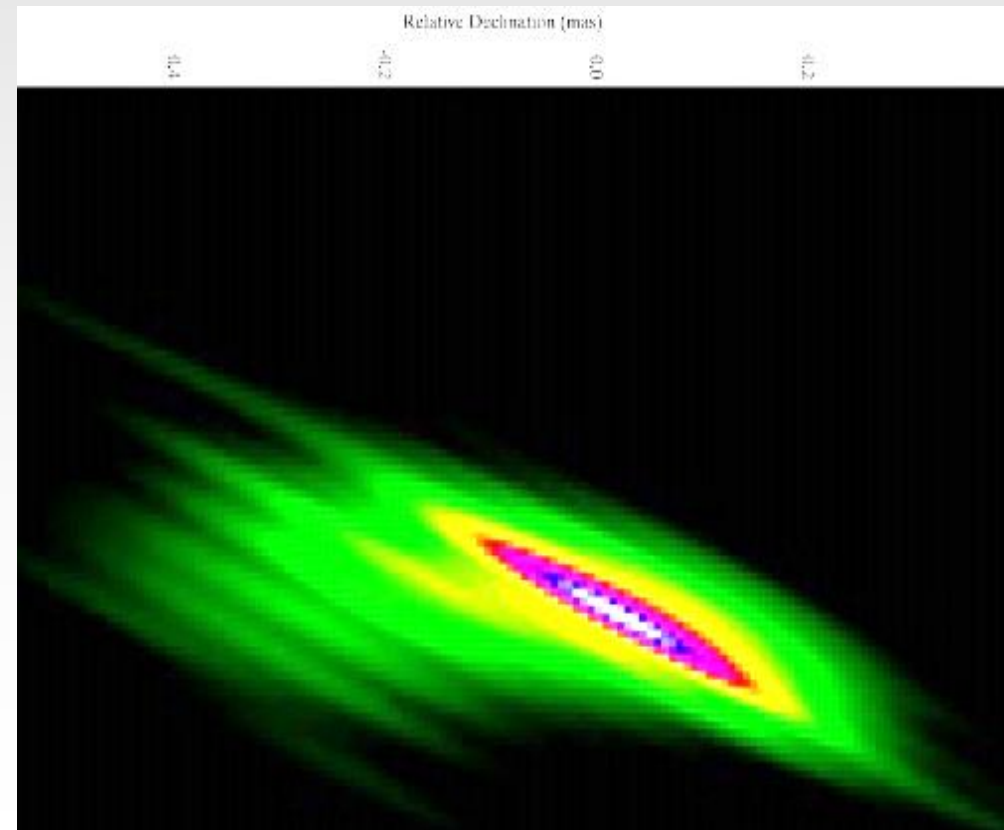
CrossMark

PROBING THE INNERMOST REGIONS OF AGN JETS AND THEIR MAGNETIC FIELDS WITH *RADIOASTRON*. I. IMAGING BL LACERTAE AT $21 \mu\text{as}$ RESOLUTION

JOSÉ L. GÓMEZ¹, ANDREI P. LOBANOV^{2,3}, GABRIELE BRUNI², YURI Y. KOVALEV^{2,4}, ALAN P. MARSCHER⁵, SVETLANA G. JORSTAD^{5,6},
YOSUKE MIZUNO⁷, UWE BACH², KIRILL V. SOKOLOVSKY^{4,8,9}, JAMES M. ANDERSON^{2,10}, PABLO GALINDO¹,
NIKOLAY S. KARDASHEV⁴, AND MIKHAIL M. LISAKOV⁴

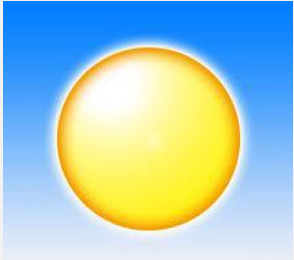
RadioAstron polarimetric space VLBI images of BL Lac at 22 GHz (λ 13.6 mm)

Space-ground fringe detections were obtained up to
a projected baseline length of 7.9 Earth diameters.



**Highest-resolution
imaging in the optical ?**

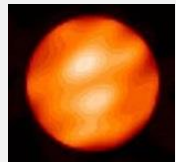
ANGULAR SCALES IN ASTRONOMY



Sun, Moon ~ 30 arcmin



Planets ~ 30 arcsec



Largest stars ~ 30 mas



Typical bright stars ~ 1 mas



History of optical interferometry

COMPTES RENDUS

HEBDOMADAIRES

DES SÉANCES

DE L'ACADÉMIE DES SCIENCES.

(1008)

MÉMOIRES LUS.

ASTRONOMIE PHYSIQUE. — *Sur l'extrême petitesse du diamètre apparent des étoiles fixes.* Note de M. STÉPHAN.

(Commissaires : MM. Le Verrier, Fizeau, Janssen.)

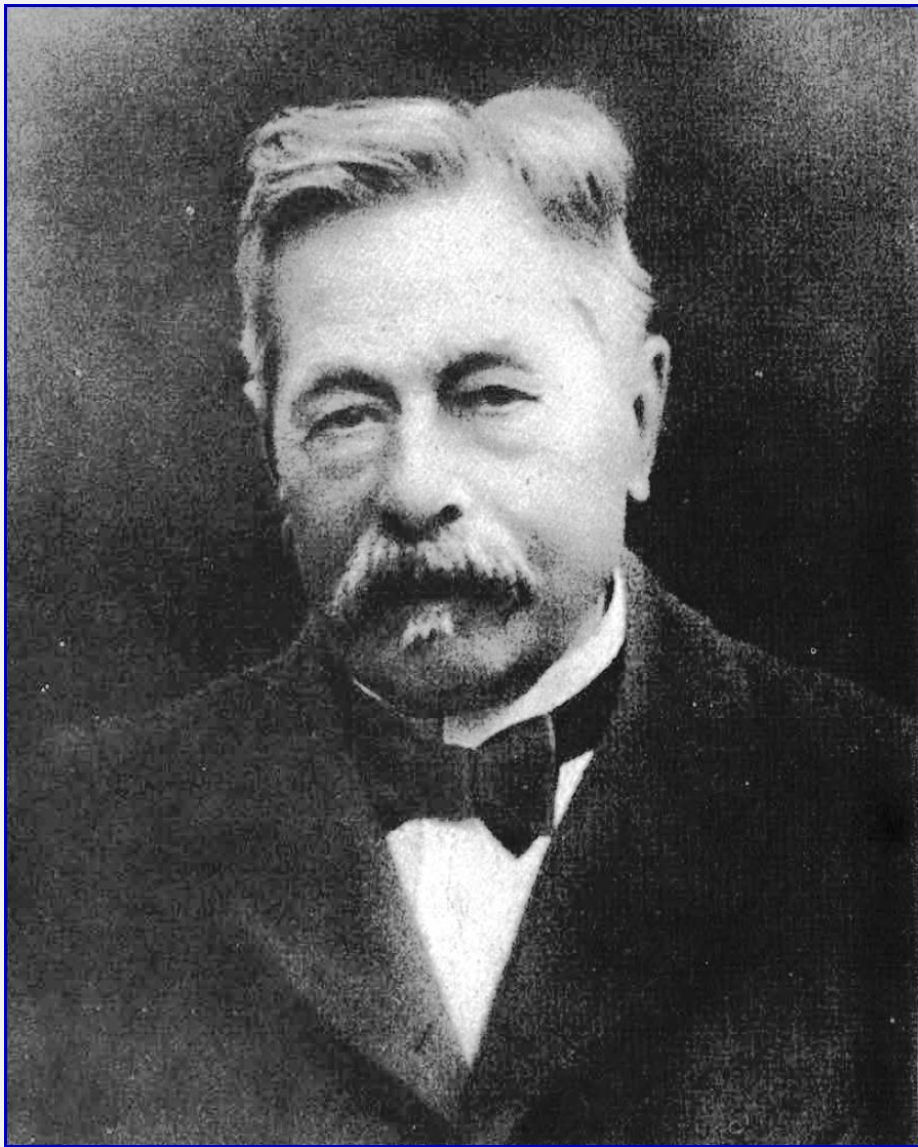
« Dans une Communication précédente (*Comptes rendus*, t. LXXVI, p. 1008), j'ai eu l'honneur de rappeler à l'Académie une idée anciennement émise par M. Fizeau sous forme de simple aperçu et qui, jusque-là, semblait être restée dans l'oubli, bien que renfermant le germe de conséquences fort importantes. Cette idée peut se formuler comme il suit : Dans plusieurs cas, en donnant naissance à certains phénomènes d'interférence, on peut augmenter la sensibilité des instruments d'optique ordinaires.

» Guidé par l'illustre physicien, j'ai cherché à déduire de cette conception originale quelques notions précises sur le diamètre apparent des étoiles fixes, et, dans la Note citée plus haut, j'ai fait connaître à l'Académie le résultat de quelques expériences préliminaires dont il convient de rappeler le principe général.

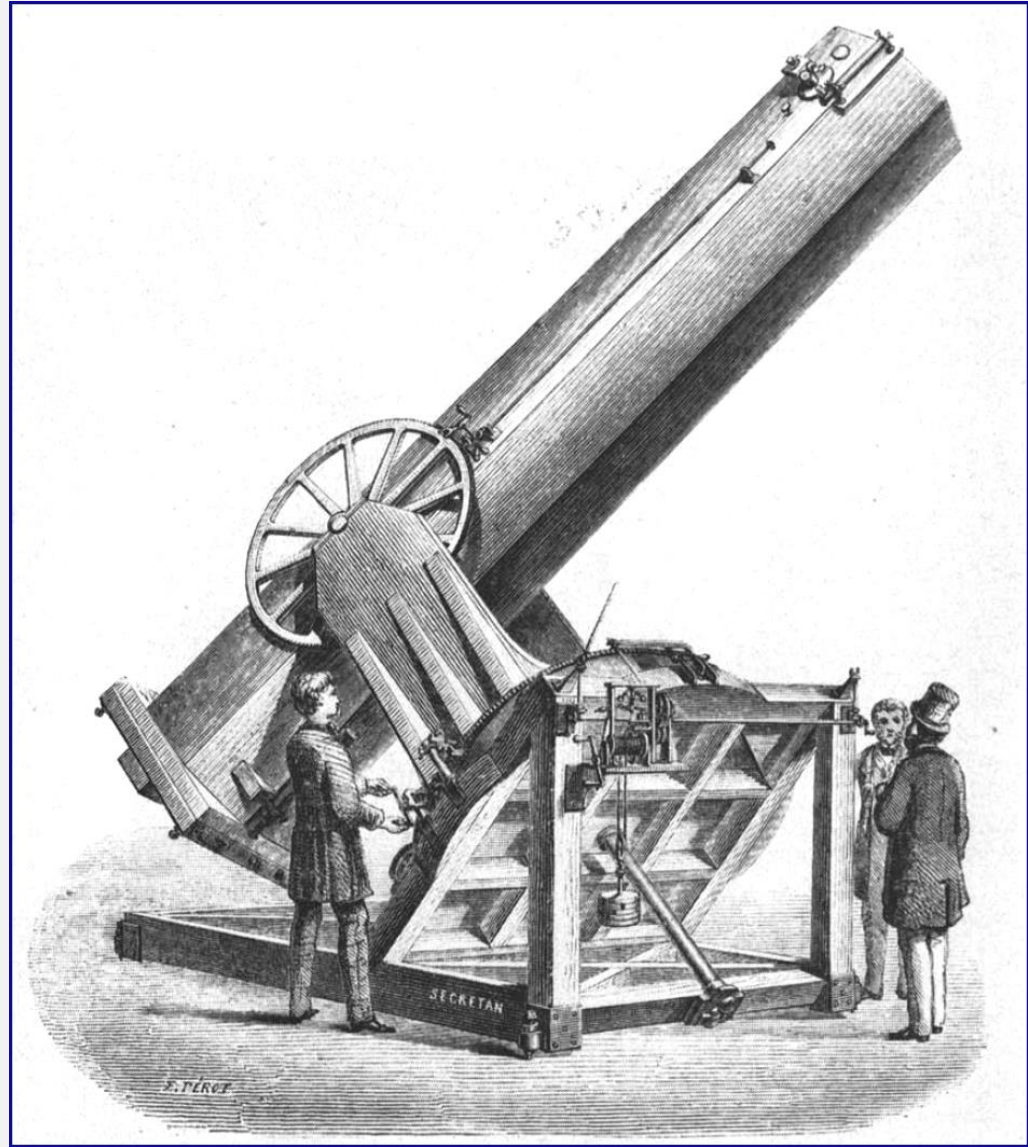
E. Stéphan:

Sur l'extrême petitesse du diamètre apparent des étoiles fixes

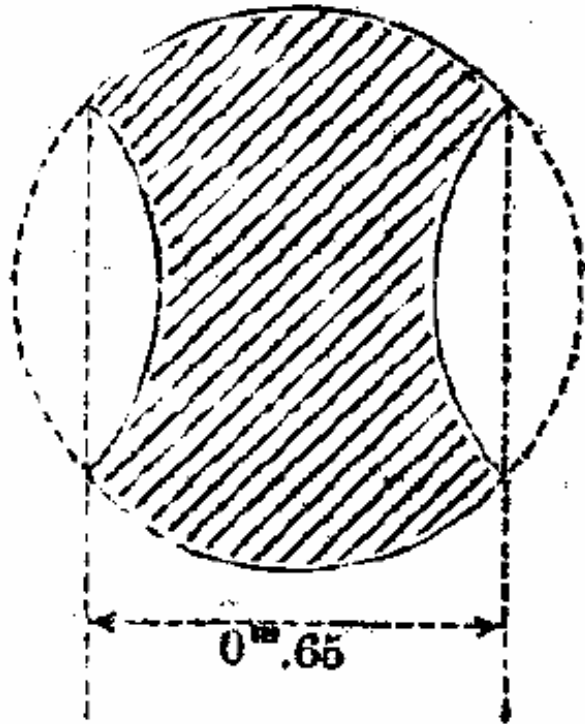
Compt. Rend. Acad. Sci. Paris **78**, 108 (1874)



Edouard Stéphan (1837-1923)



80-cm telescope at *Observatoire de Marseille*
La Nature 1, 371 (1873)



» L'instrument dont j'ai fait usage à Marseille est le grand télescope Foucault, de 80 centimètres de diamètre, muni d'un écran lunulaire; les lunules sont limitées par des cercles égaux de 80 centimètres; leurs grands axes sont parallèles et distants de 65 centimètres.

En d'autres termes, les expériences citées ne prouvent pas seulement que le diamètre apparent des étoiles examinées est inférieur à $0",158$, elles montrent encore que ce diamètre est une très-faible fraction du nombre précédent. »

E.Stéphan:

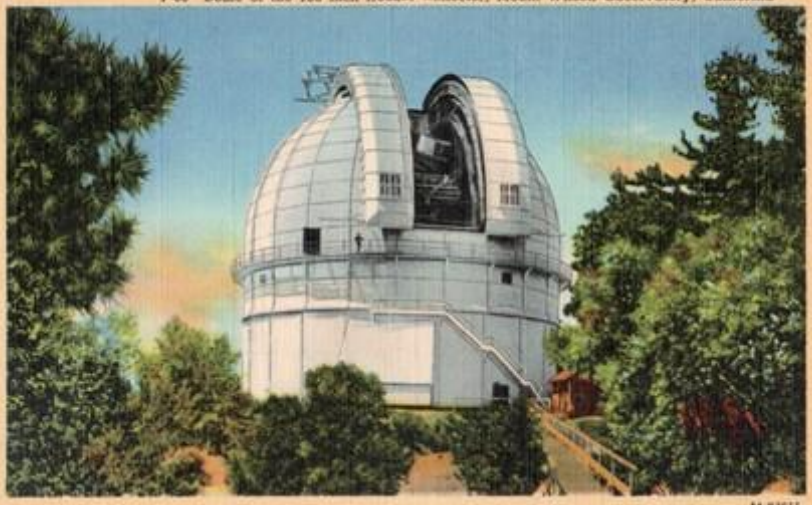
Sur l'extrême petitesse du diamètre apparent des étoiles fixes

Compt.Rend.Acad.Sci. Paris **78**, 108 (1874)

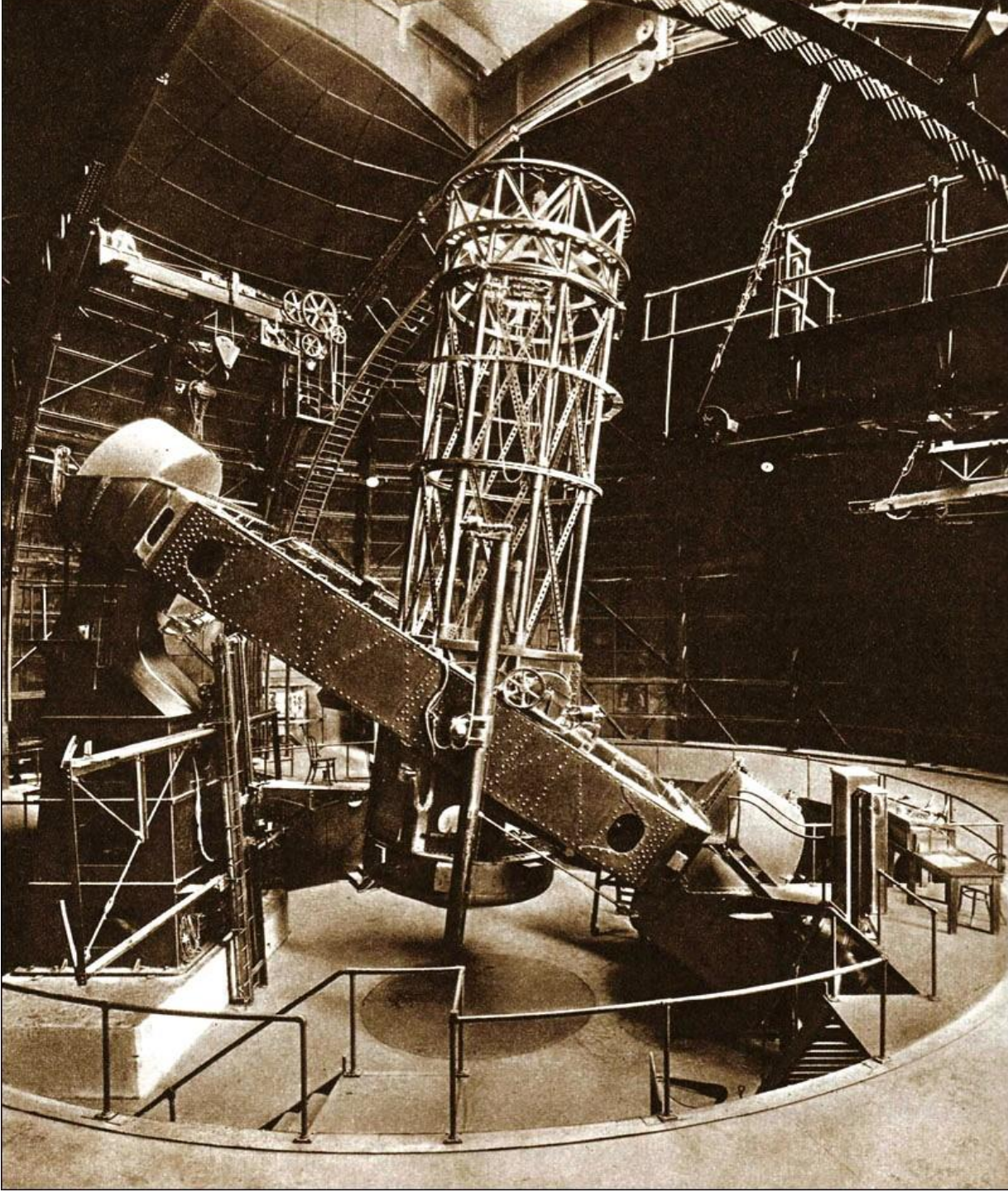


Mt. Wilson, CA, site of the 100-inch Hooker telescope

P-68 Dome of the 100 inch Hooker Reflector, Mount Wilson Observatory, California

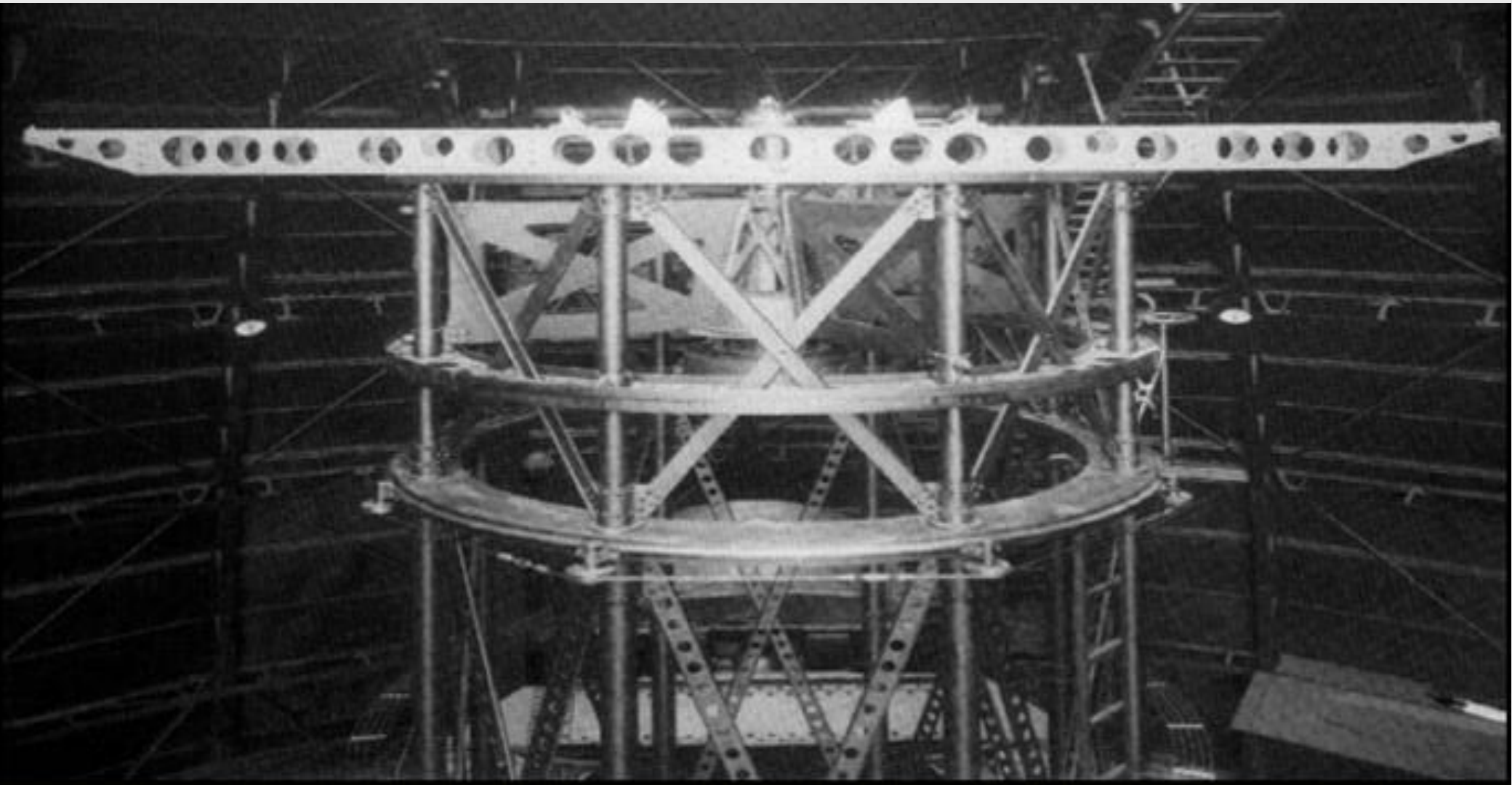


64-11302



Mt.Wilson 100-inch Hooker telescope

FIRST SUCCESSFUL STELLAR INTERFEROMETER



20-ft Michelson Stellar Interferometer c. 1919



50-ft Pease Stellar Interferometer c. 1929

Unsuccessful attempt at longer-baseline interferometry on Mt. Wilson

INTERFERENCE FRINGES OBTAINED ON VEGA WITH TWO OPTICAL TELESCOPES

ANTOINE LABEYRIE
Observatoire de Paris, 92190-Meudon, France

ApJ 196, L71, 1975



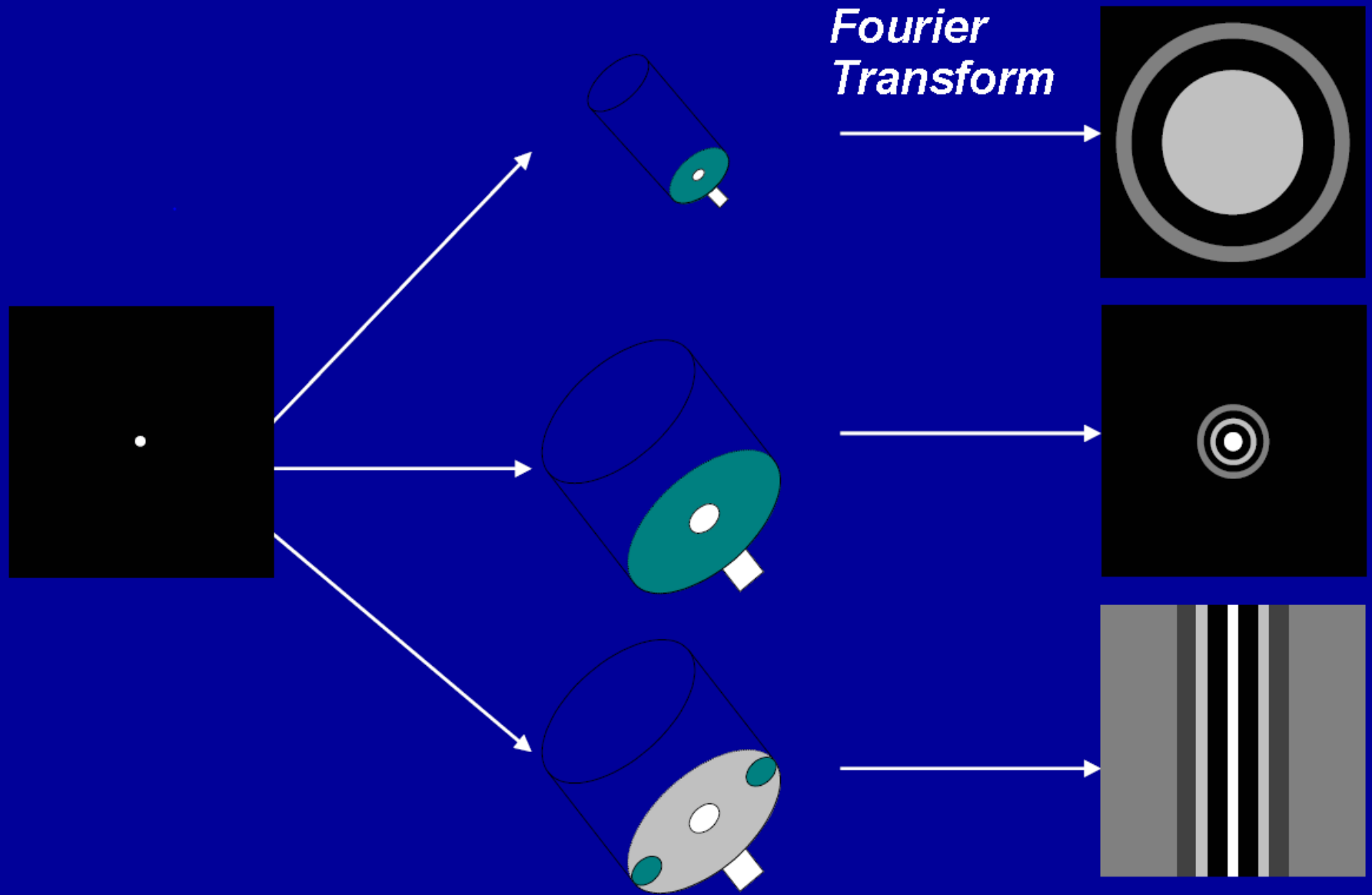
I2T.OBSERVATOIRE DE NICE . 1974 (photo: Alain Blazit)

FIRST SUCCESSFUL OPTICAL INTERFEROMETER OF THE MODERN ERA (1974)
I2T, *Interféromètre à 2 Télescopes* (Observatoire de CERGA, France)

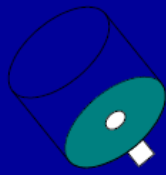
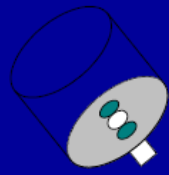
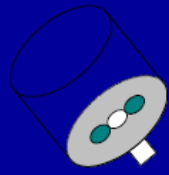
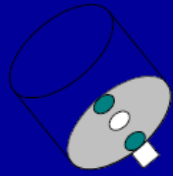
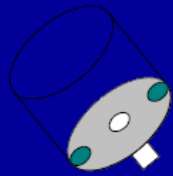
Principles of interferometry

Interference of light

Point Spread Function of Telescopes / Interferometers

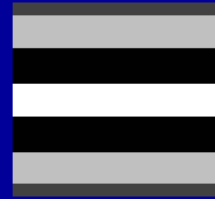
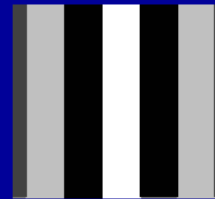
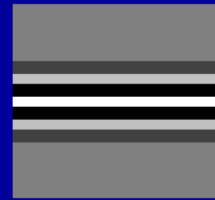


Primary Mirror Configuration



Synthetic Aperture

Point Spread Function



Synthetic PSF

Synthetic Aperture Imaging with an Interferometer

Aperture synthesis & interferometric imaging

Aperture synthesis began in the radio

THE SYNTHESIS OF LARGE RADIO TELESCOPES

M. Ryle and A. Hewish

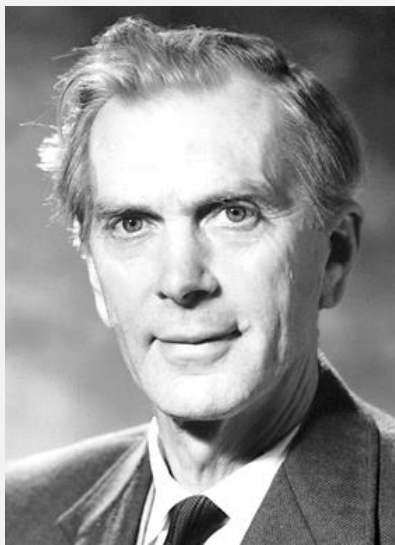
(Received 1959 August 24)

Summary

Many investigations in radio astronomy are limited by the resolving power which can be achieved by conventional methods of aerial construction.

A new method of obtaining increased resolving power has been developed, which has been applied to the construction of both "pencil-beam" systems and interferometers. In this method two aerials are arranged so that their relative position may be altered to occupy successively the whole area of a much larger equivalent aerial. By combining mathematically the information derived from these different positions, it is possible to obtain a resolving power equal to that of the large equivalent aerial. Since the combination of the individual records may be done with different phase relationships, it is possible, without extra observations, to "scan" the synthesized aerial over an appreciable solid angle; because of this the total observing time of a synthesized instrument is of the same order as that of a conventional instrument.

An interferometric system designed for the study of radio stars has been built which has an equivalent area for resolution of $8 \cdot 10^5$ sq. ft as well as a "pencil-beam" system with an equivalent area of $3 \cdot 10^6$ sq. ft. The sensitivity of both systems corresponds to a "collecting area" of about $2 \cdot 10^5$ sq. ft.



Sir Martin Ryle (1918-1984)

Nobel prize in physics 1974
"for pioneering research in radio astrophysics: for observations and inventions, in particular of the aperture synthesis technique"



The long fixed element of the radio star interferometer.



VLA: The Karl G. Jansky Very Large Array, a radio interferometer located on the Plains of San Agustin, west of Socorro, New Mexico, <http://www.vla.nrao.edu/>

ESO VLTI

Very Large Telescope Interferometer



ESO, Cerro Paranal, Chile
VLTI, Very Large Telescope Interferometer

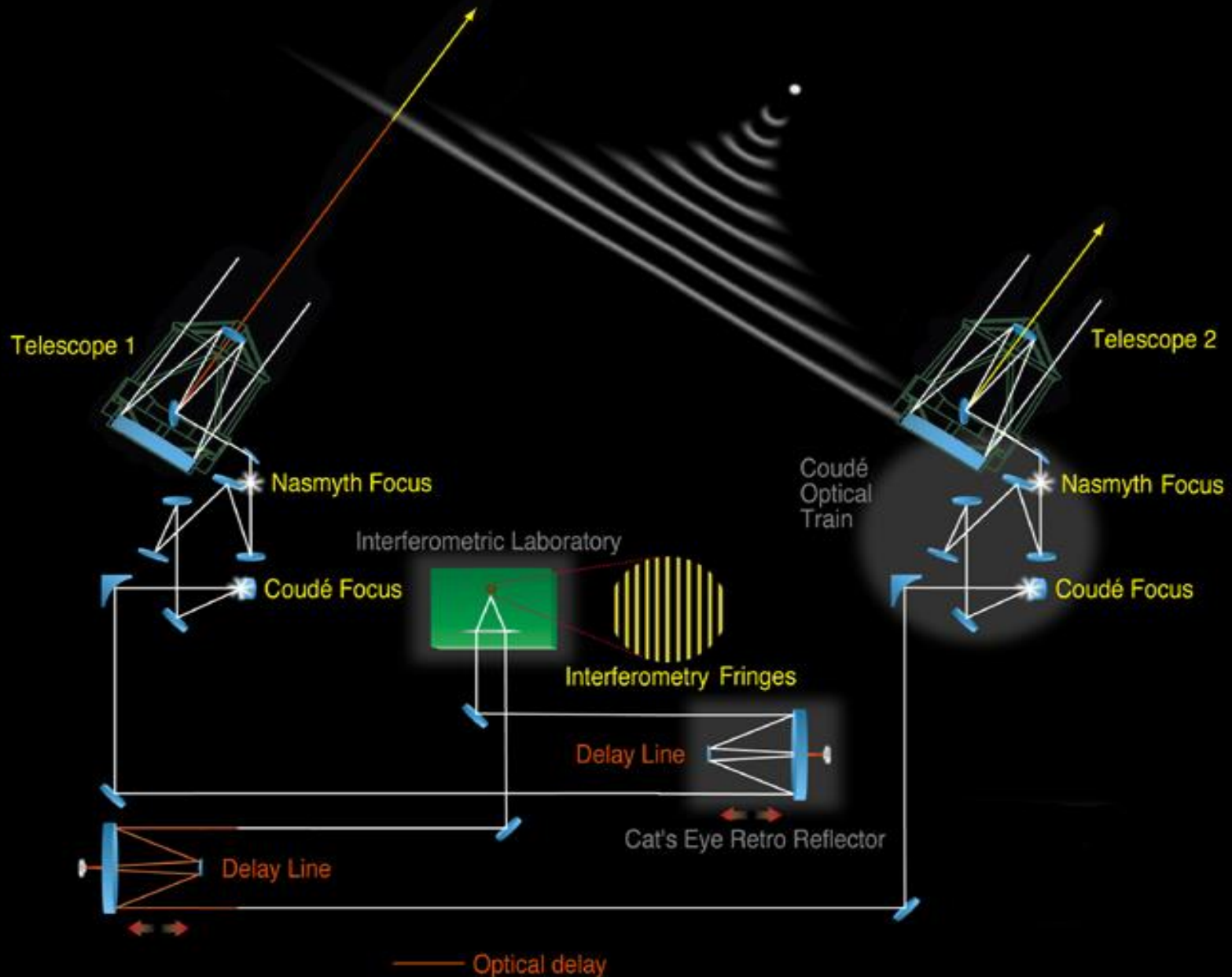


VLI auxiliary telescopes at ESO Paranal (Photo: F. Millour)



VLTI stations for auxiliary telescopes, above the ducts that lead to the interferometric tunnel

ESO Very Large Telescope Interferometer

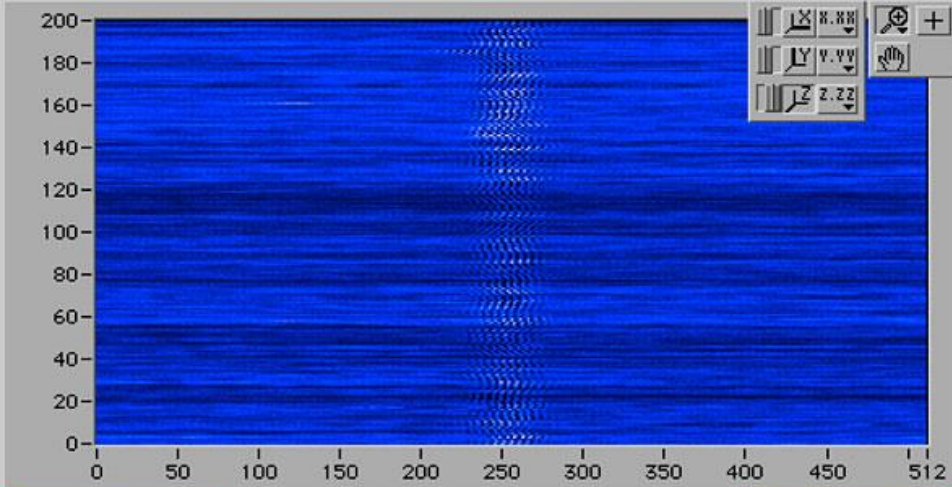




VLTI delay-line tunnel



AMBER (Astrometrical Multi BEam combineR) – VLTi three-way beam combiner.
Combines light of three telescopes, and disperses it to analyze its spectrum.
The complex optical table is required to clean up and adjust the beams from the three telescopes.



SAVE Scans to remove: **DONT SAVE**

Dump to ASCII files **Remove scans**

Comments

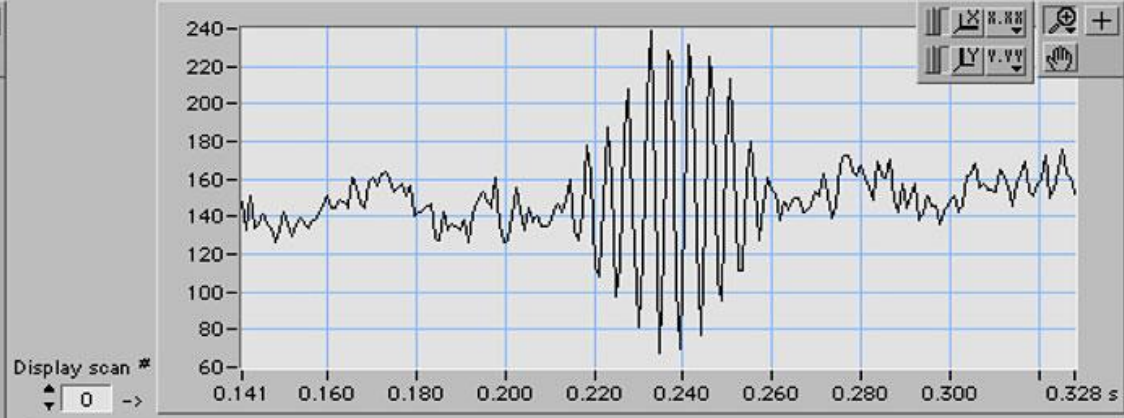
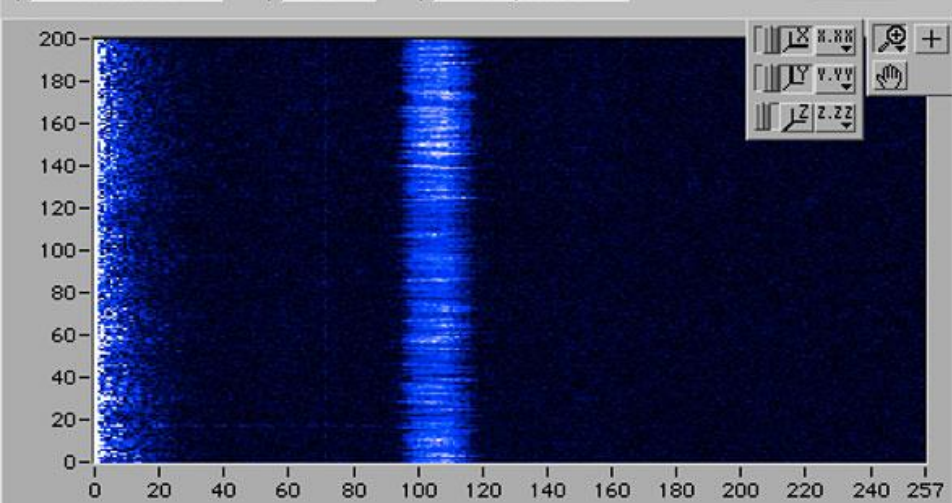
Sirius-089

Sample type: Display channel: Spectrum display:

SNR

I1	I2
21.7	17.8
PA	PB
13.50	13.61

Magnitude limit:



Plot statistics

Average:
 Median:
 Skew: Bias:

Standard deviation

Absolute	Relative
<input type="text" value="0.0575"/>	<input type="text" value="7.9 %"/>

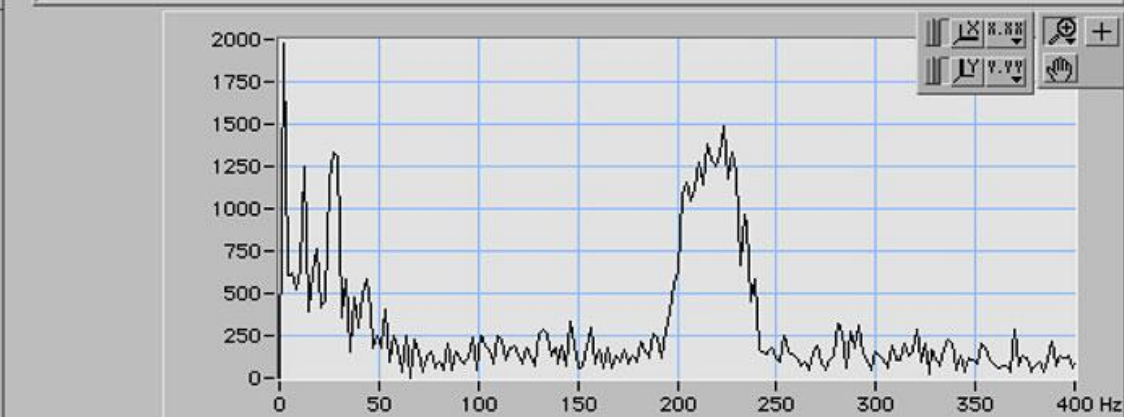
Standard error

Absolute	Relative
<input type="text" value="0.0041"/>	<input type="text" value="0.6 %"/>

Piston noise / total noise:

Correlated magnitude:

Plot vs. 200 points



VLT Fringes of Sirius

Interferometric science

Actual image of the Mira-type variable T Leporis from VLT



Image obtained by combining hundreds of interferometric measurements

Central disc shows stellar surface, surrounded by a spherical shell of expelled molecular material

Infrared wavelengths color-coded:

Blue = 1.4 – 1.6 μm

Green = 1.6 – 1.75 μm

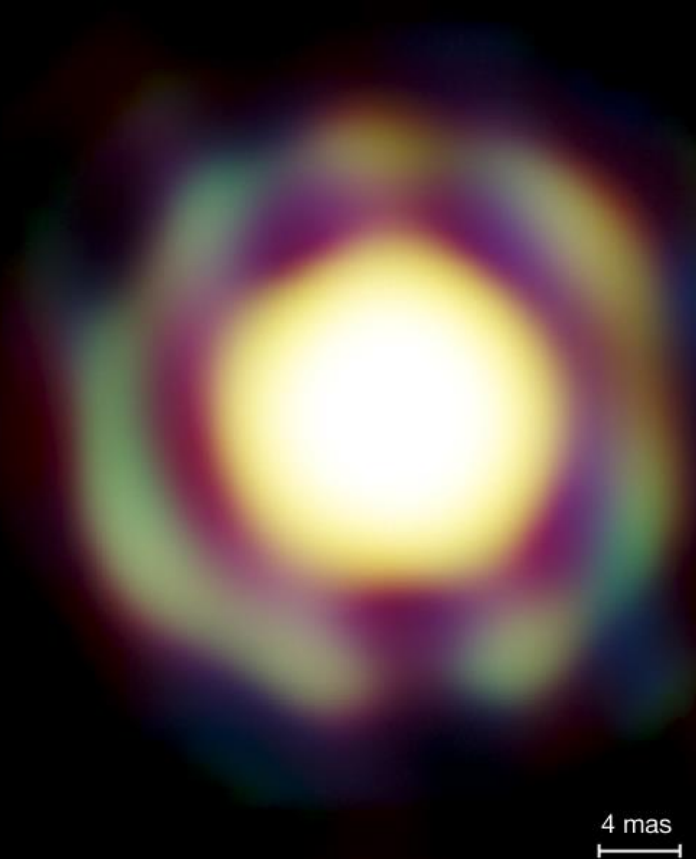
Red = 1.75 – 1.9 μm

In the green channel, the molecular envelope is thinner

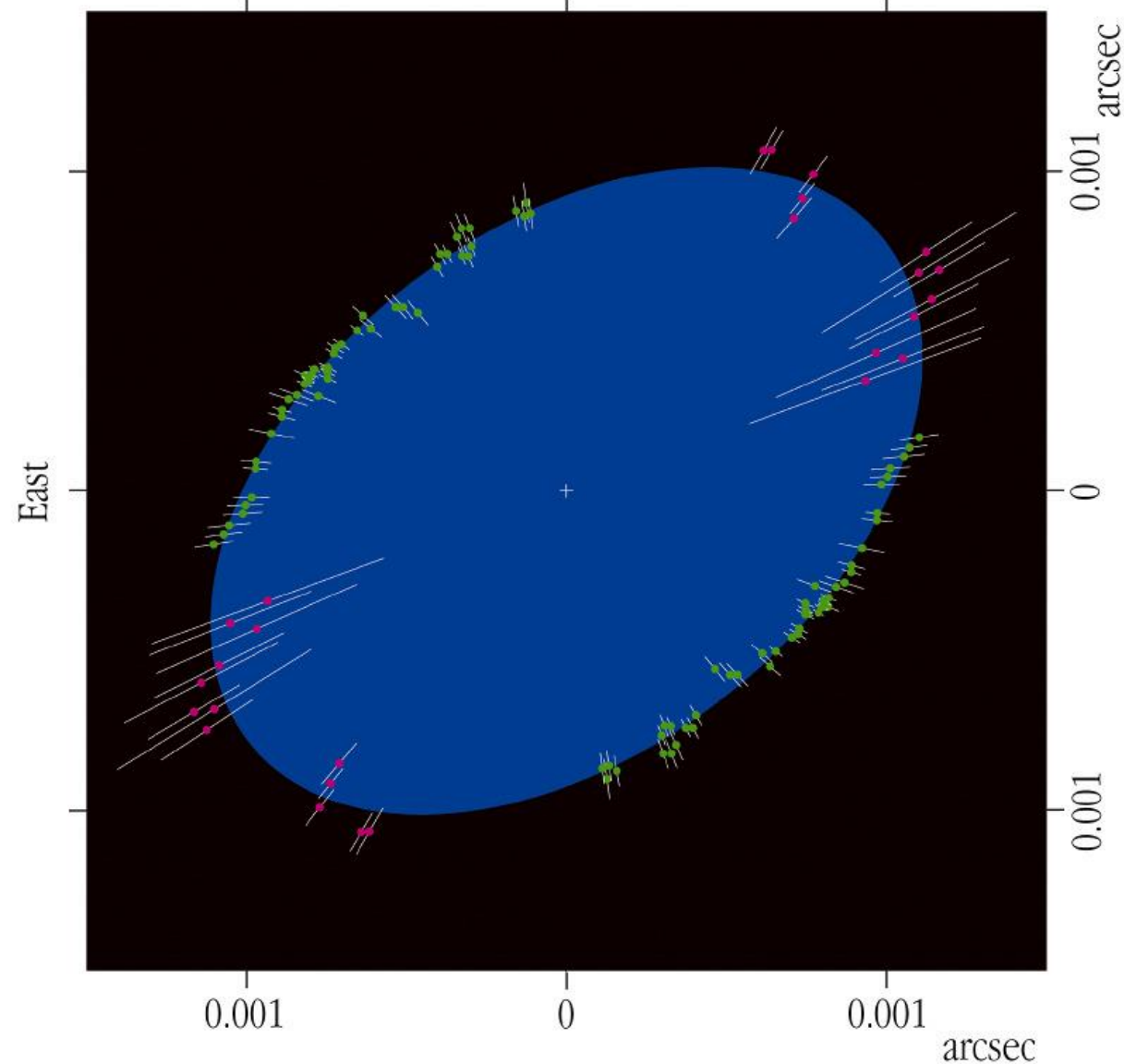
The size of Earth's orbit is marked.

Resolution = 4 milli-arcseconds

(ESO press release 0906, Feb. 2009)



North



SHAPE OF ACHERNAR

Image of the rapidly rotating ($V \sin i \approx 250$ km/s) star *Achernar* (α Eri, B3 Vpe), from VLT/VINCI observations.

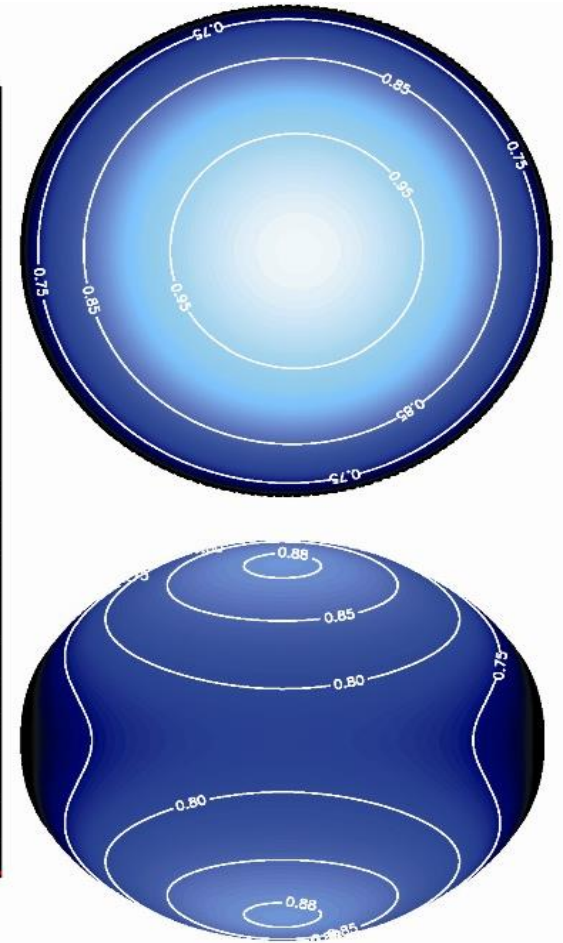
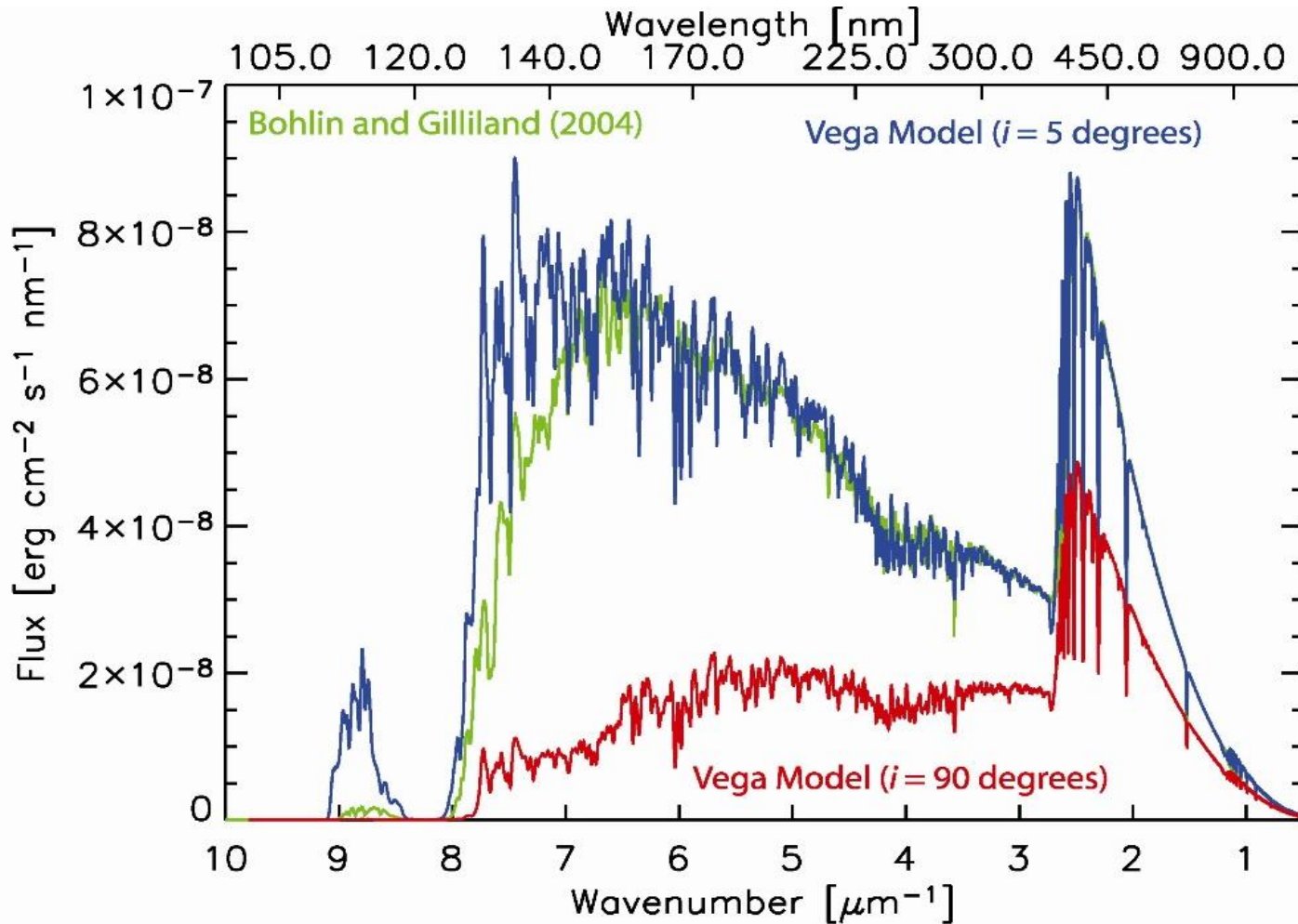
Axis ratio = 1.56, the most flattened star seen until then.

Because of the projection effect this ratio is a minimal value; the star could be even flatter.

Individual diameter measurements are shown by points with error bars.

A.Domiciano de Souza, P.Kervella, S.Jankov, L.Abe, F.Vakili, E.di Folco, F.Paresce: *Astron.Astrophys.* **407**, L47

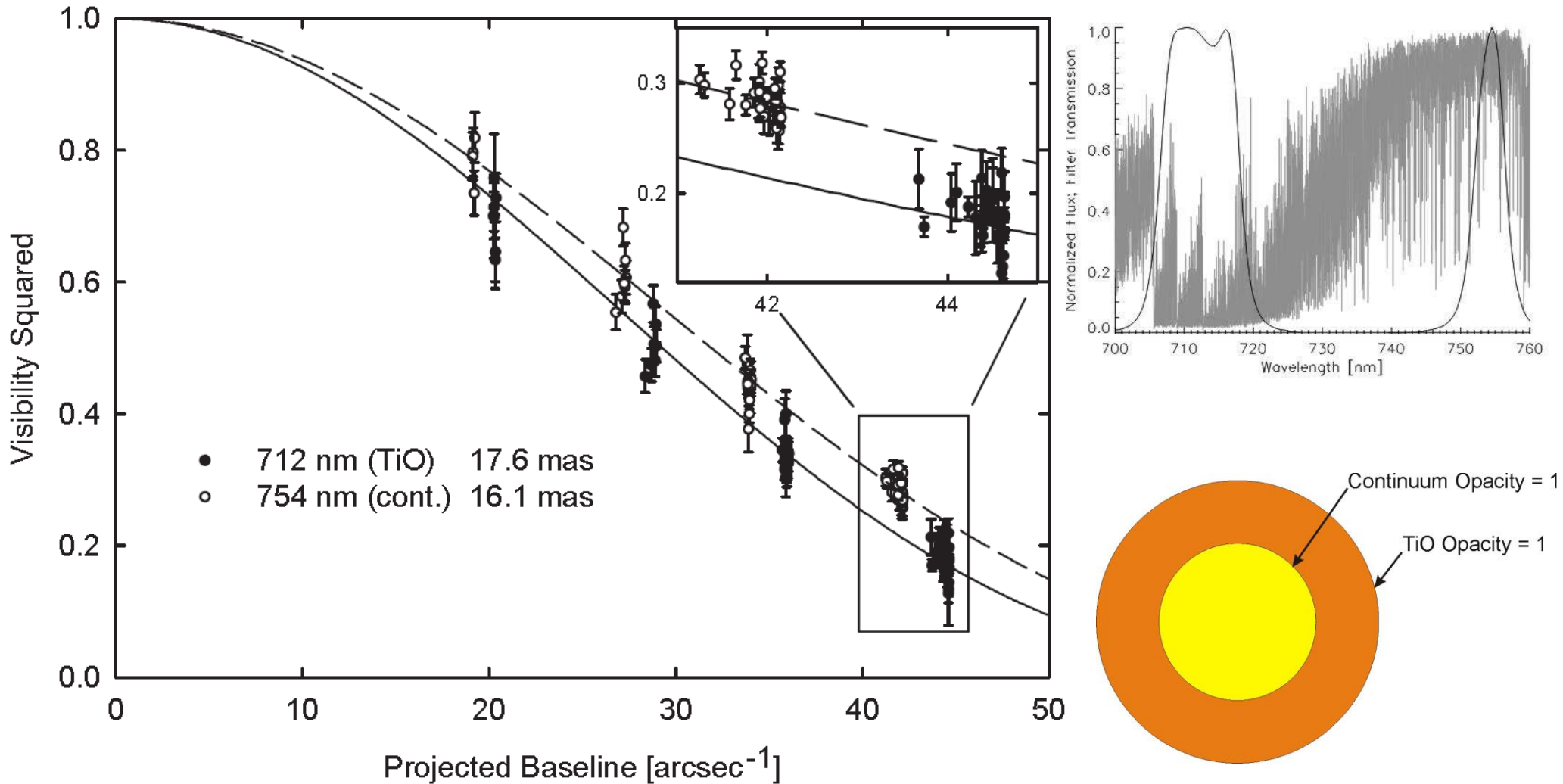
Vega (α Lyrae)



Aufdenberg et al. 2006

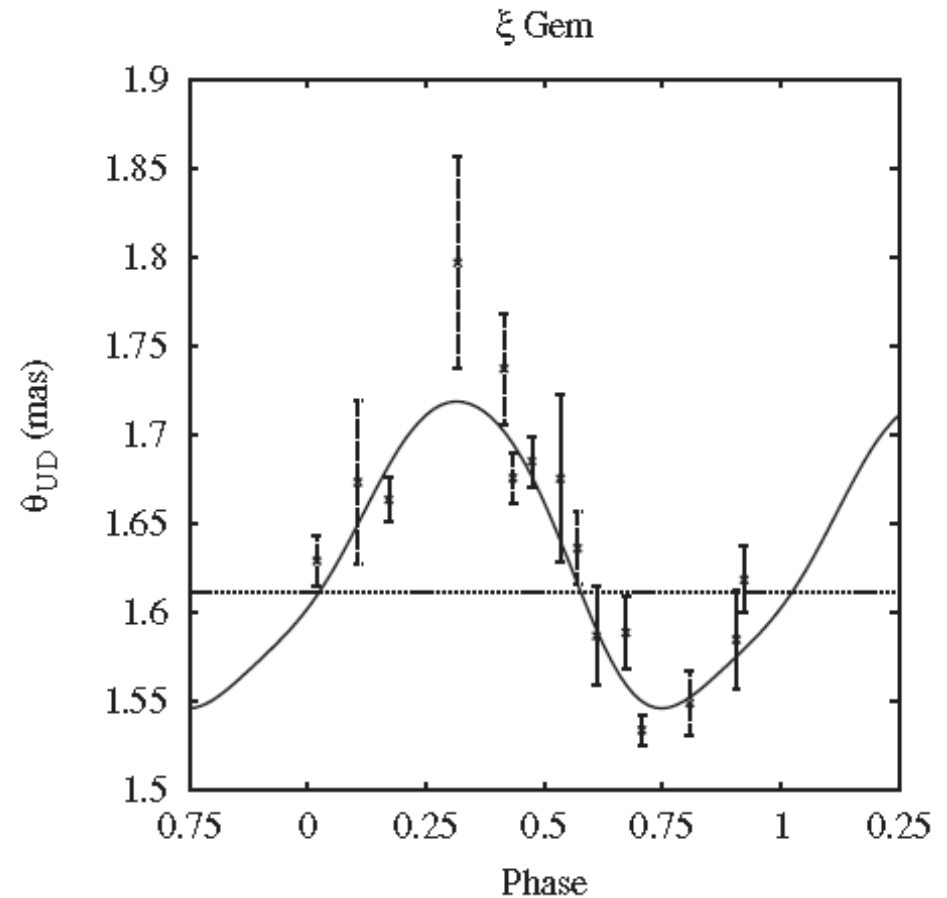
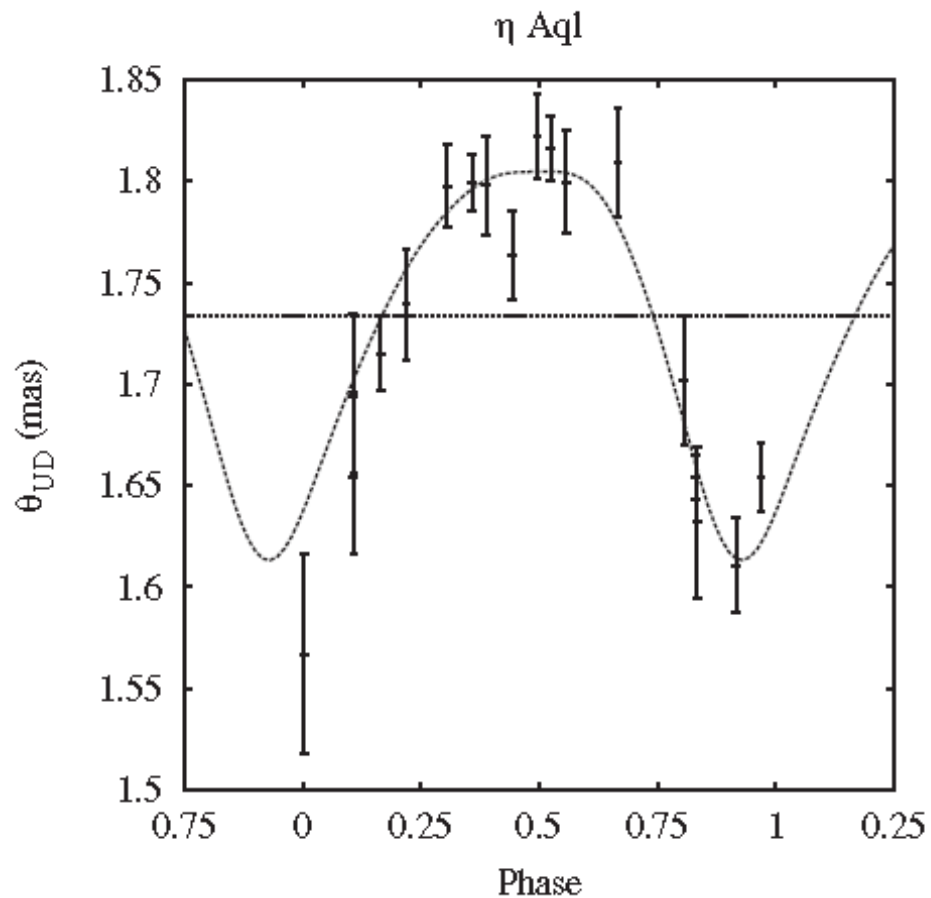
- Vega is a rapidly rotating star, seen pole-on.
- Axis inclination strongly affects values for abundances, mass, age.
- Problem, since Vega is (was?) **the** spectrophotometric standard.

Different stellar size in different wavelengths



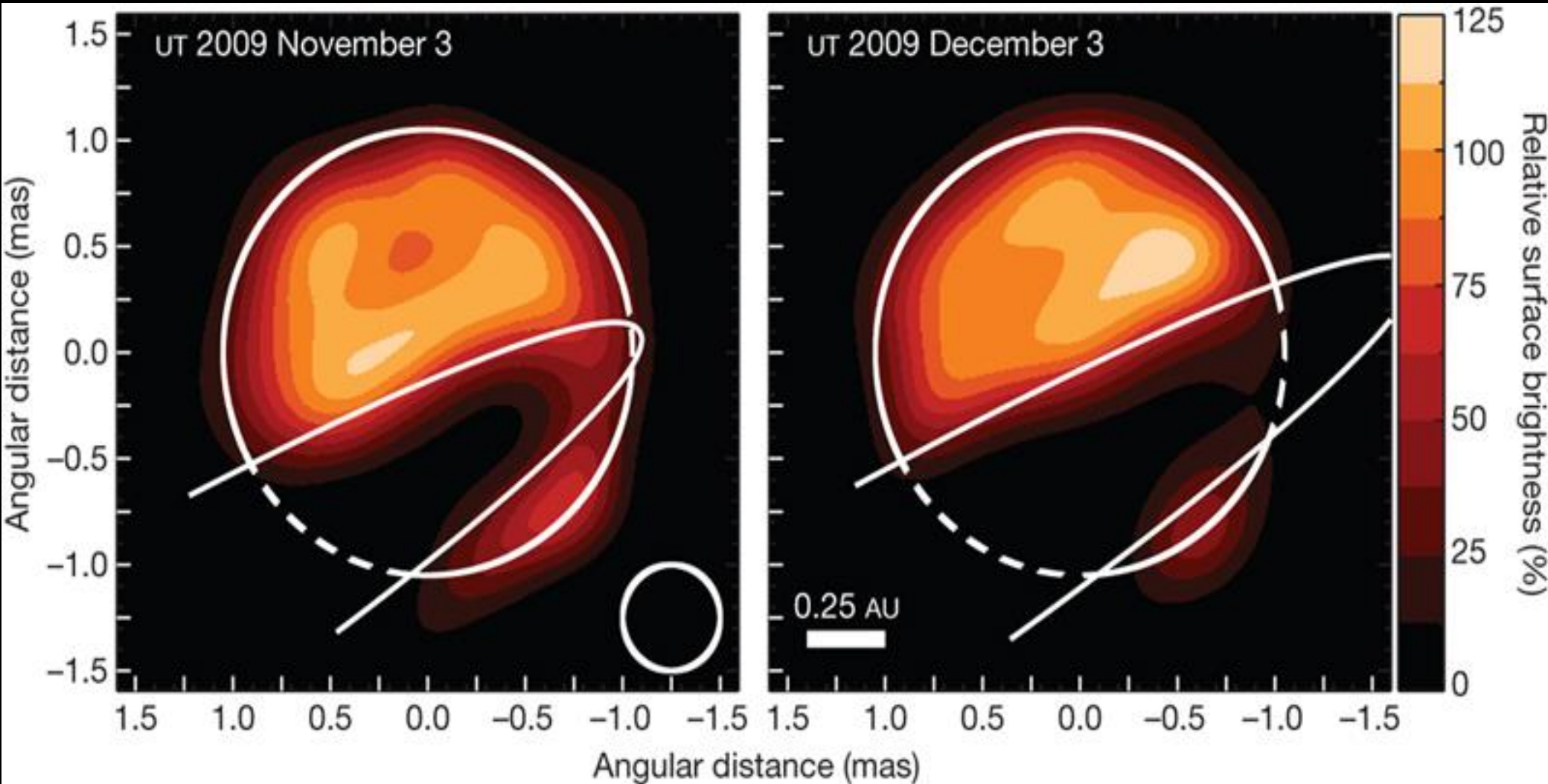
Diameters of the giant star β Pegasi

Changing stellar size during pulsation cycle



Pulsation curves for two Cepheid variables, η Aql and ζ Gem, revealing changes of stellar diameters.

Data from the PTI interferometer at $1.65\mu\text{m}$; when combined with radial velocities, accurate distances to these primary distance indicators are obtained (Lane et al., ApJ 573, 330, 2002).



Interferometric images of the F-type giant ϵ Aurigae during its month-long eclipse by an opaque disk, occurring every 27 years

B.Kloppenborg; R.Stencel; J.D.Monnier; G.Schaefer; M.Zhao; F.Baron; H.McAlister; T. ten Brummelaar; X.Che; et al.: *Infrared images of the transiting disk in the ϵ Aurigae system*, Nature **464**, 870 (2010)

NPOI

**Navy Precision Optical Interferometer
Flagstaff, Arizona**

NPOI, Navy Precision Optical Interferometer, Arizona



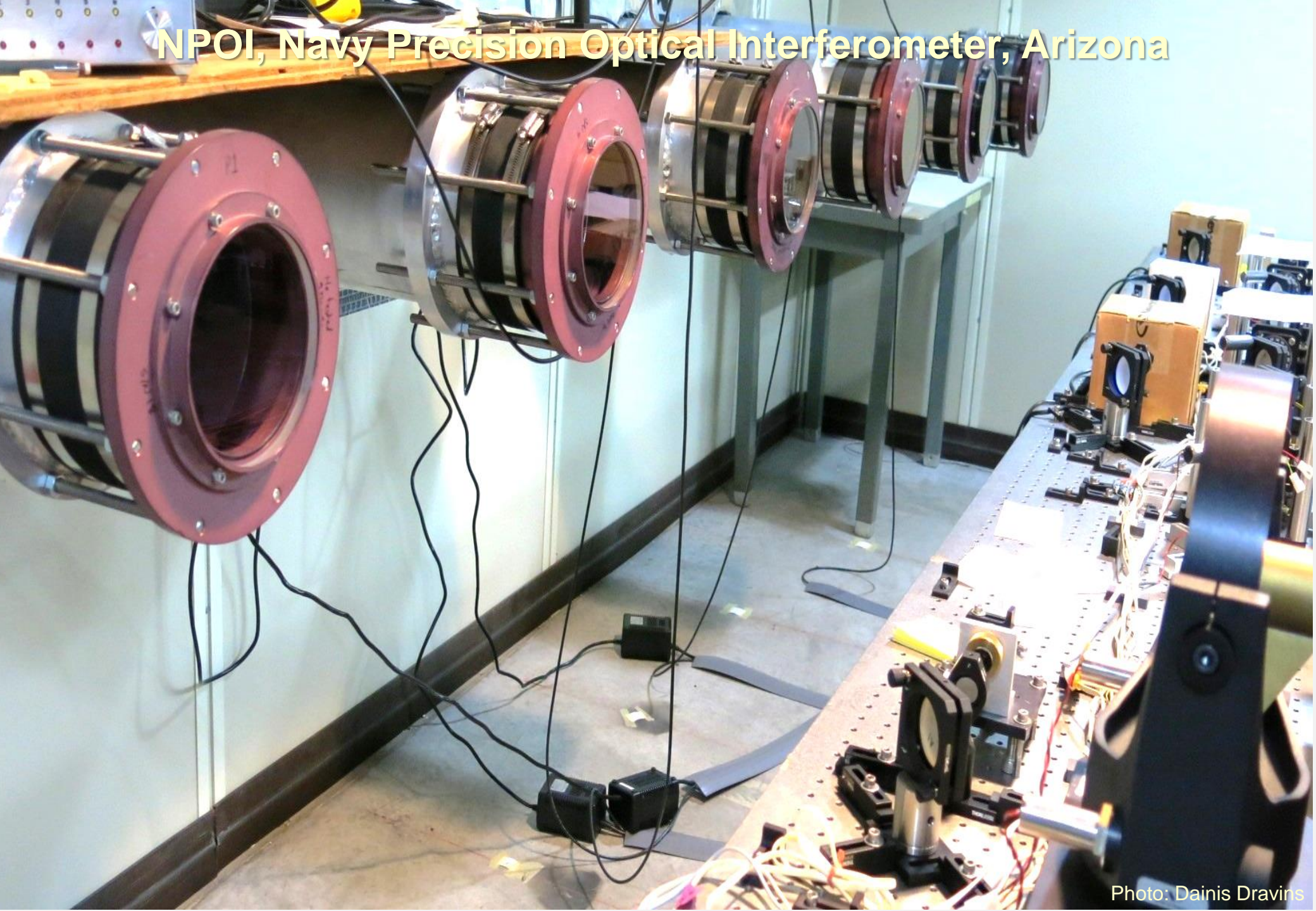
NPOI, Navy Precision Optical Interferometer



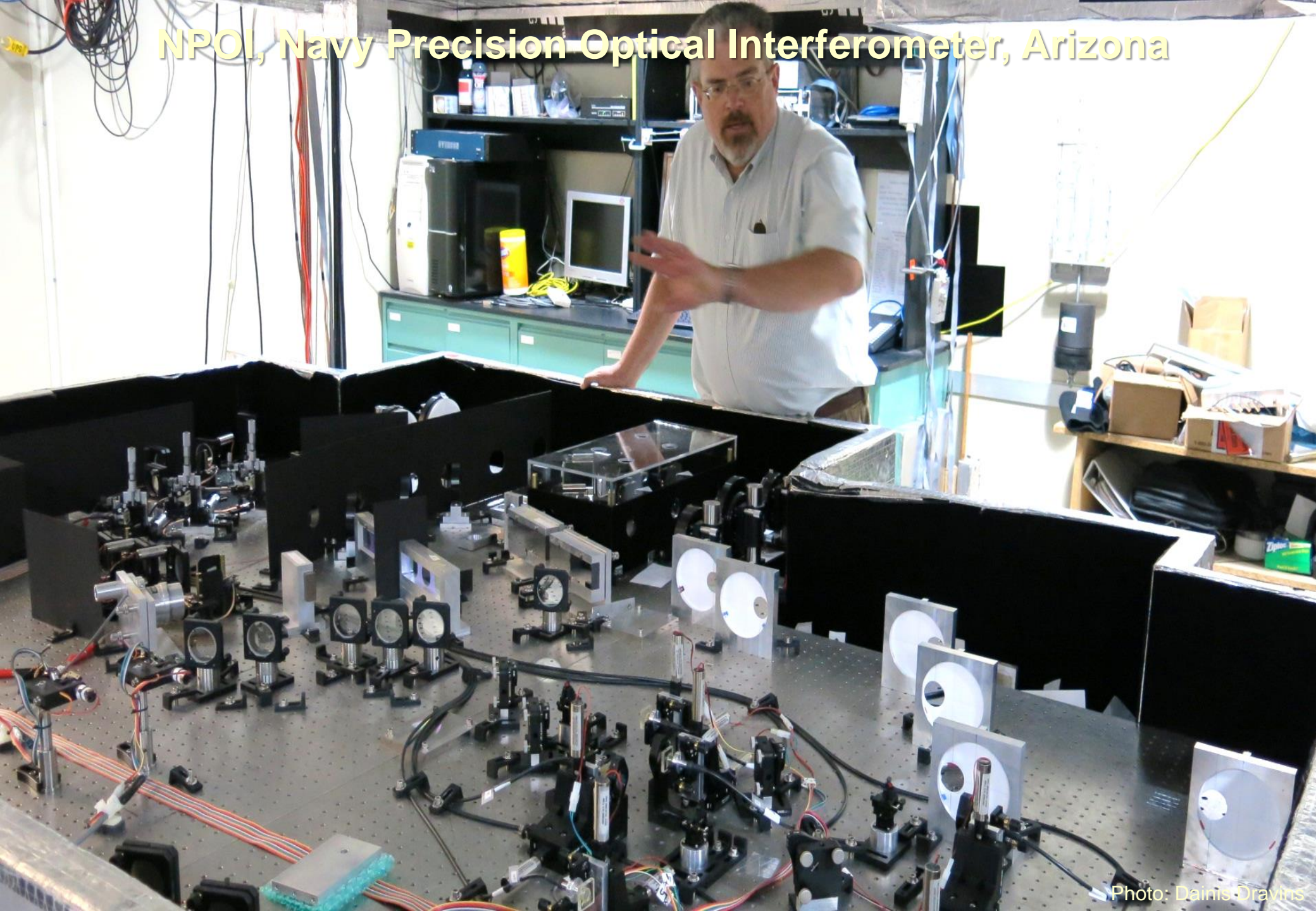
NPOI, Navy Precision Optical Interferometer, Arizona



NPOI, Navy Precision Optical Interferometer, Arizona



NPOI, Navy Precision Optical Interferometer, Arizona



GEOsat Imaging

- 2009: 1st Interferometric detection of GEOsat during “glint”

Hindsley et al. 2011, Applied Optics, 50, 2692

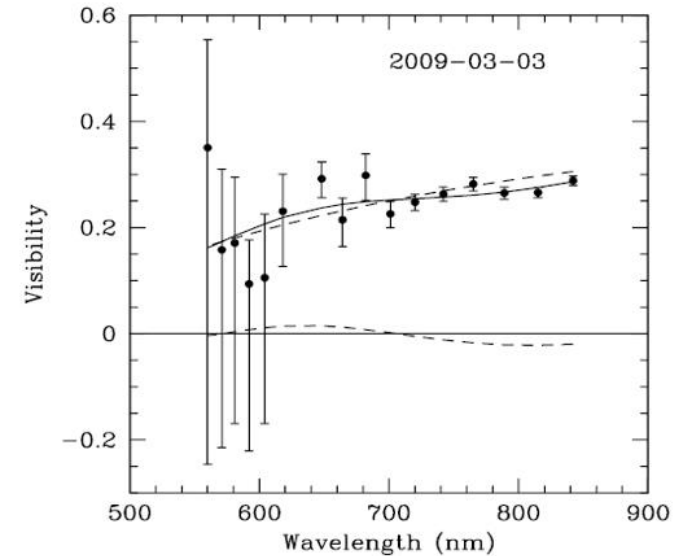


Fig. 5. Calibrated visibilities as a function of wavelength from 3 March 2009 data and from a two-component model fit to the data. The solid curve shows the flux-weighted sum of the two components from the first of the 3 March models shown in Table 1. This model consists of a smaller circular component of size 1.1 m (6.2 mas at geostationary distance) with 46% of the flux (upper dashed curve) and a larger component of 7 m (40 mas) with 54% of the flux (lower dashed curve). This larger, resolved component has a visibility amplitude of almost zero.

**IMAGING
GEOSTATIONARY
SATELLITES?**

**Many stars become
resolved surface objects
for baselines 100-1000 m**

Kilometer-scale interferometry!?

Concordia Base @ Dome C (3233 m)



http://www.esa.int/Our_Activities/Human_Spaceflight/Concordia
<http://blogs.esa.int/concordia/>

KEOPS: Kiloparsec Explorer for Optical Planet Search



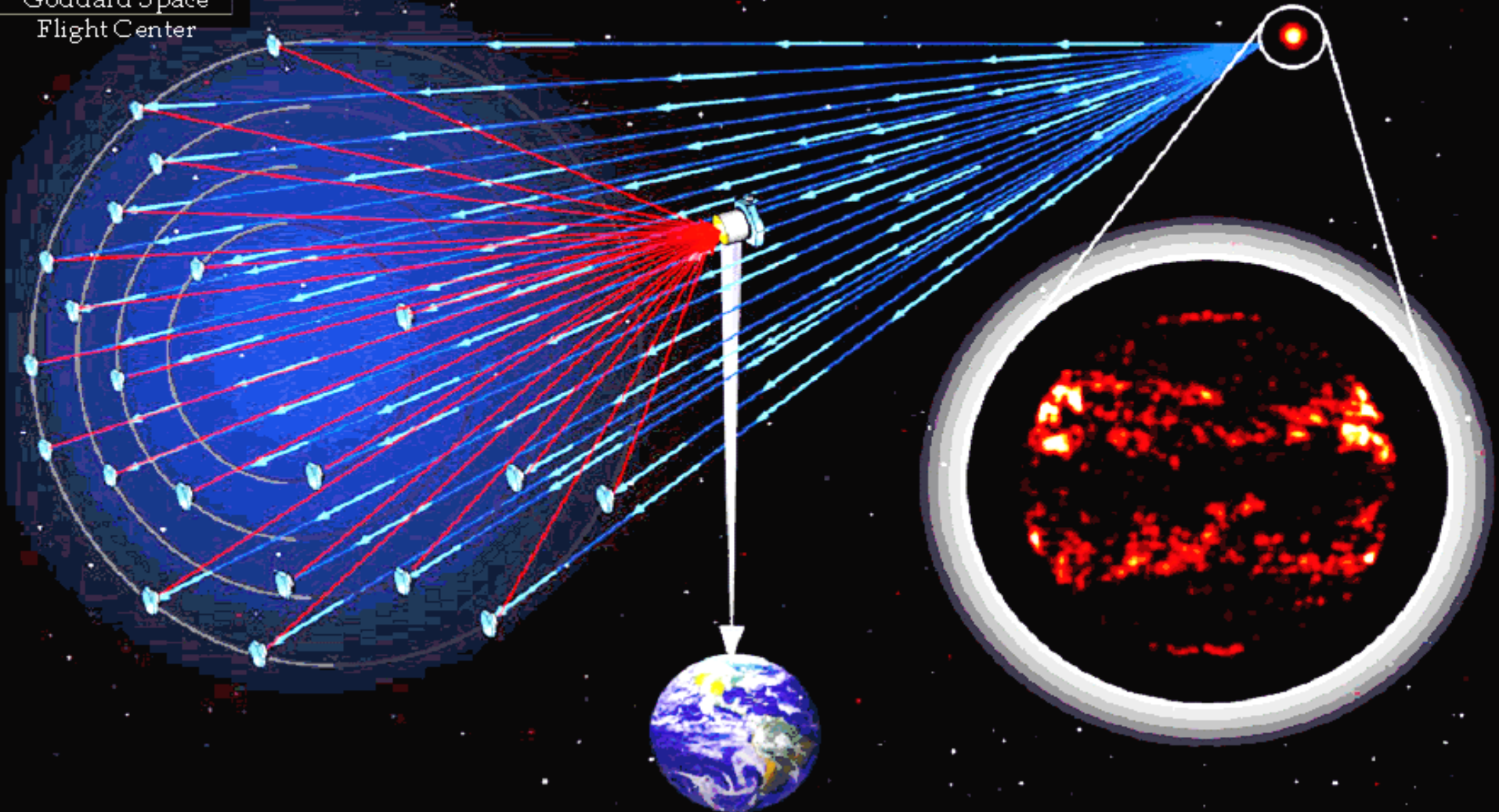
Imaging synthesis optical array proposed at Concordia Base on Dome C in Antarctica. KEOPS individual telescopes are grouped around the optical recombiner. Concordia station is visible in the distance.

F.Vakili; E.Aristidi; F.X.Schmider; S.Jankov; E.Fossat; L.Abe; A.Domiciano; A.Belu; A.Agabi; J.-B.Daban; et al.: *KEOPS: Towards Exo-Earths from Dome C of Antarctica*, EAS Publ. Ser. **14**, 211 (2005)



Goddard Space
Flight Center

Stellar Imager (SI)



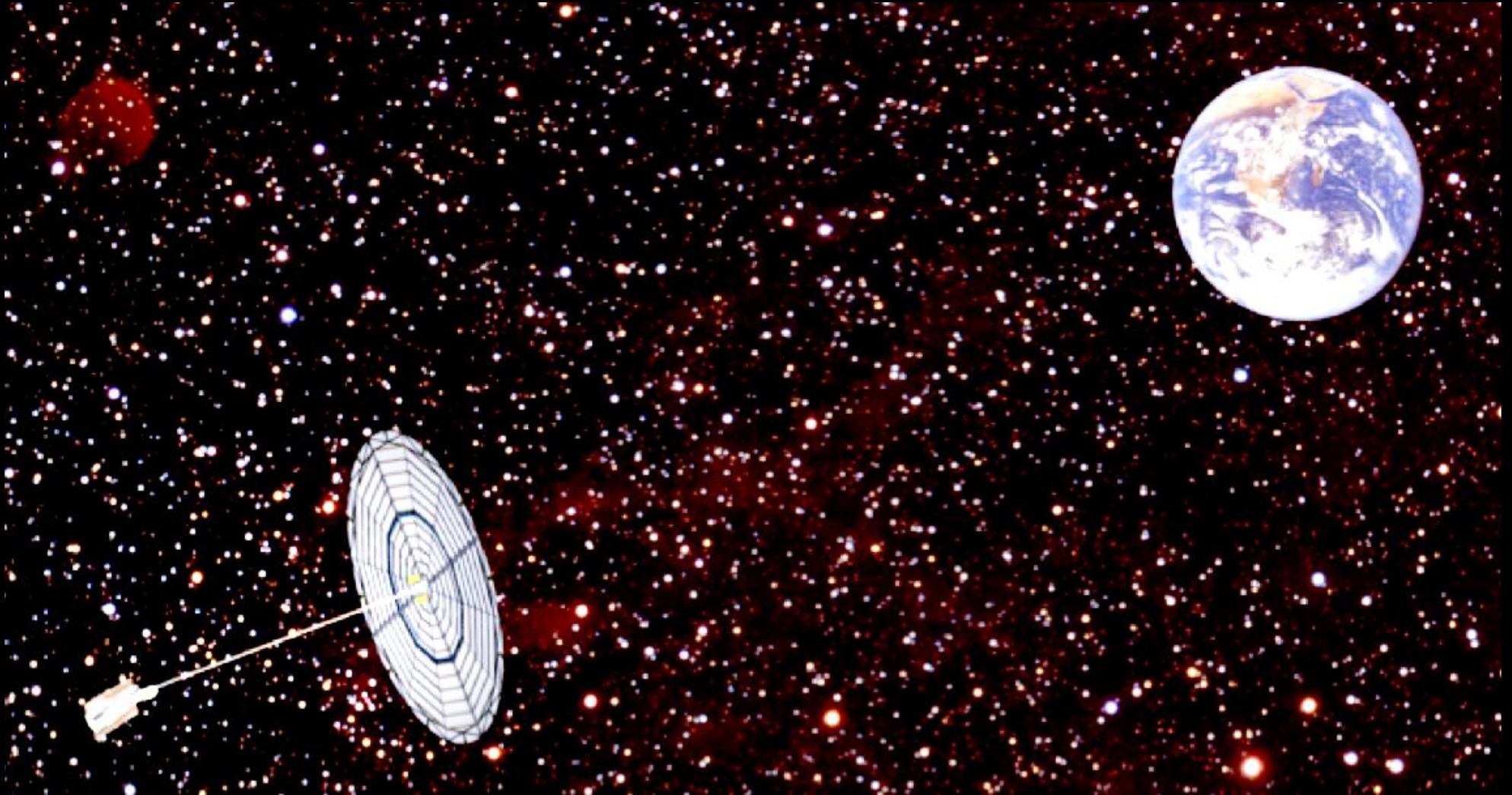
K.G.Carpenter, C.J.Schrijver, M.Karovska & SI Mission Concept Development Team;

<http://hires.gsfc.nasa.gov/si/>

ARAGOSCOPE

Webster Cash, University of Colorado

NASA Innovative Advanced Concept (NIAC) study (2015)



*Luciola** Hypertelescope

* genus of fireflies



The *Luciola* flotilla of many small collector mirrors operates like one giant diluted mirror. Focal beam-combiners independently exploit the sky image formed at the focal surface.

A.Labeyrie, H.Le Coroller, J.Dejonghe, O.Lardière, C.Aime, K.Dohlen, D.Mourard, R.Lyon, K.G.Carpenter, *Luciola hypertelescope space observatory*, *Exp.Astron.* **23**, 463 (2009)

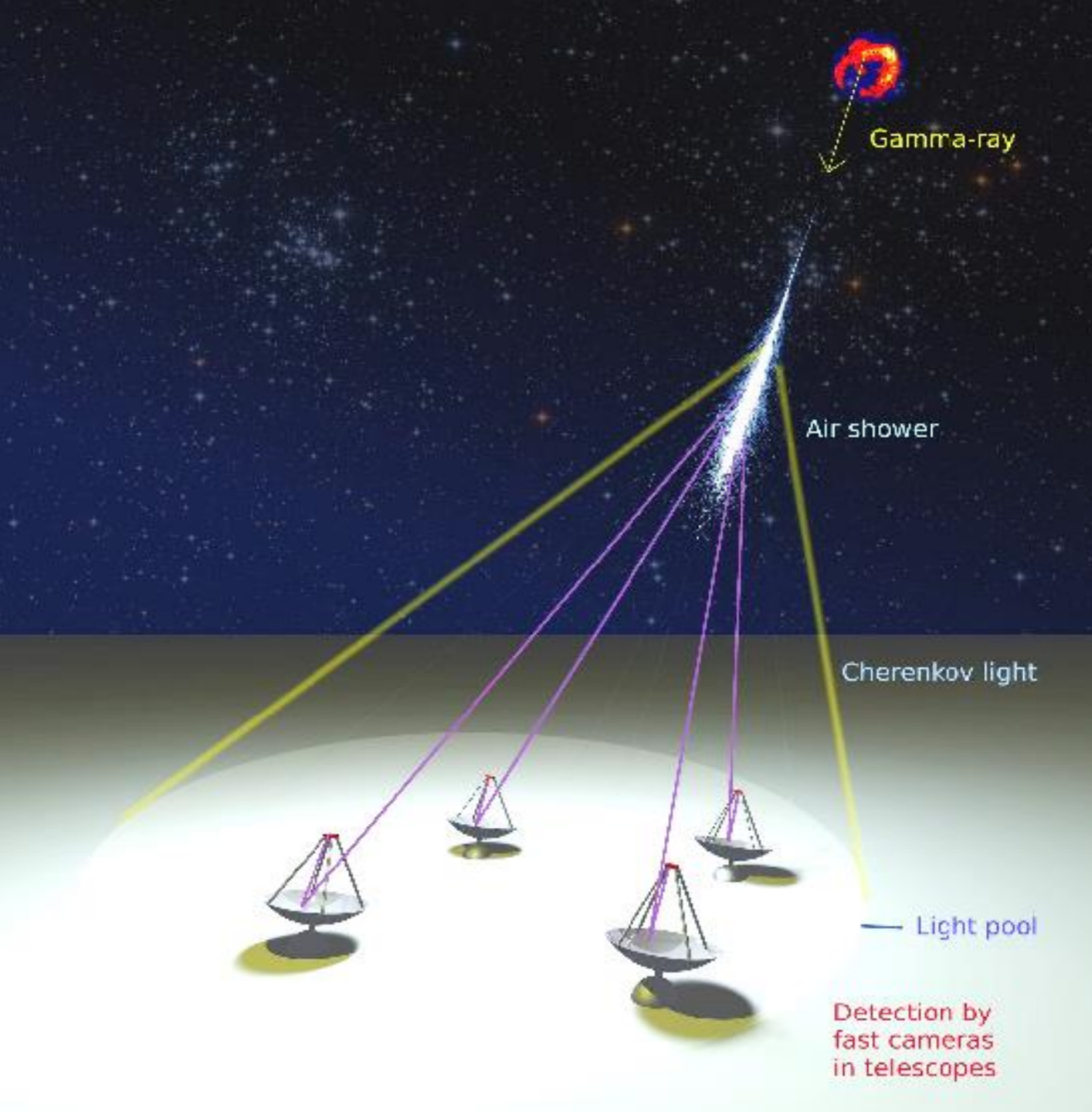


Exo-Earth Imager (150 km baseline space interferometer) with a simulated 30-min exposure of Earth at 3 parsec distance. (Antoine Labeyrie, Obs. de Haute-Provence)

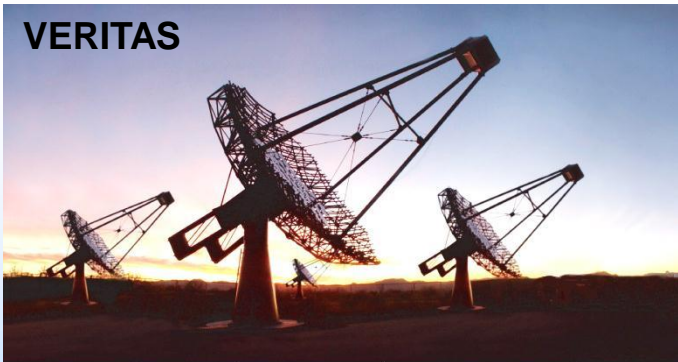
Isn't there some easier way??

Air Cherenkov Telescopes

Air Cherenkov Telescopes



VERITAS



MAGIC



HANLE



H.E.S.S.

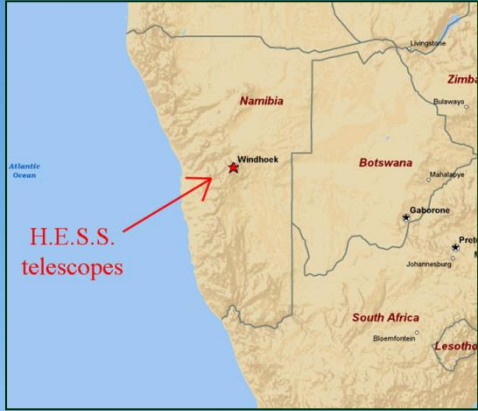
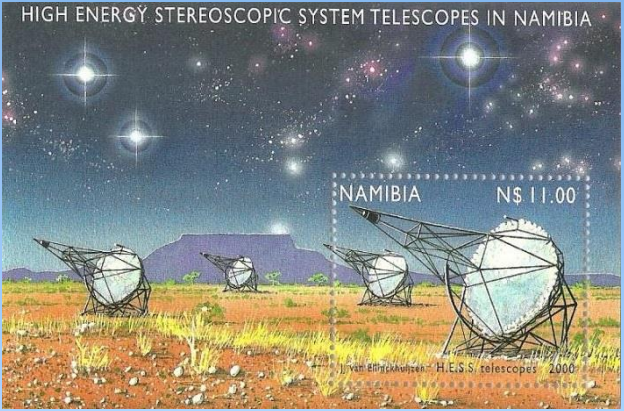


CANGAROO III

AIR CHERENKOV TELESCOPES



HIGH ENERGY STEREOSCOPIC SYSTEM TELESCOPES IN NAMIBIA



High Energy Stereoscopic System (H.E.S.S.) array of Imaging Atmospheric Cherenkov Telescopes (IACT) Telescopes, Khomas Highland, near Windhoek, Namibia

Artist's vision of CTA-North on La Palma



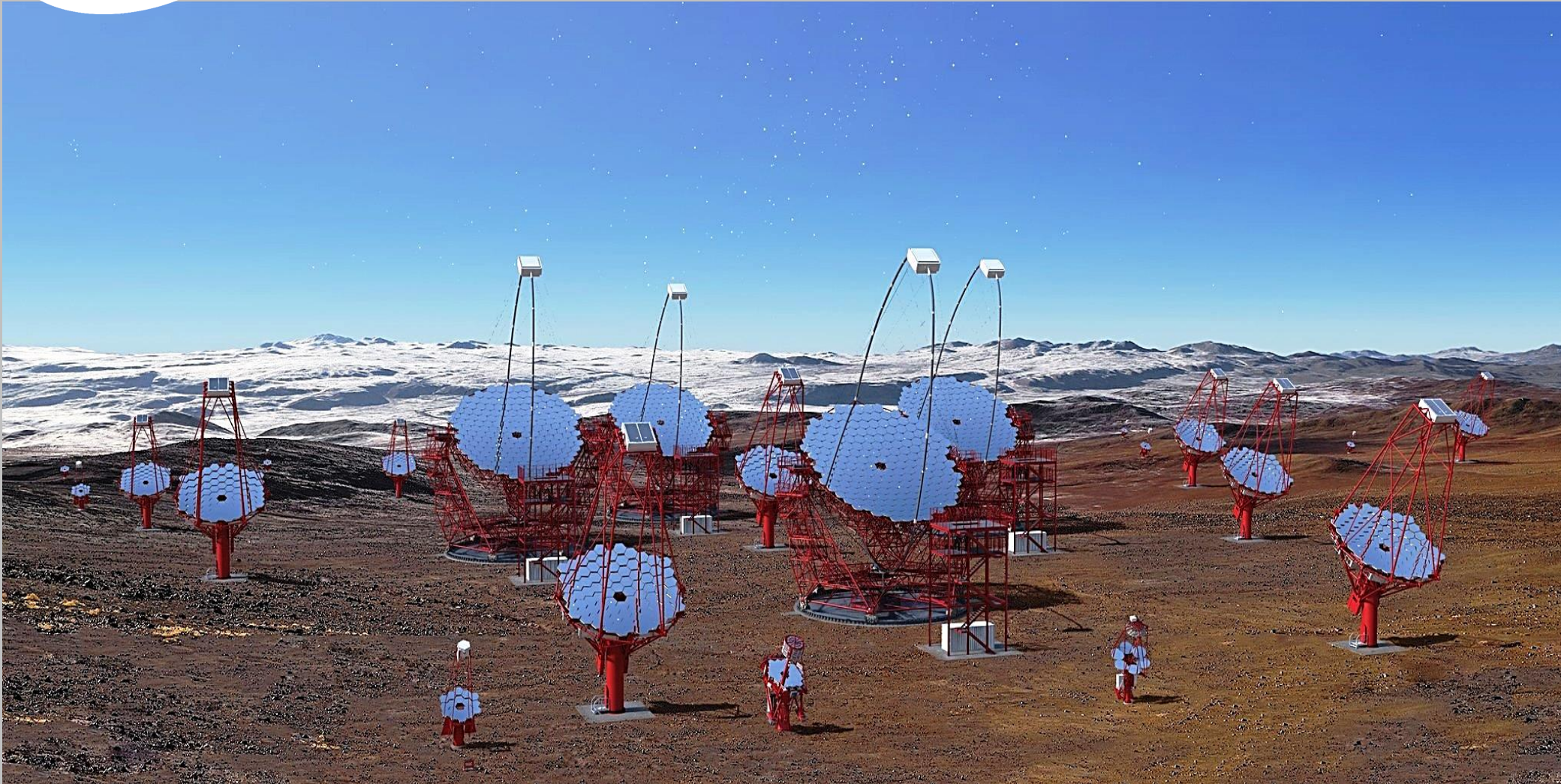
Four 23-m and fifteen 12-m telescopes will supplement two existing MAGIC 17-m dishes

Image: G.Pérez, IAC; www.cta-observatory.org

Webcam from LST-1 construction site:

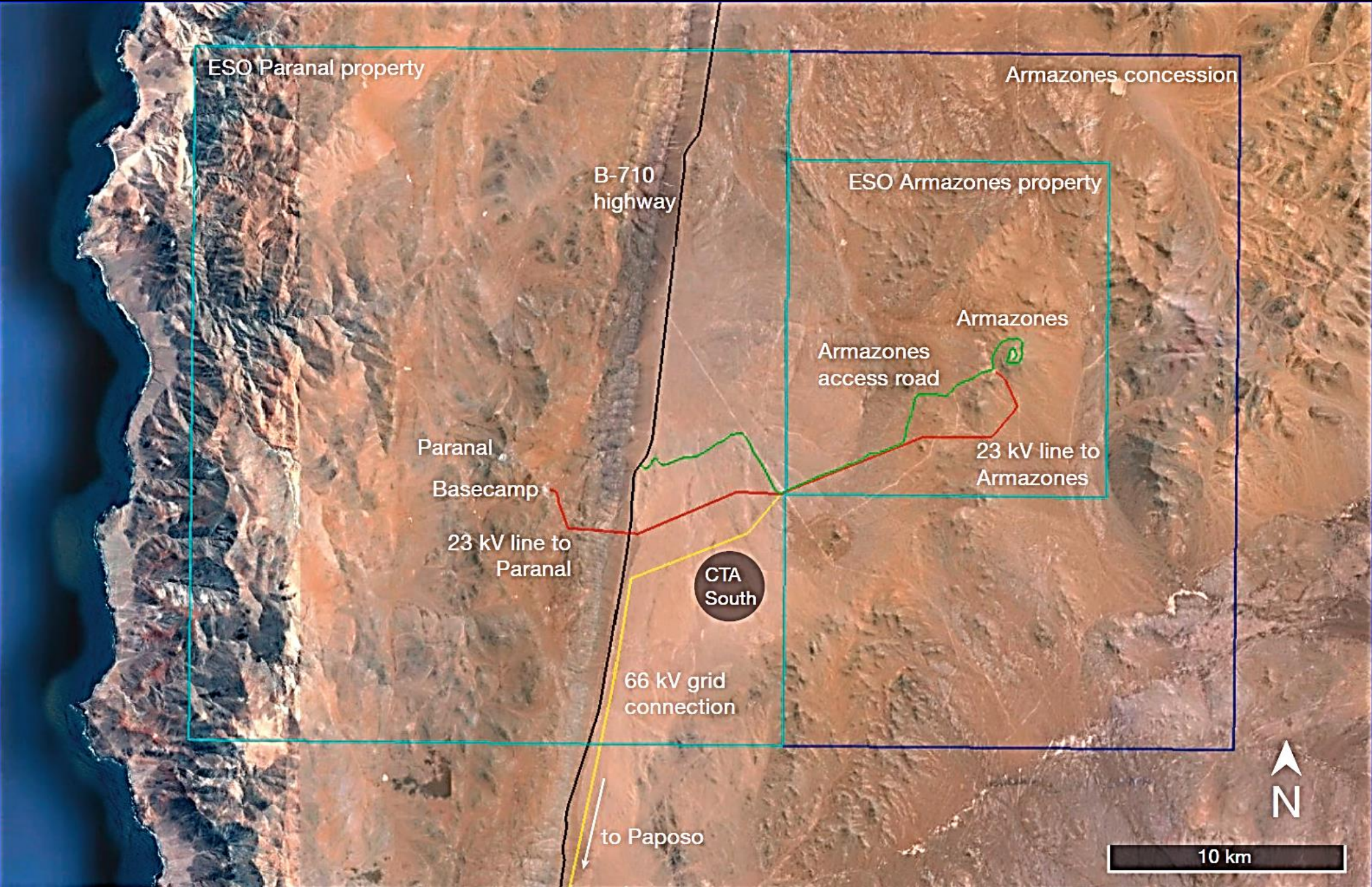
<http://www.lst1.iac.es/webcams/current1/1000.jpg>

Artist's vision of CTA-South in Chile



Artist's vision of CTA-South, with different small-, medium-, and large-size telescopes

Image: G.Pérez, IAC; www.cta-observatory.org



Paranal-Armazones area: Access road to Armazones (green), electricity grid connections, and location of CTA South. (T.de Zeeuw: *Reaching New Heights in Astronomy — ESO Long Term Perspectives*, ESO Messenger 166, 2, 2016)



Cerro Paranal



Future site of CTA-south, ~10 km south-east from the ESO Paranal observatory
(ESO Announcement ann15058)

Vulcano Lullillaco
6739 m, 190 km east

Cerro Armazones
ELT

Proposed Site for the
Cherenkov Telescope Array

Cerro Paranal
Very Large Telescope

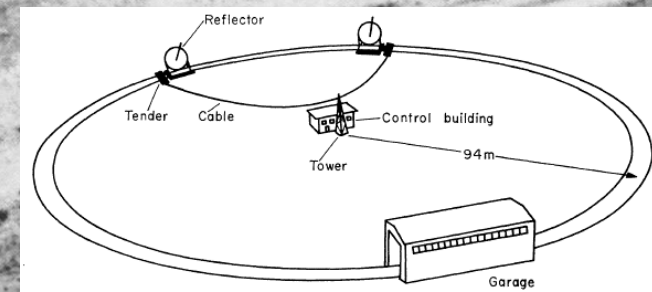


Intensity interferometry

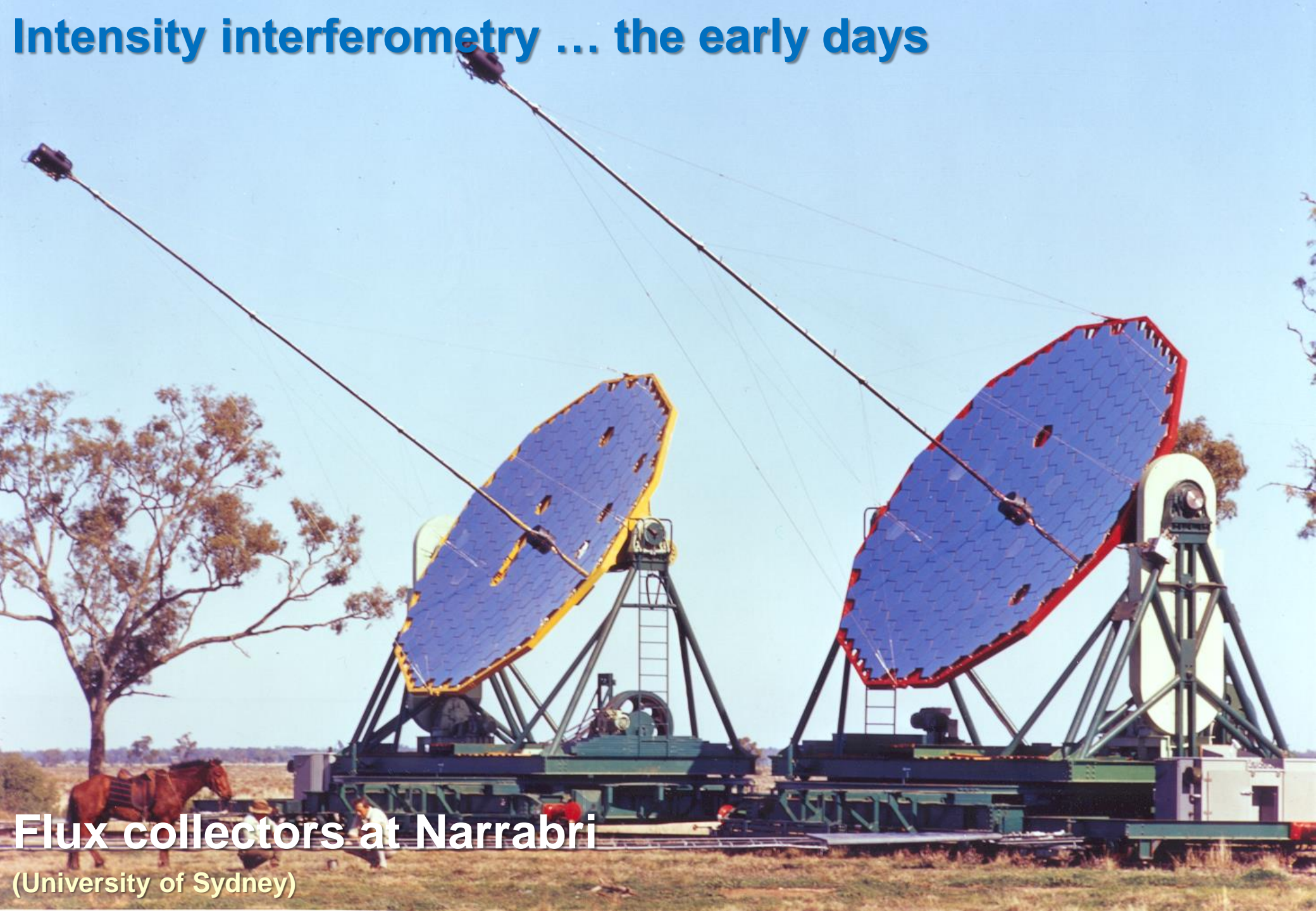
Intensity interferometry ... the early days

Narrabri observatory with its circular railway track

R.Hanbury Brown: *BOFFIN. A Personal Story of the Early Days of Radar, Radio Astronomy and Quantum Optics* (1991)

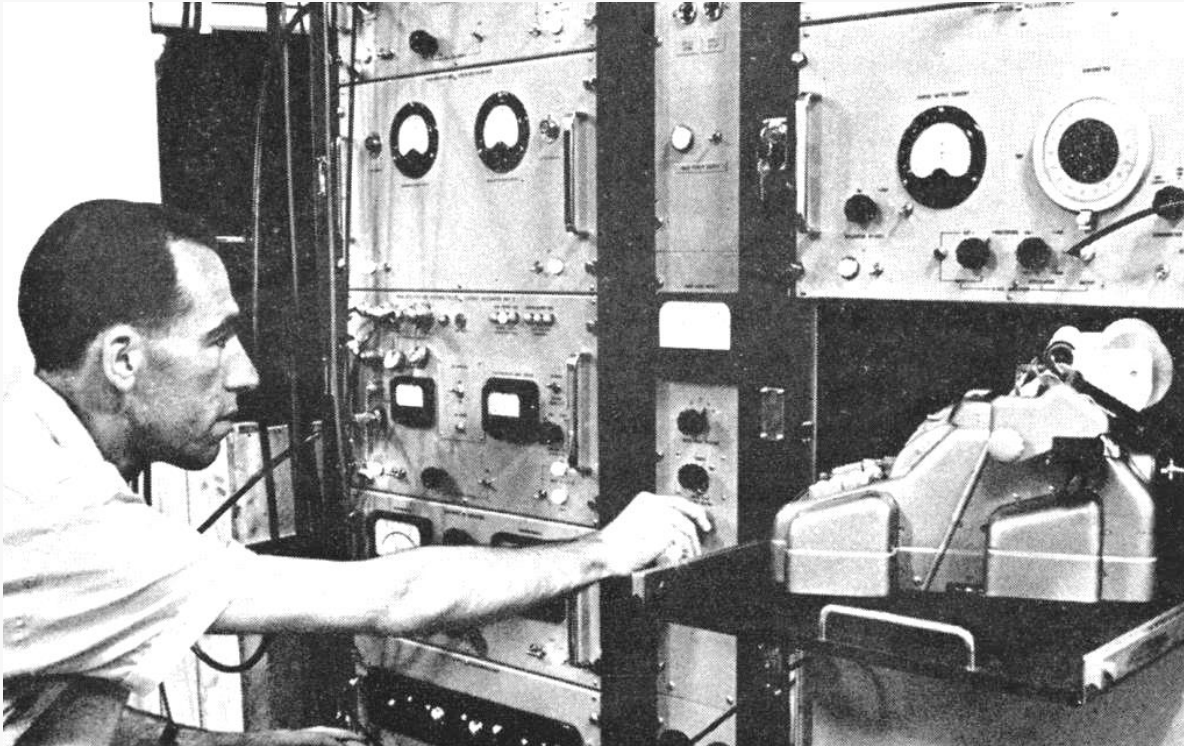


Intensity interferometry ... the early days



Flux collectors at Narrabri
(University of Sydney)

Intensity interferometry ... the early days



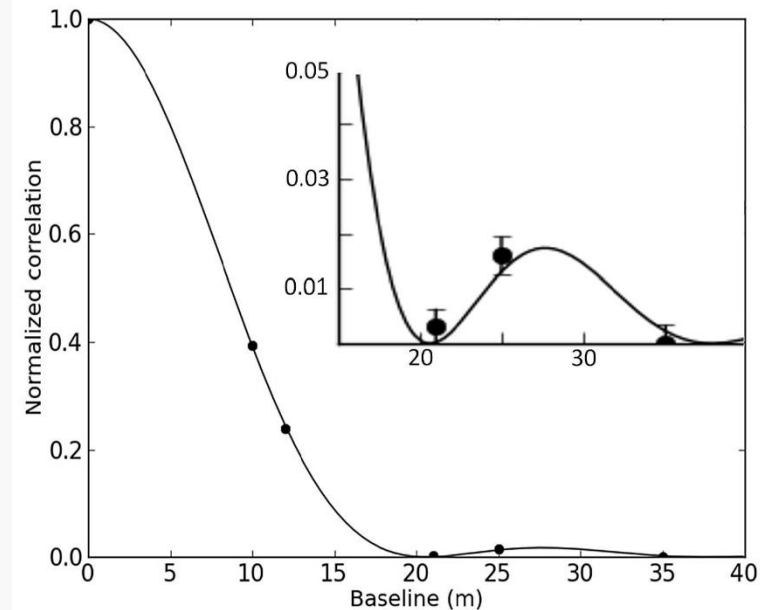
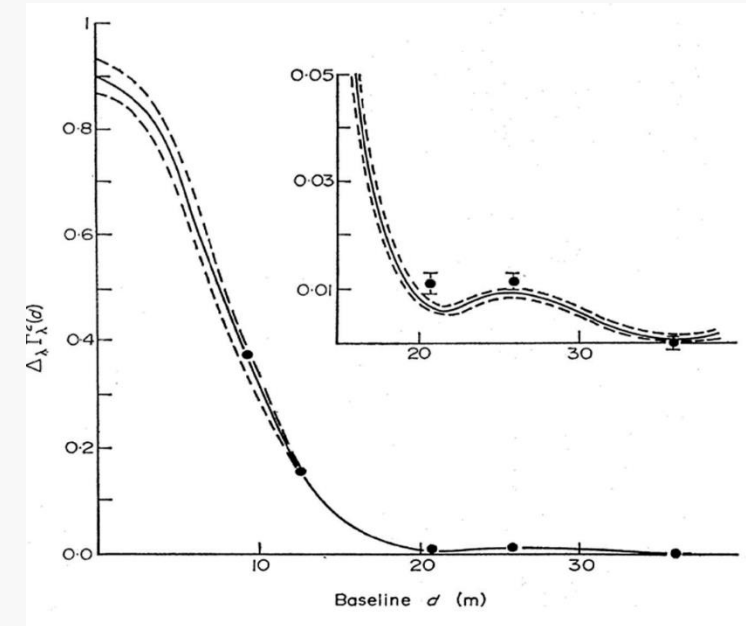
Left: Narrabri electronics of the 1960's

Top right: Sirius observed from Narrabri

(Hanbury Brown et al., MNRAS **167**, 475, 1974)

Bottom right: Simulated Narrabri observations
using current software

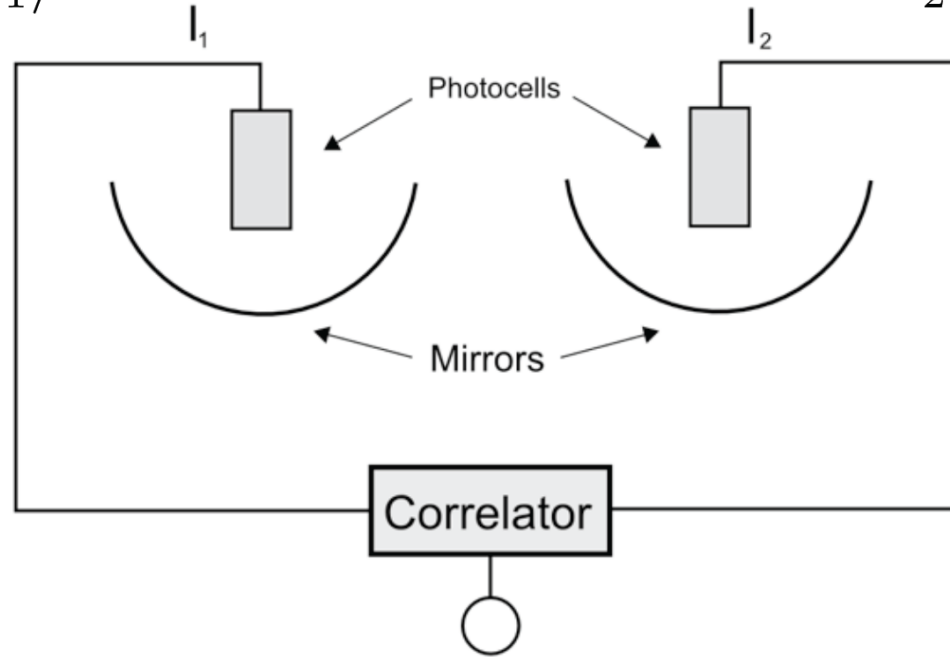
Dravins et al., New Astron. Rev. **56**, 143, 2012)



INTENSITY INTERFEROMETRY

$$P_1 = \alpha_1 \langle I_1 \rangle \Delta t$$

$$P_2 = \alpha_2 \langle I_2 \rangle \Delta t$$



$$P_{12} = \alpha_1 \alpha_2 \langle I_1 \rangle \langle I_2 \rangle (1 + |\gamma_{12}|^2) \Delta t^2$$

↑
Photon clumping

PHOTON CORRELATIONS*

Roy J. Glauber

Lyman Laboratory, Harvard University, Cambridge, Massachusetts

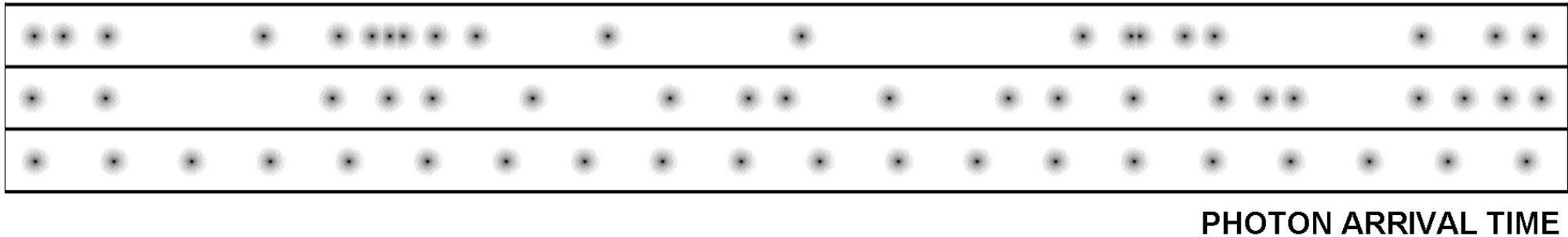
(Received 27 December 1962)

In 1956 Hanbury Brown and Twiss¹ reported that the photons of a light beam of narrow spectral width have a tendency to arrive in correlated pairs. We have developed general quantum mechanical methods for the investigation of such correlation effects and shall present here results for the distribution of the number of photons counted in an incoherent beam. The fact that photon correlations are enhanced by narrowing the spectral bandwidth has led to a prediction² of large-scale correlations to be observed in the beam of an optical maser. We shall indicate that this prediction is misleading and follows from an inappropriate model of the maser beam. In considering these problems we shall outline

a method of describing the photon field which appears particularly well suited to the discussion of experiments performed with light beams, whether coherent or incoherent.

The correlations observed in the photoionization processes induced by a light beam were given a simple semiclassical explanation by Purcell,³ who made use of the methods of microwave noise theory. More recently, a number of papers have been written examining the correlations in considerably greater detail. These papers^{2,4-6} retain the assumption that the electric field in a light beam can be described as a classical Gaussian stochastic process. In actuality, the behavior of the photon field is considerably more

PHOTON STATISTICS



Top: Bunched photons (Bose-Einstein; ‘quantum-random’)

Center: Antibunched photons (like fermions)

Bottom: Coherent and uniformly spaced (like ideal laser)

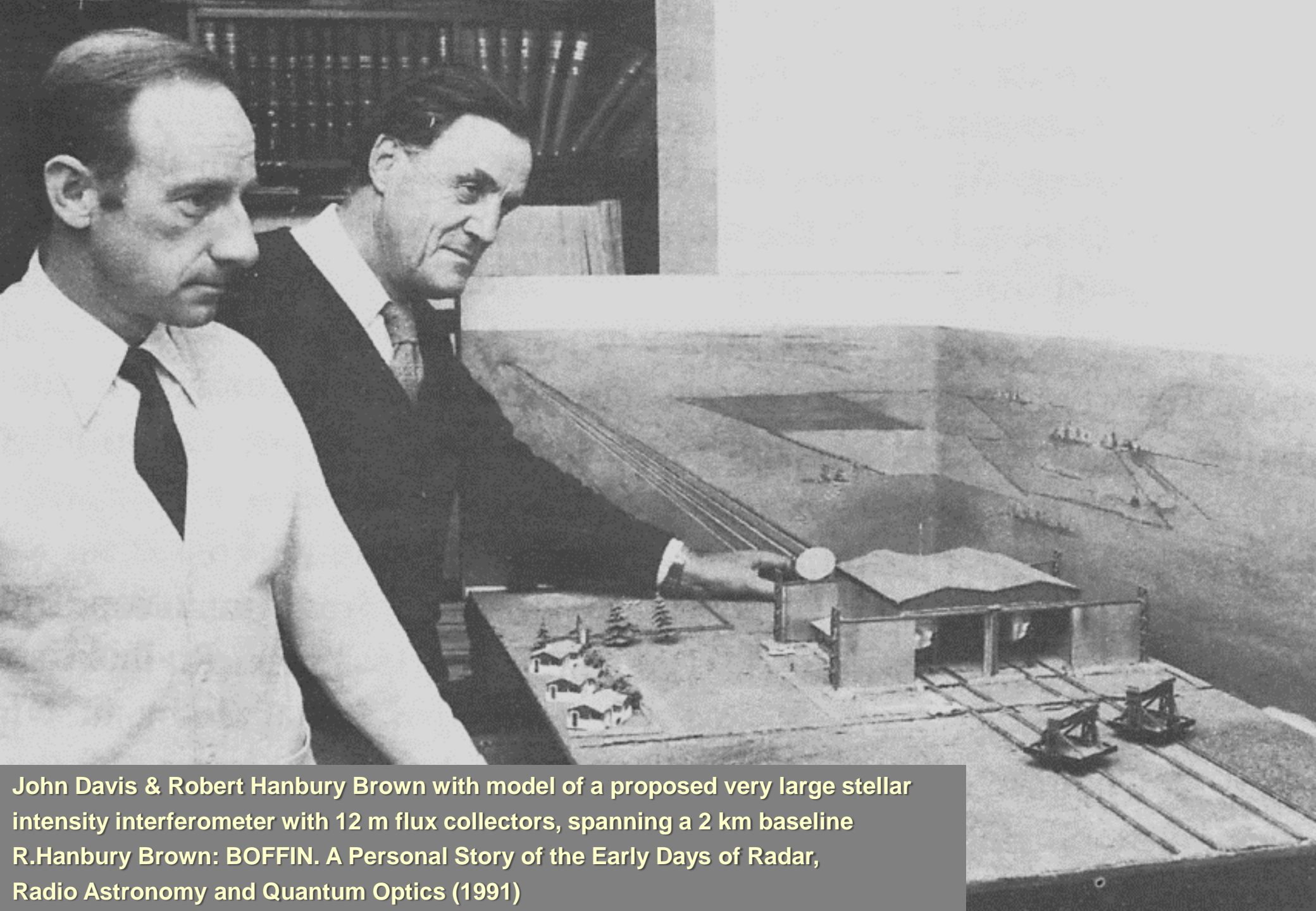
Roy Glauber

Nobel prize in physics

Stockholm, December 2005



**"For his contribution to the
quantum theory of optical coherence"**

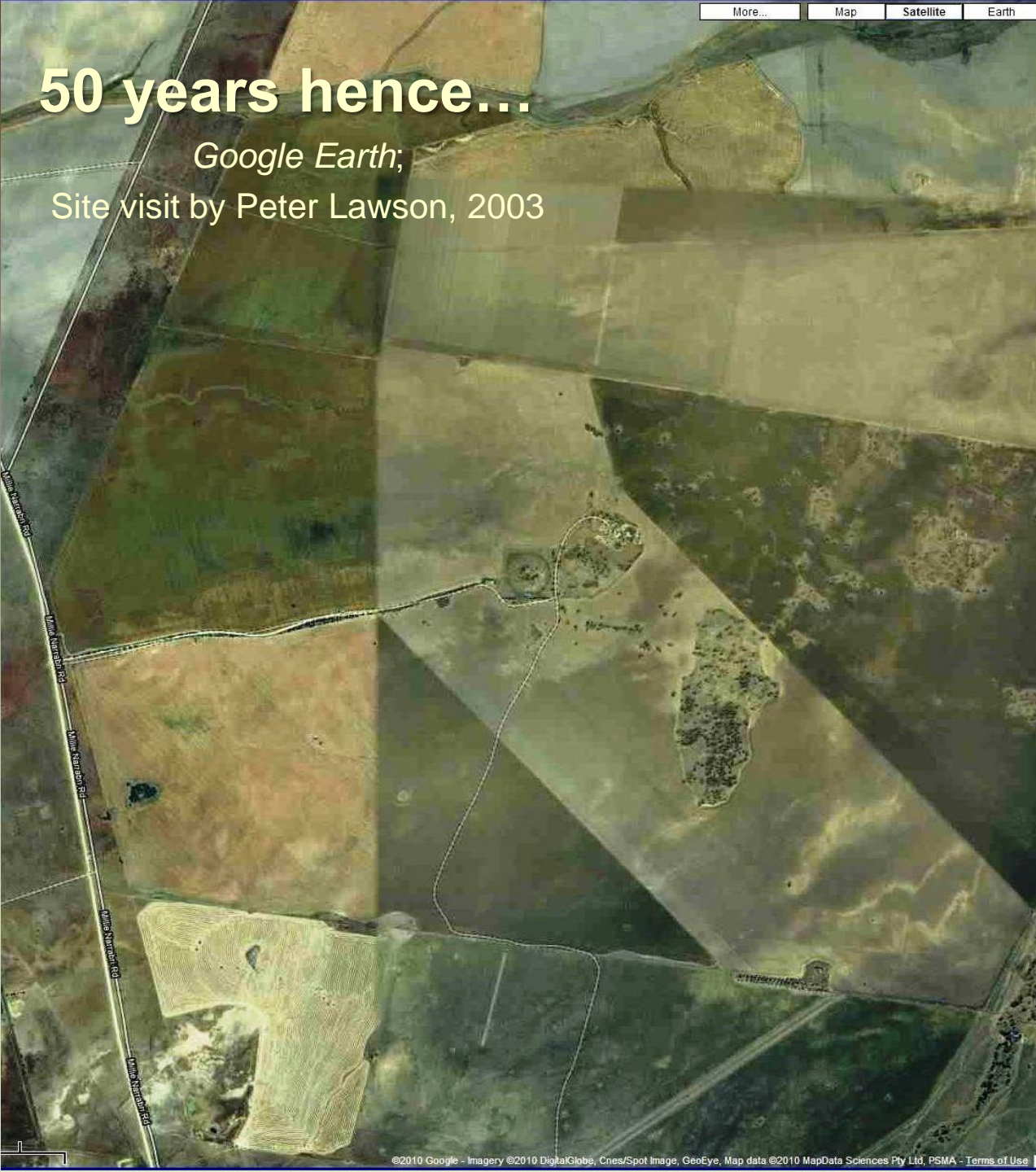


John Davis & Robert Hanbury Brown with model of a proposed very large stellar intensity interferometer with 12 m flux collectors, spanning a 2 km baseline
R.Hanbury Brown: BOFFIN. A Personal Story of the Early Days of Radar, Radio Astronomy and Quantum Optics (1991)

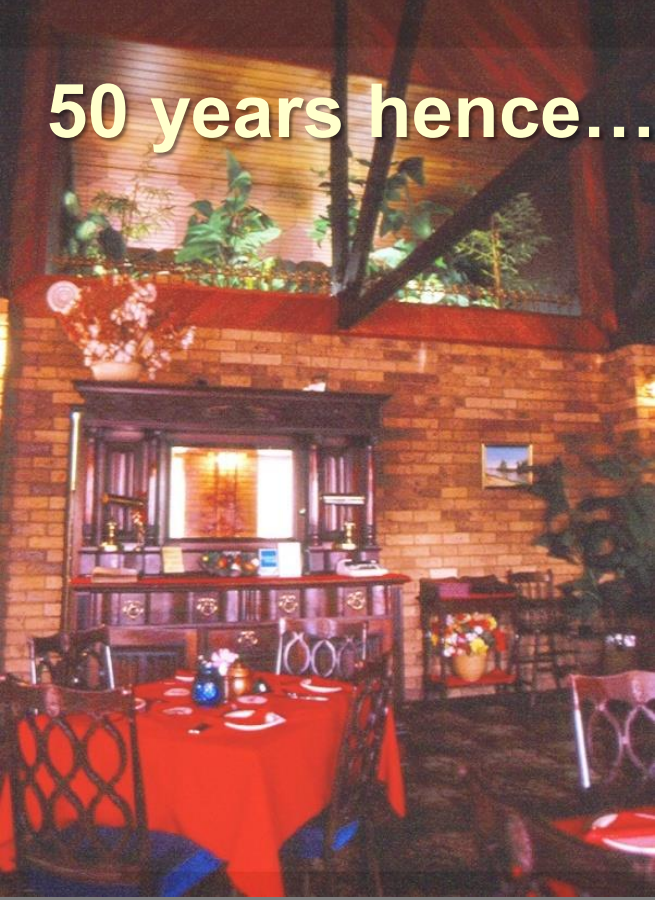
50 years hence...

Google Earth;

Site visit by Peter Lawson, 2003



50 years hence...



Sic transit gloria mundi...

Motel restaurant and bar in Narrabri,
its wall covered with mirrors from the
former observatory.

Photos: Dainis Dravins

**Astronomy out ...
particle physics in**

PARTICLE PHYSICS

PHYSICAL REVIEW

VOLUME 120, NUMBER 1

OCTOBER 1, 1960

Influence of Bose-Einstein Statistics on the Antiproton-Proton Annihilation Process*

GERSON GOLDHABER, SULAMITH GOLDHABER, WONYONG LEE, AND ABRAHAM PAIS†

Lawrence Radiation Laboratory and Department of Physics, University of California, Berkeley, California

(Received May 16, 1960)

Recent observations of angular distributions of π mesons in \bar{p} - p annihilation indicate a deviation from the predictions of the usual Fermi statistical model. In order to shed light on these phenomena, a modification of the statistical model is studied. We retain the assumption that the transition rate into a given final state is proportional to the probability of finding N free π mesons in the reaction volume, but express this probability in terms of wave functions symmetrized with respect to particles of like charge. The justification of this assumption is discussed. The model reproduces the experimental results qualitatively, provided the radius of the interaction volume is between one-half and three-fourths of the pion Compton wavelength; the depend-

ence of angular correlation effects on the value of the radius is rather sensitive. Quantitatively, there seems to remain some discrepancy, but we cannot say whether this is due to experimental uncertainties or to some other dynamic effects. In the absence of information on π - π interactions and of a fully satisfactory explanation of the mean pion multiplicity for annihilation, we wish to emphasize the preliminary nature of our results. We consider them, however, as an indication that the symmetrization effects discussed here may well play a major role in the analysis of angular distributions. It is pointed out that in this respect the energy dependence of the angular correlations may provide valuable clues for the validity of our model.

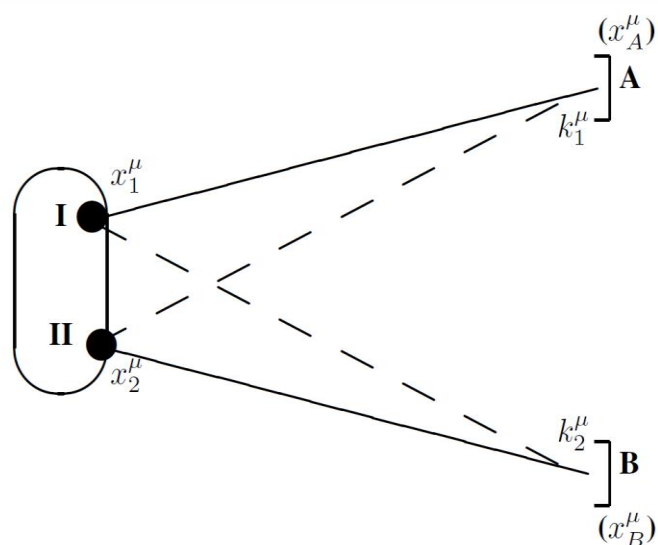
HBT Interferometry: Historical Perspective

Sandra S. Padula

Instituto de Física Teórica - UNESP, Rua Pamplona 145, 01405-900 São Paulo, Brazil

Received on 15 December, 2004

I review the history of HBT interferometry, since its discovery in the mid 1950's, up to the recent developments and results from BNL/RHIC experiments. I focus the discussion on the contributions to the subject given by members of our Brazilian group.



1.2 GGLP

In 1959, Goldhaber, Goldhaber, Lee and Pais performed an experiment at the Bevalac/LBL, in Berkeley, CA, USA, aiming at the discovery of the ρ^0 resonance[4]. In the experiment, they considered $\bar{p}p$ collisions, at 1.05 GeV/c. They were searching for the resonance by means of the decay $\rho^0 \rightarrow \pi^+\pi^-$, by measuring the unlike pair, $\pi^+\pi^-$, mass-distribution and comparing it with the ones for like pairs, $\pi^\pm\pi^\pm$. Afterwards, they concluded that there was not enough statistics for establishing the existence of ρ^0 . Nevertheless, they observed an unexpected angular correlation among identical pions! Later, in 1960, they successfully reproduced the empirical angular distribution by a detailed multi- π phase-space calculation using symmetrized wave functions for LIKE particles. Being so, they concluded the effect was a consequence of the Bose-Einstein nature of $\pi^+\pi^+$ and $\pi^-\pi^-$. They were not aware of the experiment Hanbury-Brown and Twiss had performed previously. Thus, they had discovered, by chance, the counterpart of the HBT effect in high energy collisions.

Figure 3. Simplified picture: two point sources, I and II, emit quanta considered as plane waves, which are observed in detectors A and B, respectively, with momenta k_1^μ and k_2^μ . Since the quanta are indistinguishable, there are two possible combinations for this observation, illustrated by the two continuous and the two dashed lines.

PARTICLE PHYSICS

HBT Interferometry: Historical Perspective

Sandra S. Padula

Instituto de Física Teórica - UNESP, Rua Pamplona 145, 01405-900 São Paulo, Brazil

Received on 15 December, 2004

I review the history of HBT interferometry, since its discovery in the mid 1950's, up to the recent developments and results from BNL/RHIC experiments. I focus the discussion on the contributions to the subject given by members of our Brazilian group.

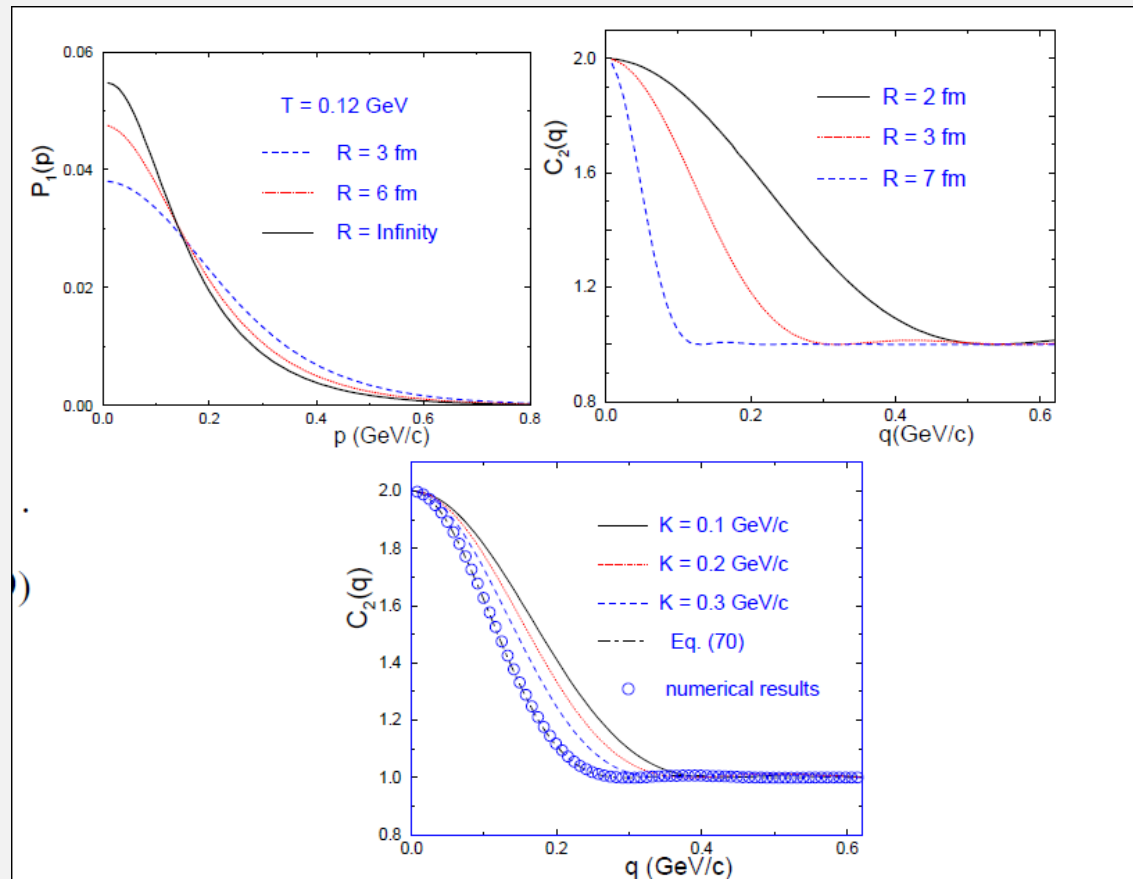
1.5 Further applications

In the 1970's, Kopylov, Podgoretskiĭ, and Grishin[8] used second-order interferometry to study several interesting problems. For example, they modelled the nucleus as a static sphere with radius R , emitting pions from its surface and got the following correlation function

$$C(k_1, k_2) = 1 \pm \left[\frac{2J_1(q_T R)}{q_T R} \right]^2 [1 + (q_0 \tau)^2]^{-1}, \quad (13)$$

2.1 Expansion effects in HBT

In the first paper on the subject, we started by making the hypothesis that the Quark-Gluon Plasma was already being produced in pp and $\bar{p}p$ collisions at the CERN/ISR. We considered[25] that the system produced in such collisions expanded before emitting the final particles (hadrons), according to the one-dimensional Landau Hydrodynamical Model [26]. In the initial stage, the system was formed in the QGP phase at a certain temperature, T_0 , started expanding and cooling down, until it reached the critical temperature, T_c , which we assumed to be of order of pion mass. It could be imagined that, once T_c was reached, the hadronization occurred instantaneously, followed by the particle emission.



The top plot shows the spectrum in the example of pions confined in the sphere of radius R . The top right plot shows $C_{\pi\pi}(q)$ versus q , for three different values of the source radius. The plot in the bottom shows that the correlation function shrinks for increasing average momentum

HBT Interferometry: Historical Perspective

Sandra S. Padula

Instituto de Física Teórica - UNESP, Rua Pamplona 145, 01405-900 São Paulo, Brazil

Received on 15 December, 2004

I review the history of HBT interferometry, since its discovery in the mid 1950's, up to the recent developments and results from BNL/RHIC experiments. I focus the discussion on the contributions to the subject given by members of our Brazilian group.

PARTICLE PHYSICS

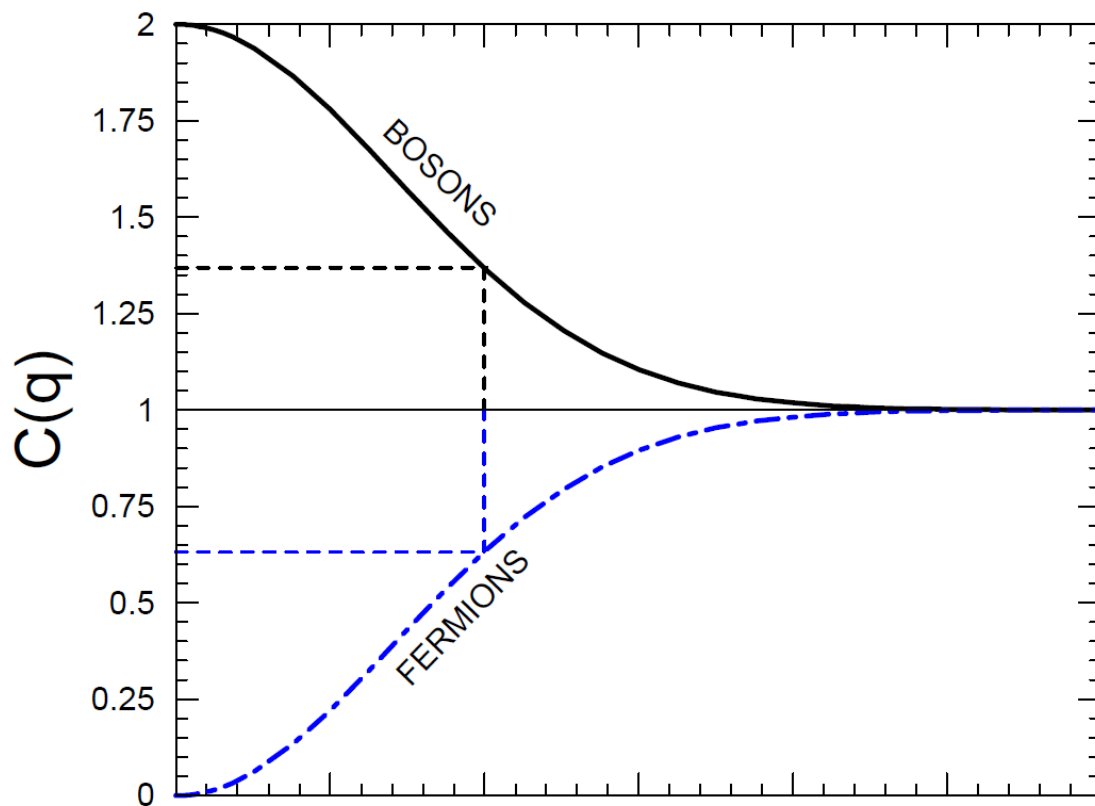


Figure 4. Simple illustration corresponding to the ideal Gaussian source. The upper curve represents to the bosonic case, while the lower curve, the fermionic one. The parameter R is the r.m.s. radius of the emitting region.

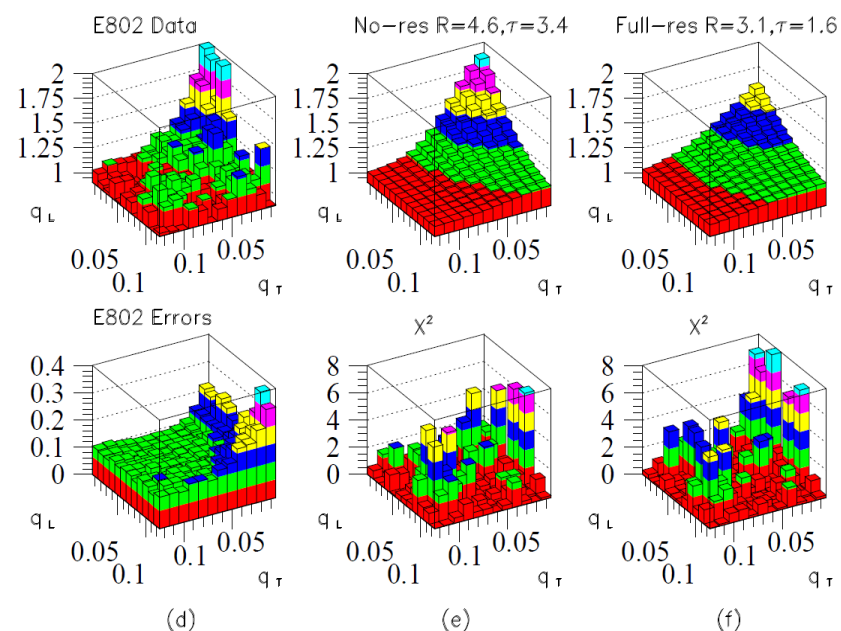
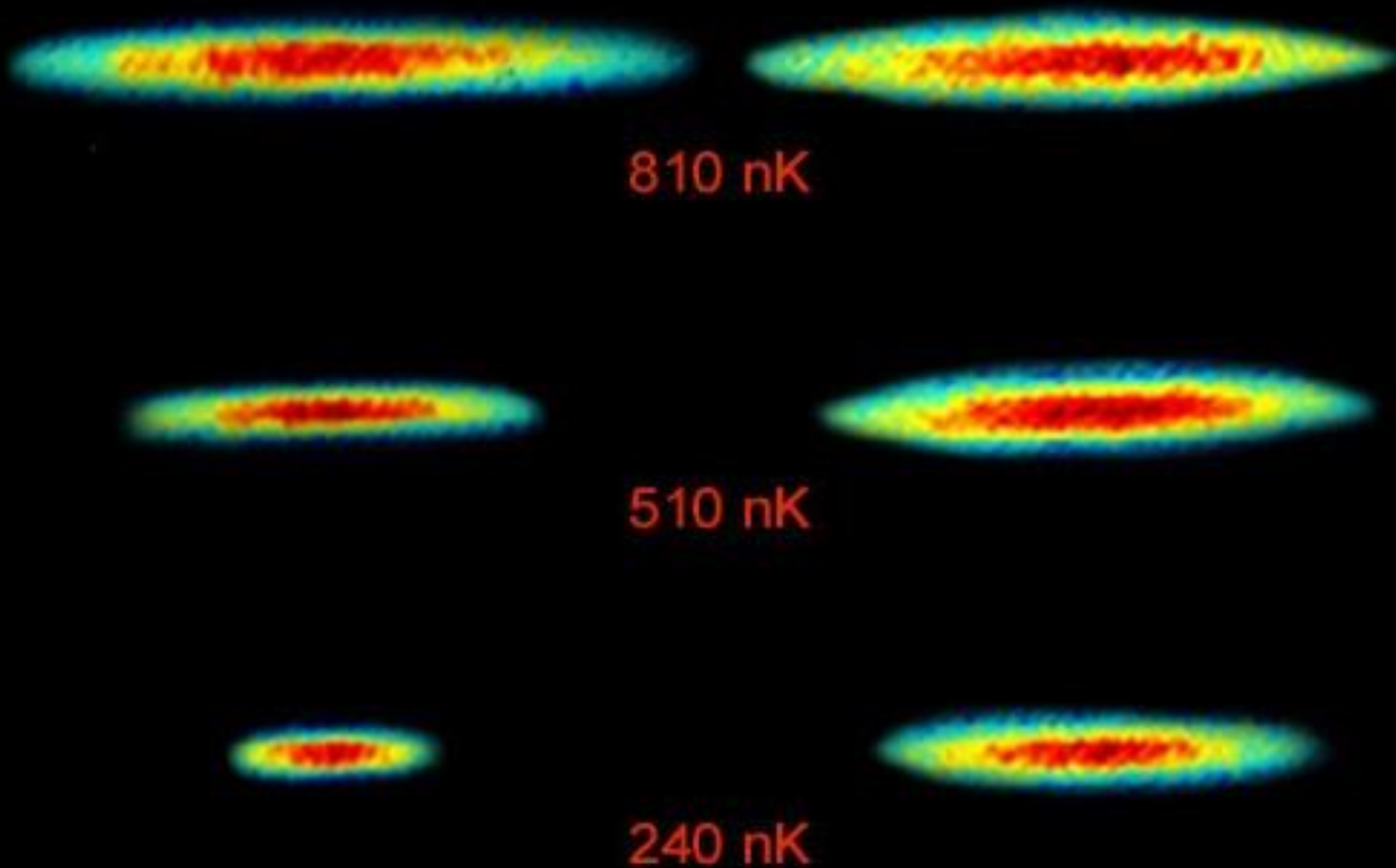


Figure 13. $\pi^- \pi^-$ correlations in central Si+Au collisions is shown as a function of q_T and q_L . The preliminary E802 data[43] corrected for acceptance and Coulomb effects are shown in part (a). Parts (b) and (c) show theoretical correlation functions filtered with the E802 acceptance. They correspond, respectively, to cases without and with resonance production.

Bosons

Fermions



BOSONS BUNCH TOGETHER, FERMIONS DON'T

Pauli exclusion principle:
Fermions cannot share the same quantum state

(but bosons can! 😊)

Bose-Einstein condensates of lithium isotopes;

Left: ${}^7\text{Li}$ bosons (integer spin)

Right: ${}^6\text{Li}$ fermions

As temperature drops, bosons bunch together, while fermions keep their distance

Truscott & Hulet (Rice Univ.)

PARTICLE PHYSICS

HBT Interferometry: Historical Perspective

Sandra S. Padula

Instituto de Física Teórica - UNESP, Rua Pamplona 145, 01405-900 São Paulo, Brazil

Received on 15 December, 2004

I review the history of HBT interferometry, since its discovery in the mid 1950's, up to the recent developments and results from BNL/RHIC experiments. I focus the members of our Brazilian group.

Review of HBT or Bose-Einstein correlations in high energy heavy ion collisions

T. Csörgő

MTA KFKI RMKI, H - 1525 Budapest 114, P.O.Box 49, Hungary

Abstract. A brief review is given on the discovery and the first five decades of the Hanbury Brown - Twiss effect and its generalized applications in high energy nuclear and particle physics, that includes a meta-review. Interesting and inspiring new directions are also highlighted, including for example source imaging, lepton and photon interferometry, non-Gaussian shape analysis as well as many other new directions. Existing models are compared to two-particle correlation measurements and the so-called RHIC HBT puzzle is resolved. Evidence for a (directional) Hubble flow is presented and the conclusion is confirmed by a successful description of the pseudorapidity dependence of the elliptic flow as measured in Au+Au collisions by the PHOBOS Collaboration.

Annu. Rev. Nucl. Part. Sci. 1992. 42:77-100
Copyright © 1992 by Annual Reviews Inc. All rights reserved.

HADRONIC INTERFEROMETRY IN HEAVY-ION COLLISIONS

Wolfgang Bauer and Claus-Konrad Gelbke

National Superconducting Cyclotron Laboratory and Department of Physics and Astronomy, Michigan State University, East Lansing, Michigan 48824

Scott Pratt

Department of Physics, University of Wisconsin, Madison, Wisconsin 53706

KEY WORDS: intensity interferometry, Hanbury Brown and Twiss effect, two-particle correlation functions, transport theory

THE PHYSICS OF HANBURY BROWN-TWISS INTENSITY INTERFEROMETRY: FROM STARS TO NUCLEAR COLLISIONS *

GORDON BAYM

Department of Physics, University of Illinois at Urbana-Champaign
1110 W. Green St., Urbana, IL 61801, USA

(Received April 14, 1998)

In the 1950's Hanbury Brown and Twiss showed that one could measure the angular sizes of astronomical radio sources and stars from correlations of signals received at two antennas.

Their surprising discovery that the correlation function of photon counts in quantum optics experiments has become a powerful tool for understanding the basic physics of matter and light in high energy collisions.



ELSEVIER

25 May 1995

Physics Letters B 351 (1995) 293-301

Bose-Einstein effects and W mass determinations

Leif Lönnblad, Torbjörn Sjöstrand¹
Theory Division, CERN, CH-1211 Geneva 23, Switzerland

Received 30 January 1995
Editor: R. Gatto

Abstract

In $e^+e^- \rightarrow W^+W^- \rightarrow q\bar{q}_1 q\bar{q}_2$ events at LEP 2, the two W decay vertices are much closer to each other than typical hadronization distances. Therefore the Bose-Einstein effects, associated with the production of identical bosons (mainly pions), may provide a 'cross-talk' between the W^+ and the W^- decay products. If so, the observable W masses are likely to be affected. We develop algorithms for the inclusion of Bose-Einstein effects in multi-hadronic events. In this way we can study potential uncertainties in the W mass determination. In some scenarios the effects are significant, so that this source of uncertainty cannot be neglected.

TWO-PARTICLE CORRELATIONS IN RELATIVISTIC HEAVY-ION COLLISIONS

Ulrich Heinz

Theory Division, CERN, CH-1211 Geneva 23, Switzerland;

e-mail: ulrich.heinz@cern.ch, and Institut für Theoretische Physik, Universität Regensburg, D-93040 Regensburg, Germany

Barbara V. Jacak

Department of Physics, State University of New York at Stony Brook, Stony Brook, New York 11794; e-mail: jacak@skipper.physics.sunysb.edu

Key Words Hanbury Brown-Twiss interferometry, Bose-Einstein correlations, collective expansion, source size/lifetimes

■ **Abstract** Two-particle momentum correlations between pairs of identical particles produced in relativistic heavy ion collisions.

Annu. Rev. Nucl. Part. Sci. 2005. 55:537-402
doi: 10.1146/annurev.nucl.55.090704.151533
Copyright © 2005 by Annual Reviews. All rights reserved

FEMTOSCOPY IN RELATIVISTIC HEAVY ION COLLISIONS: Two Decades of Progress

Michael Annan Lisa

Department of Physics, The Ohio State University, Columbus, Ohio 43210;
email: lisa@mps.ohio-state.edu

Scott Pratt

Department of Physics and Astronomy, Michigan State University, East Lansing, Michigan 48824; email: pratts@pa.msu.edu

Ron Soltz

N-Division, Livermore National Laboratory, 7000 East Avenue, Livermore, California 94550; email: soltz1@lnl.gov

Urs Wiedemann

Theory Division, CERN, Geneva, Switzerland; email: urs.wiedemann@cern.ch

Key Words HBT, intensity interferometry, heavy ion collisions, femtoscopy

■ **Abstract** Analyses of two-particle correlations have provided the chief means for determining spatio-temporal characteristics of relativistic heavy ion collisions. We discuss the theoretical formalism behind these studies and the experimental methods used in carrying them out. Recent results from RHIC are put into context in a systematic review of correlation measurements performed over the past two decades. The current understanding of these results is discussed in terms of model comparisons and overall trends.

Back to astronomy ...

Intensity interferometry

Pro: Time resolution of 10 ns, say, implies 3 m light travel time; no need for more accurate optics nor atmosphere.

Permitted error budget is ~meter, not ~wavelength of light!

Virtually immune to atmospheric turbulence!!

Con: Require high photometric precision, large flux collectors.

Method not pursued in astronomy since numerous large and widely spread telescopes have not been available.

GCT



SCT



LST



LST

SST-1M



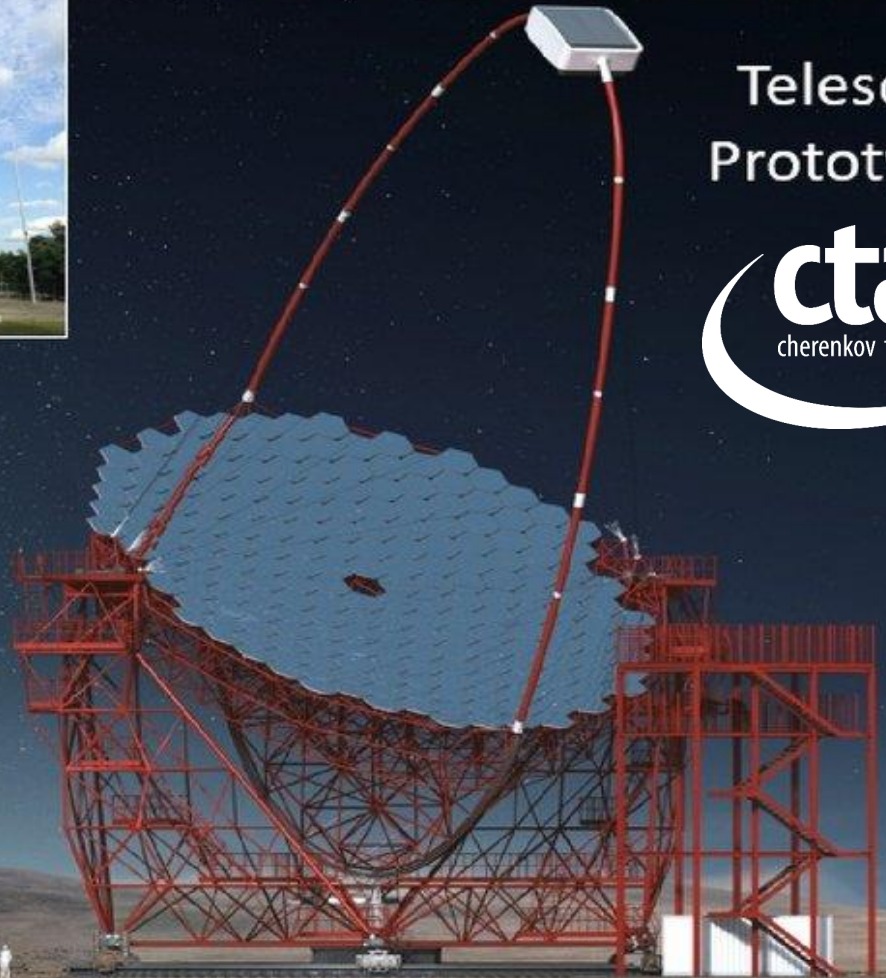
MST



Telescope Prototypes



ASTRI



Proposed configurations of the Cherenkov Telescope Array

Image: G.Pérez, IAC

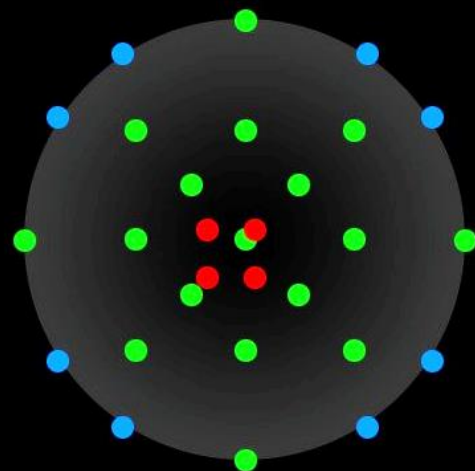
CTA - North

CTA - South

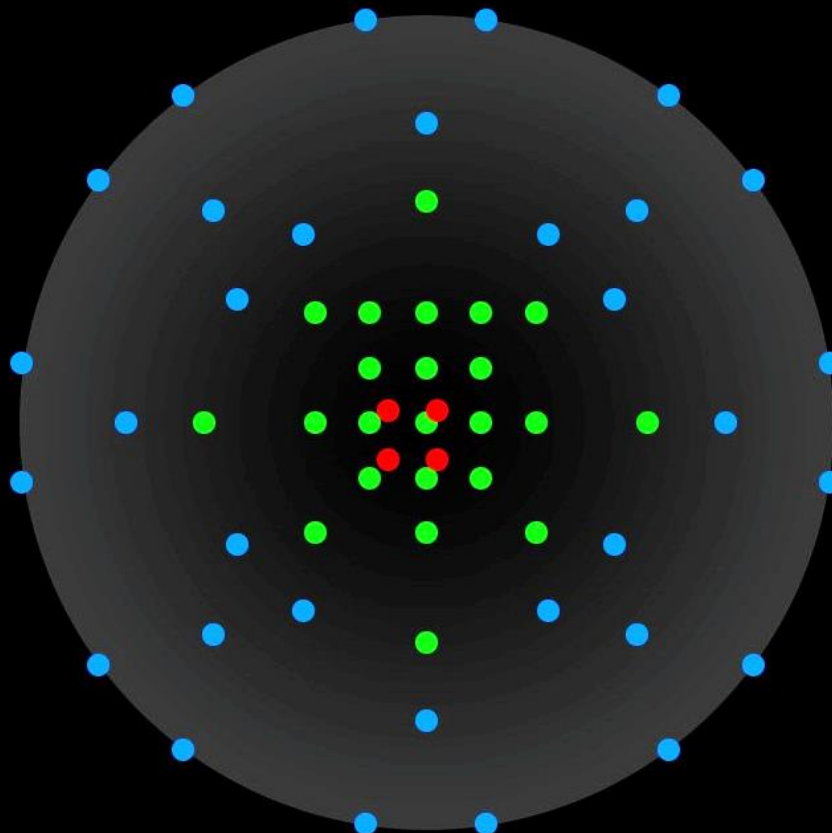
LST
24 m

MST
12 m

SST
6 m



1 km²



3 km²

Software telescopes in radio and the optical



LOFAR

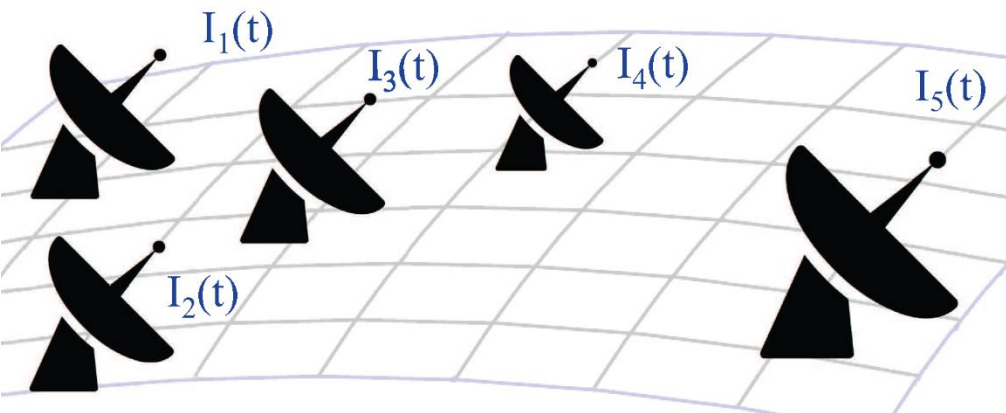


LOFAR low-band antennas at Onsala Space Observatory

Low-frequency radio waves, ~100 MHz

Many antennas, huge data flows.
Radio-wave amplitude sampled 12 bits deep.
Spectral resolution ~1 kHz, bandwidth 32 MHz.
Measures first-order coherence.
Large, central on-line data processing facility.

Optical Intensity Interferometer



Low-frequency optical fluctuations, ~100 MHz

Many telescopes, moderate data flows.
Photon counts recorded (1 bit).
Spectral resolution by optical filters.
Measures second-order coherence.
On-line or off-line data processing.

Laboratory & field experiments

Verify operation of an intensity interferometer; understand detector properties, issues in data handling



VERITAS telescopes at Basecamp, Arizona

Site of first full-scale tests of digital intensity interferometry

- * Digitally correlated pairs of 12-m telescopes*
- * Photon rates >30 MHz per telescope*
- * Real-time cross correlation, $\Delta t = 1.6$ ns*

(D.Dravins & S.LeBohec, Proc. SPIE 6986)





STAR BASE UTAH (near Salt Lake City)

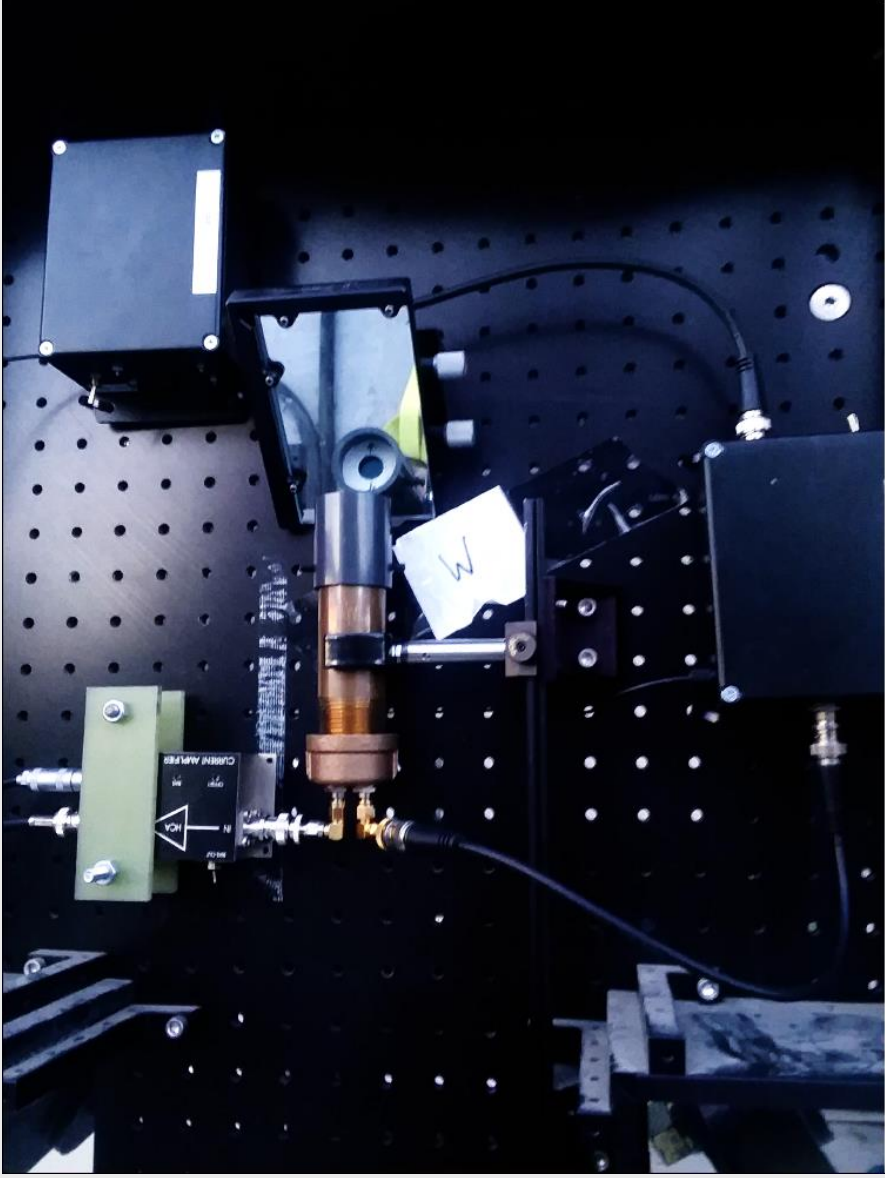
**Testbed for intensity interferometry
& Cherenkov telescope instrumentation**



The StarBase 3 m Cherenkov telescopes are protected by buildings which can be rolled open for observation. The control room is located between the two telescopes.

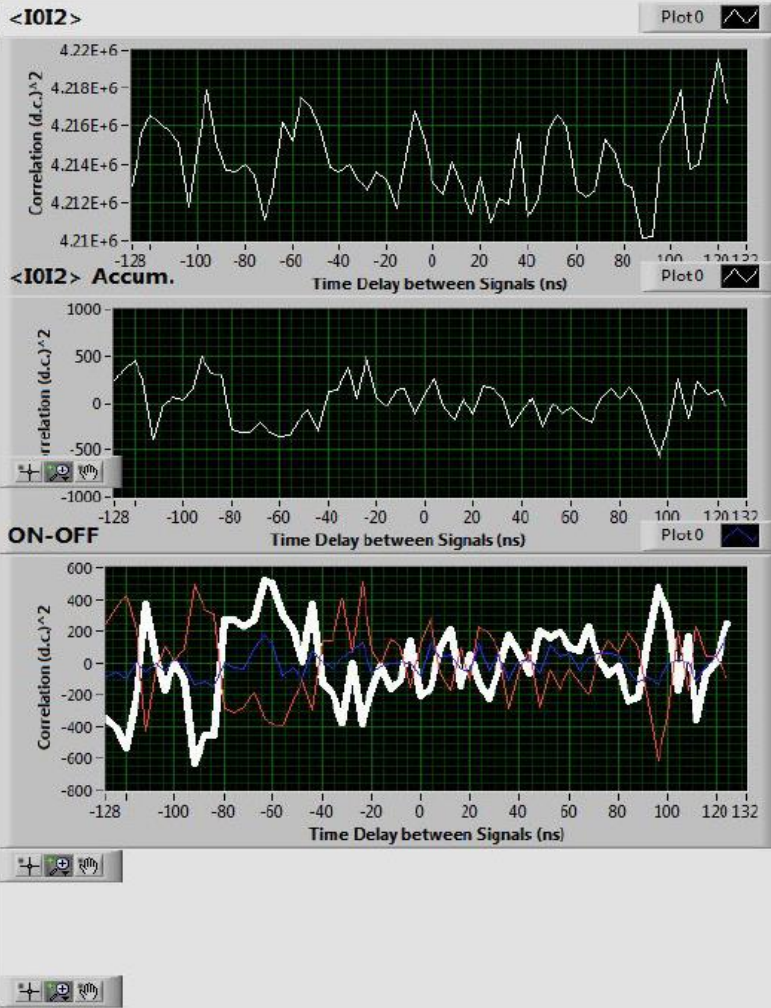
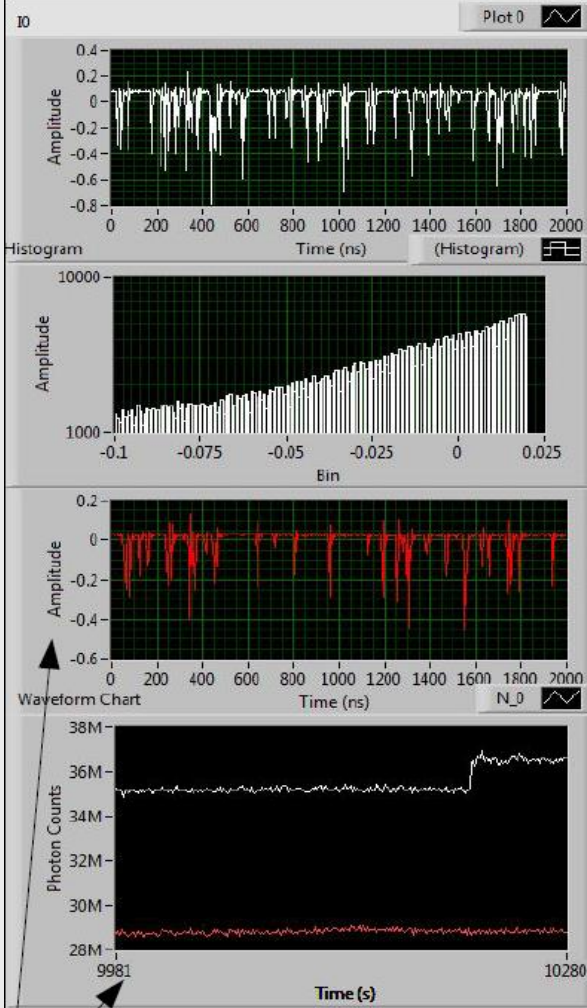
D.Dravins, S.LeBohec, H.Jensen, P.D.Nuñez:

Stellar Intensity Interferometry: Prospects for sub-milliarsecond optical imaging, New Astron. Rev. **56**, 143 (2012)



Left: One of the StarBase telescopes, having 19 hexagonal mirror facets with total diameter of 3 m. Right: Light is detected by the intensity interferometry camera consisting of a single PMT 'pixel'

N.Matthews, O.Clarke, S.Snow, S.LeBohec, D.Kieda
Implementation of an intensity interferometry system on the StarBase observatory
SPIE Proc. **10701**, 107010W (2018)



Run Control:

Run Type (ON/OFF) Recording

OFF

START RUN

STOP RUN

STOP CODE

Correlator Parameters:

Accumulator Reset Rate (sec): 1

Delay Channels: 64

of Correlation Inverals per run: 600

Discriminator Level CH0: -0.1

Discriminator Level CH2: -0.05

Use Discrim.?:

Monitoring:

FPGA Writes: 10281

Host Reads: 10281

FIFO Elements Remaining: 0

Configuration Error:

Stop SPI Loop:

A10 Counts: 36.590M

A12 Counts: 28.790M

-Display traces of both channels (segment of data)
 -Bottom left: photon rates over observation of Bellatrix

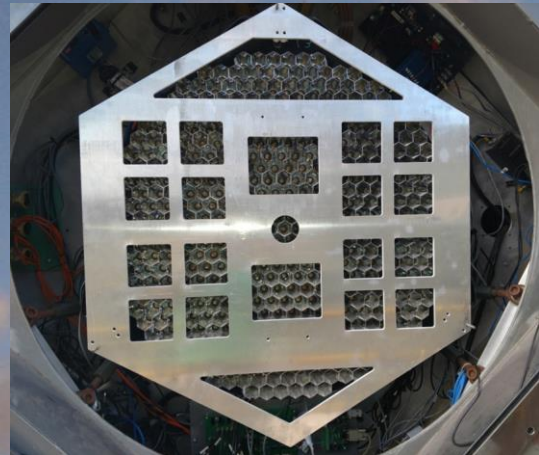
-Real-time correlation - $\Delta t = 4$ ns
 -Correlation saved to disk every second
 -Post-processing for ON/OFF subtraction + path delay compensation

Observing interface at StarBase during stellar observations

N.Matthews, O.Clarke, S.Snow, S.LeBohec, D.Kieda
 Implementation of an intensity interferometry system on the StarBase observatory
 SPIE Proc. **10701**, 107010W (2018)



VERITAS Cherenkov telescope on Mt. Hopkins, Arizona

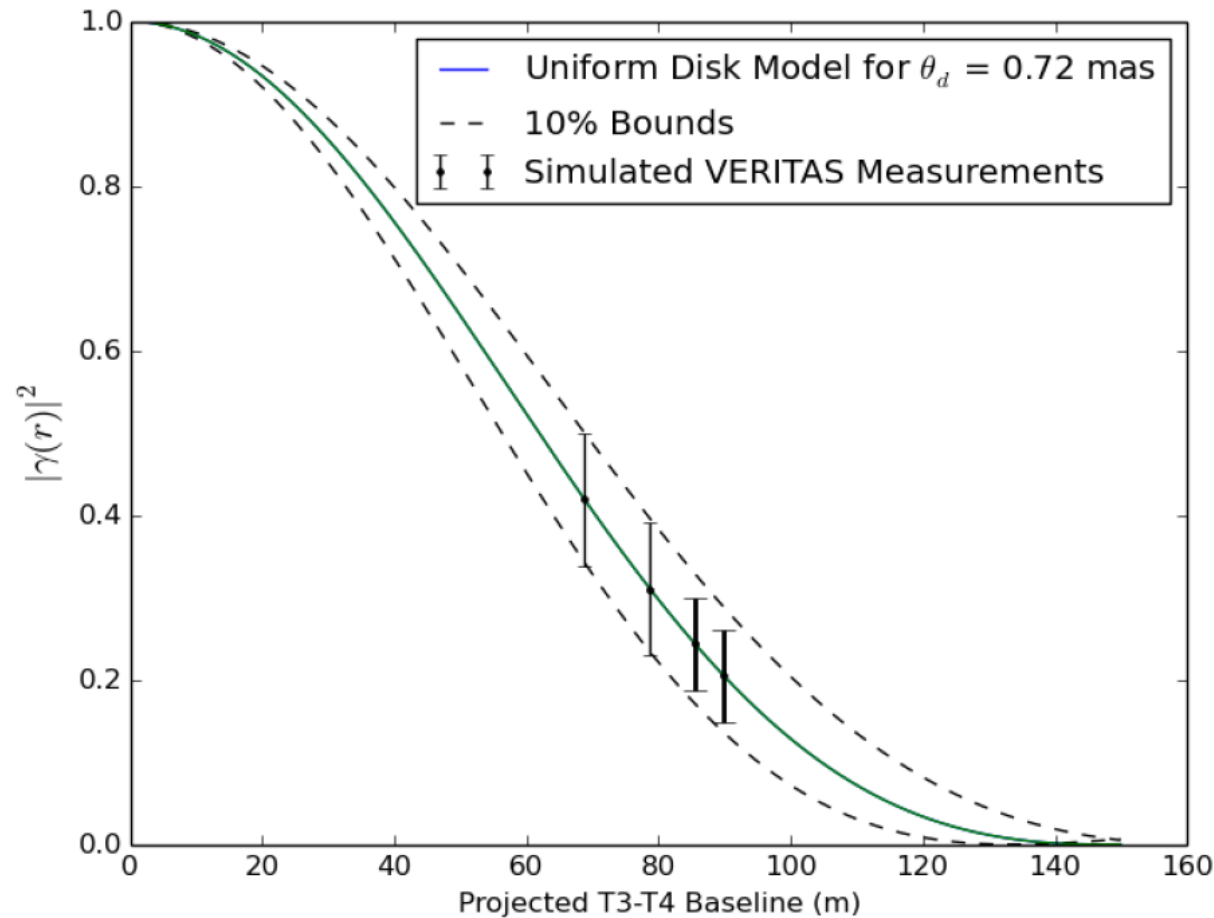


Camera baseplate for interferometry
(David Kieda, Univ. of Utah, Sept. 2018)





Initial Target Source – Bellatrix



-Simulations of a 6-hr observation of Bellatrix (gamma Orionis) about the meridian using T3-T4 telescopes.

-Solid line is model curve based on known angular diameter

-Dashed lines show curve +/- 10% of expected diameter (quick literature search shows something like 7% precision in current measurement)

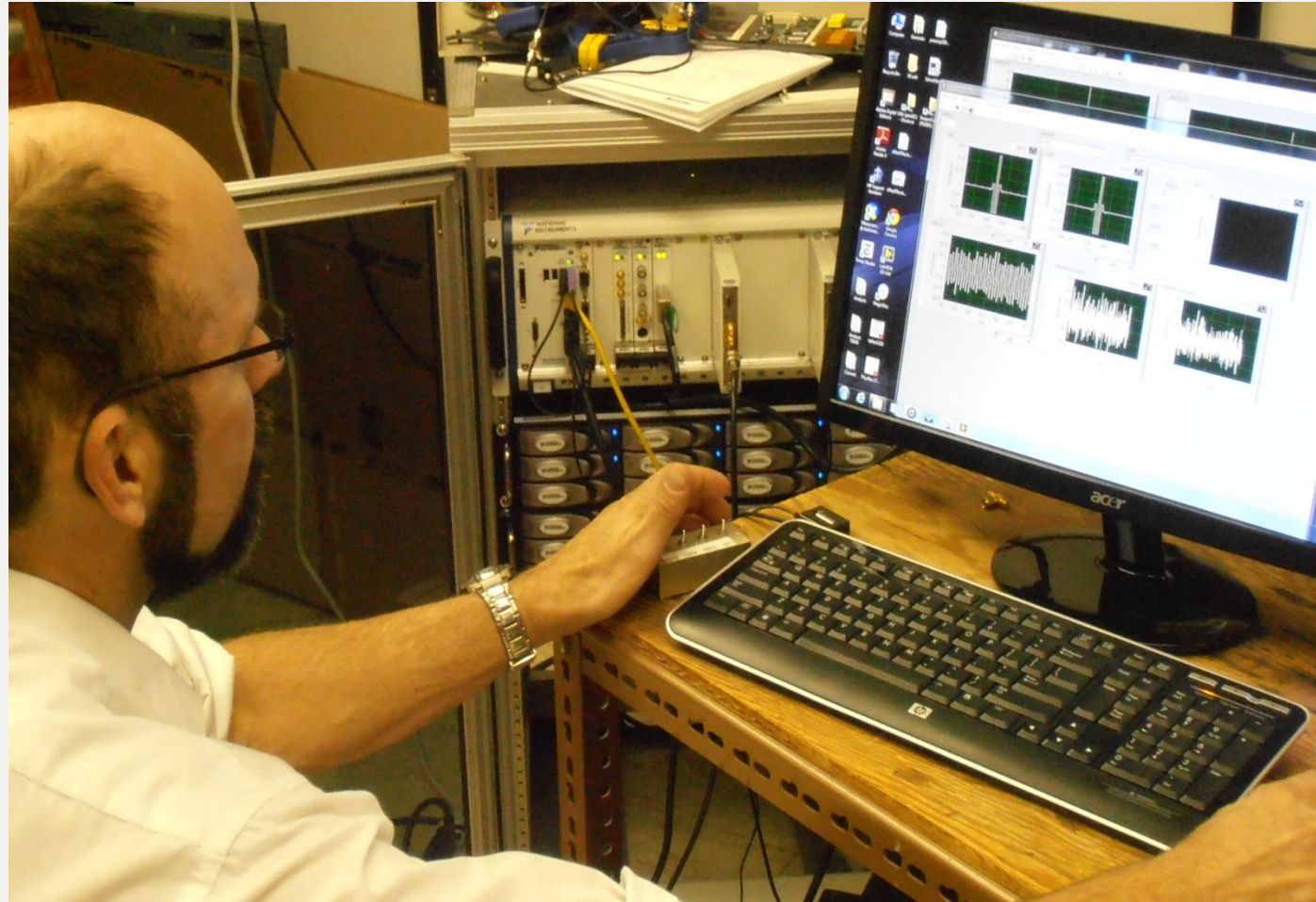
-Uncertainties estimated by scaling from StarBase count rate by mirror areas

→ Does not include systematics

→ Possible to observe earlier/later for shorter baseline coverage

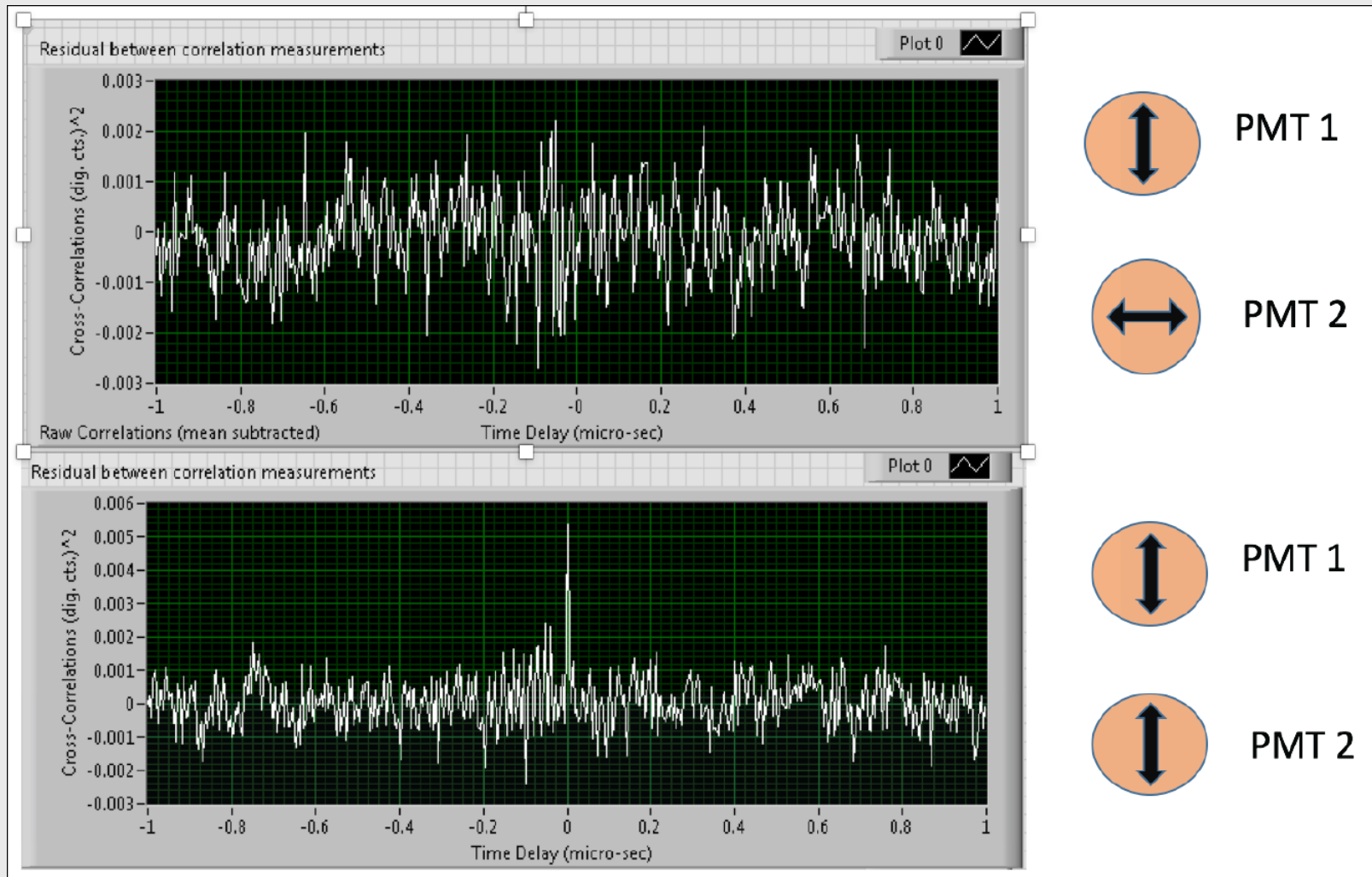
Stellar Intensity Interferometry

VERITAS upgrade & laboratory experiments @ The University of Utah



The ongoing VERITAS upgrade includes provisions also for intensity interferometry. Here, David Kieda examines correlation functions computed off-line in electronics for real-time digitization and storage of photomultiplier signals.

Intensity fluctuations in polarized light



Temporal coherence from a Hg arc lamp in the laboratory. Upper plot: Non-correlation with perpendicular polarizations. Lower: Observed 2-photon correlation with parallel polarizer configuration.

D.Kieda, N.Matthews

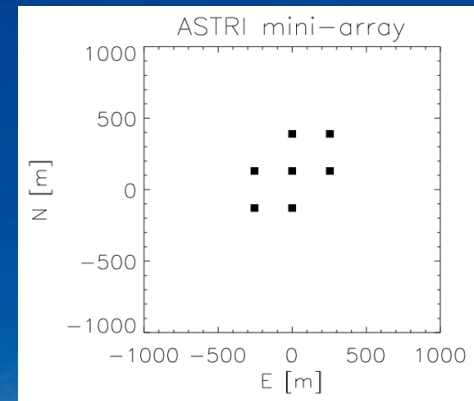
Stellar intensity interferometric capabilities of IACT arrays

Proc.Science, arXiv:1709.03956 (2017)

ASTRI* small-size telescope array

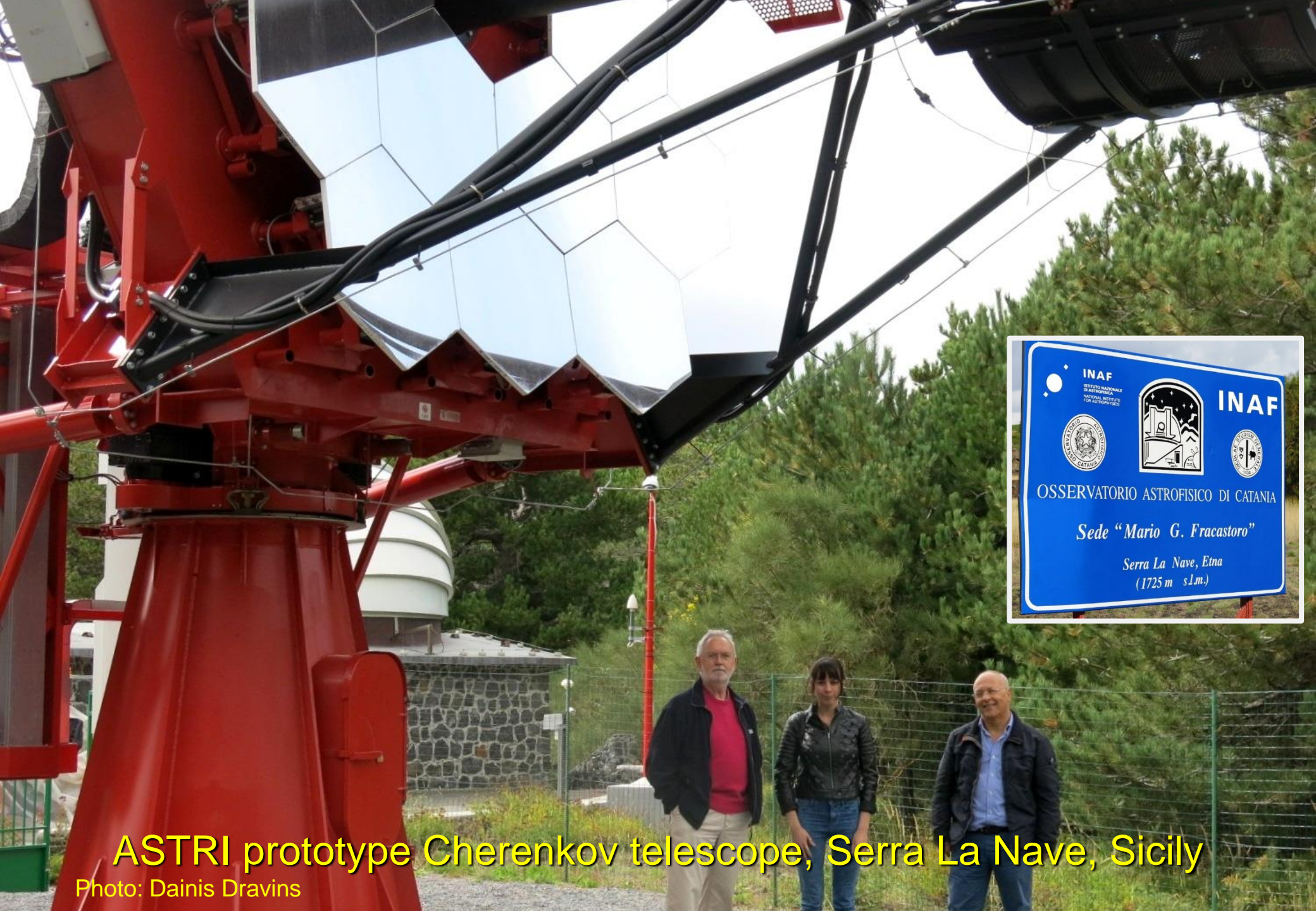
To be set up the CTA Southern site

Telescope spacing ~ 250 m (drawing here not to scale),
well suitable for intensity interferometry



**Astrofisica con Specchi a Tecnologia Replicante Italiana*

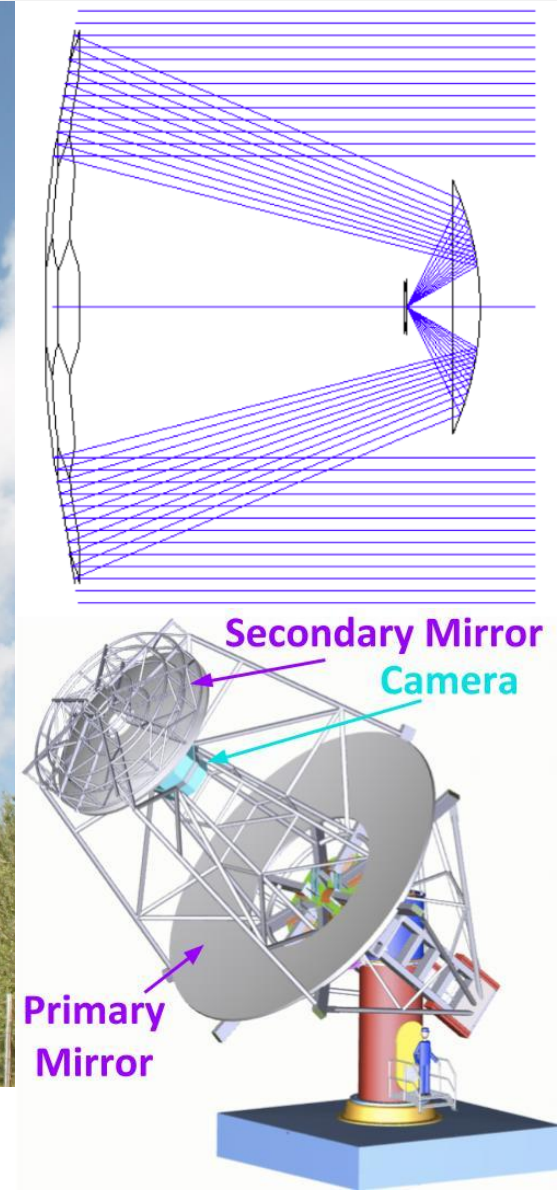
Luca Zampieri, Gabriele Rodeghiero, Giampiero Naletto, for the ASTRI collaboration



ASTRI prototype Cherenkov telescope, Serra La Nave, Sicily
Photo: Dainis Dravins

Schwarzschild-Couder air Cherenkov telescope

ASTRI project; inaugurated at *Serra La Nave* observatory on Sicily, 2014



First Schwarzschild-Couder telescope completed since its invention in 1905!
Very fast wide-field optics, $f/0.5$. Telescope diameter 4.3 m.

Schwarzschild-Couder: A wide-angle design

Astronomische Mittheilungen
der
Königlichen Sternwarte zu Göttingen.

Zehnter Theil.

Herausgegeben von
K. Schwarzschild,
Direktor der Sternwarte.

Untersuchungen zur geometrischen Optik. II.

Theorie der Spiegeltelescope.

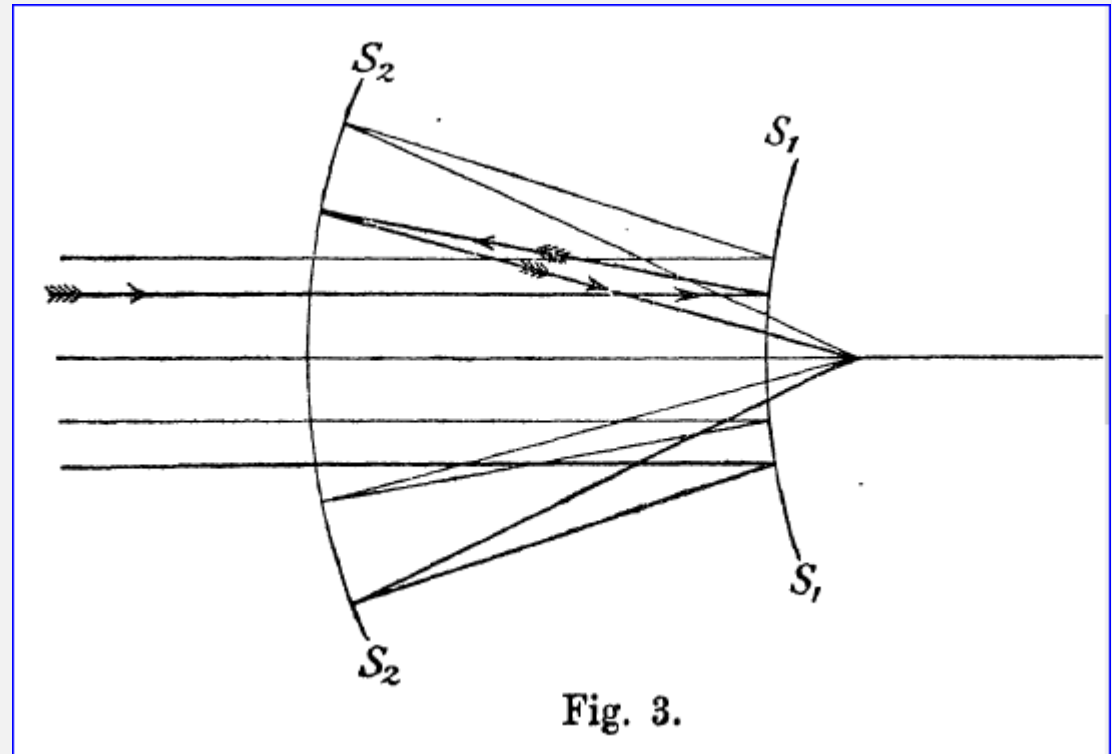
Von
K. Schwarzschild.

Mit 9 Figuren im Text.

(Aus den Abhandlungen der Königl. Gesellschaft der Wissenschaften zu Göttingen.
Mathematisch-physikalische Klasse. Neue Folge. Band IV. No. 2.)

Göttingen 1905.

Druck der Dieterich'schen Univ.-Buchdruckerei
(W. Fr. Kaestner).



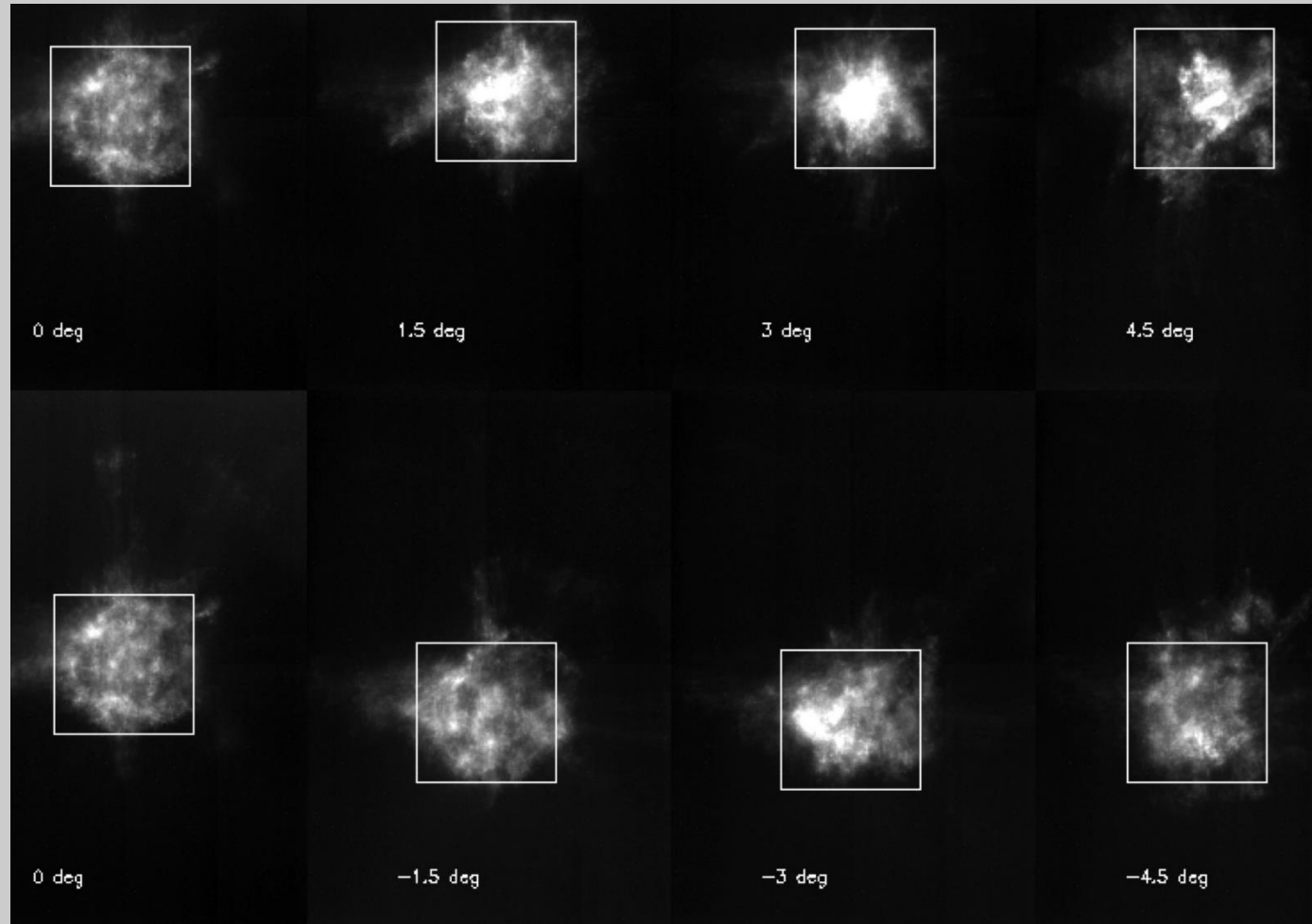
Karl Schwarzschild (1873-1916)



André Couder (1897-1979)

Basic concept proposed by Karl Schwarzschild in 1905; developed by André Couder.
Challenging optical polishing and alignment requirements; design overtaken by Schmidt telescopes.

ASTRI prototype
Cherenkov telescope,
Serra La Nave, Sicily

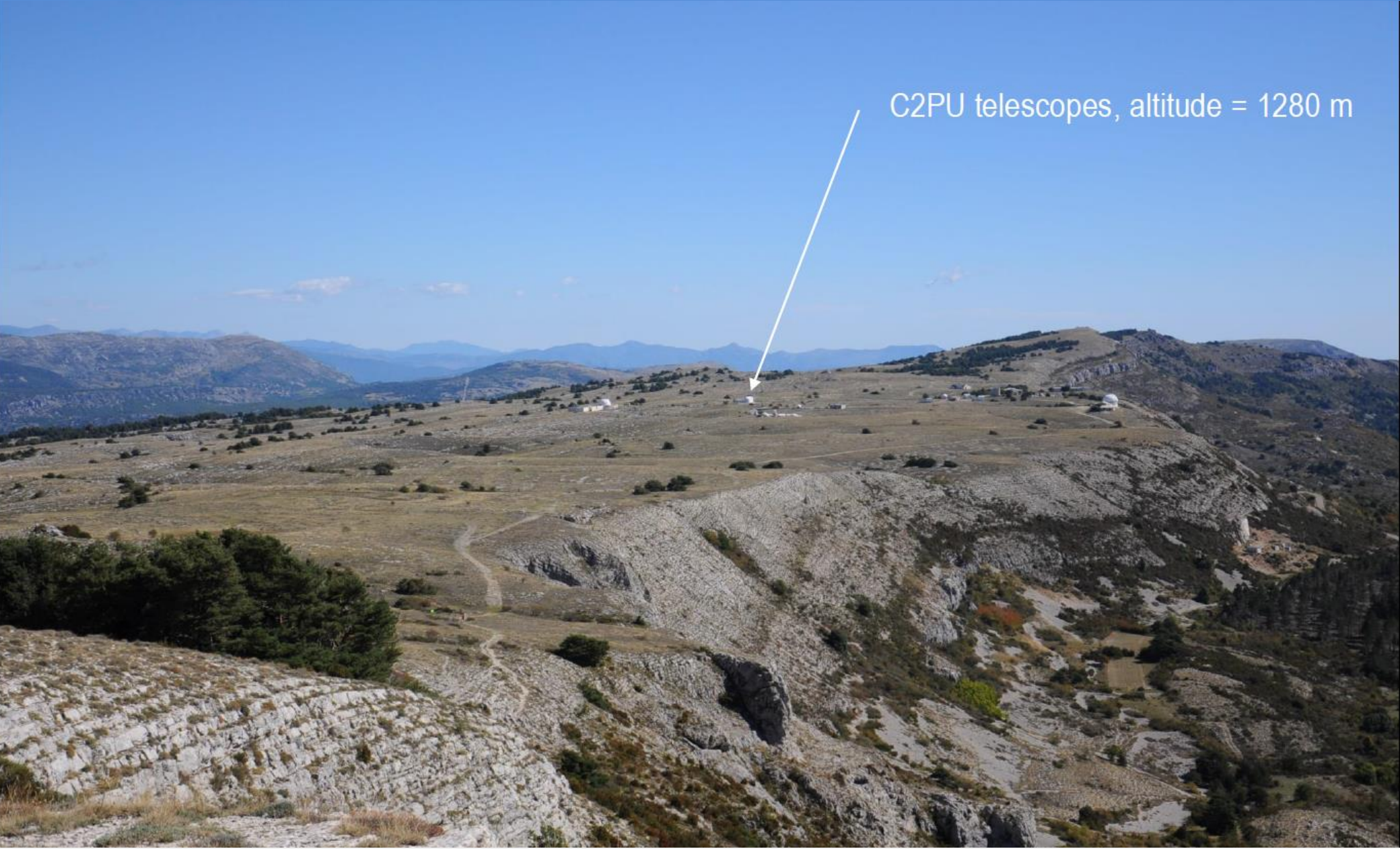


Observations of *Polaris* (Oct. 2016) demonstrate constant PSF over a wide 10-deg field

(E.Giro, R.Canestrari, S.Scuderi, G.Sironi, INAF Padova, Brera & Catania; www.cta-observatory.org)

Plateau de Calern, Observatoire de la Côte d'Azur

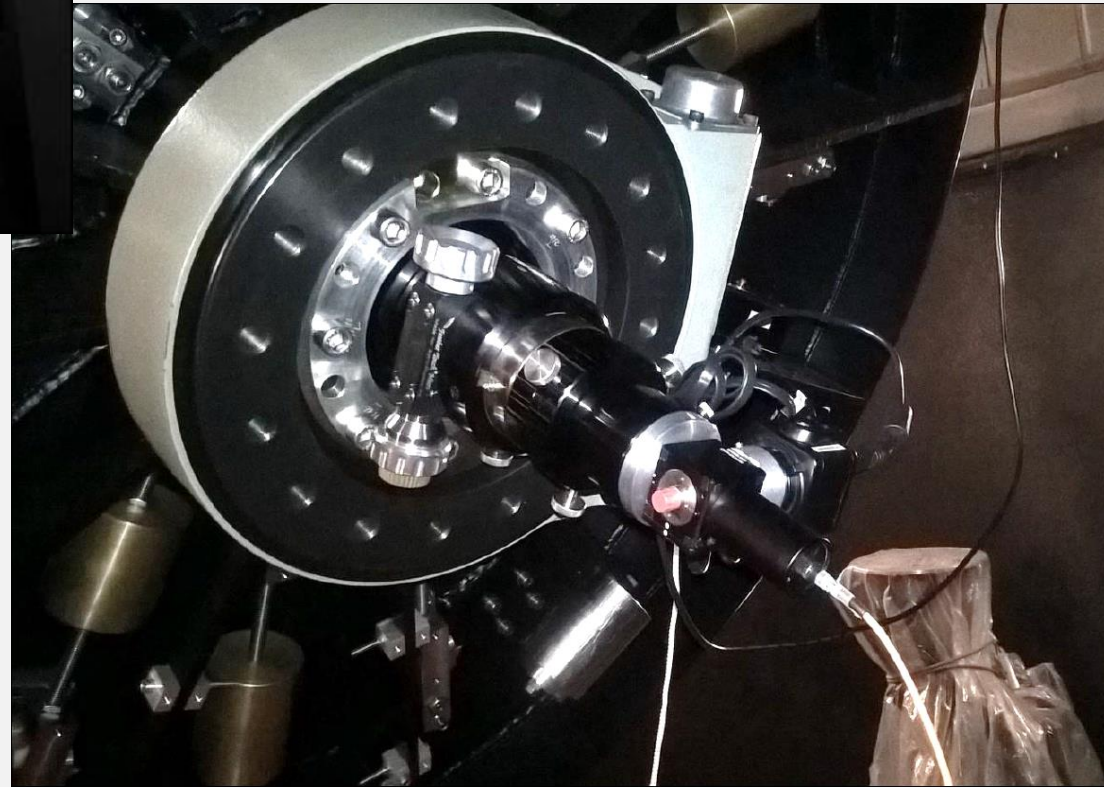
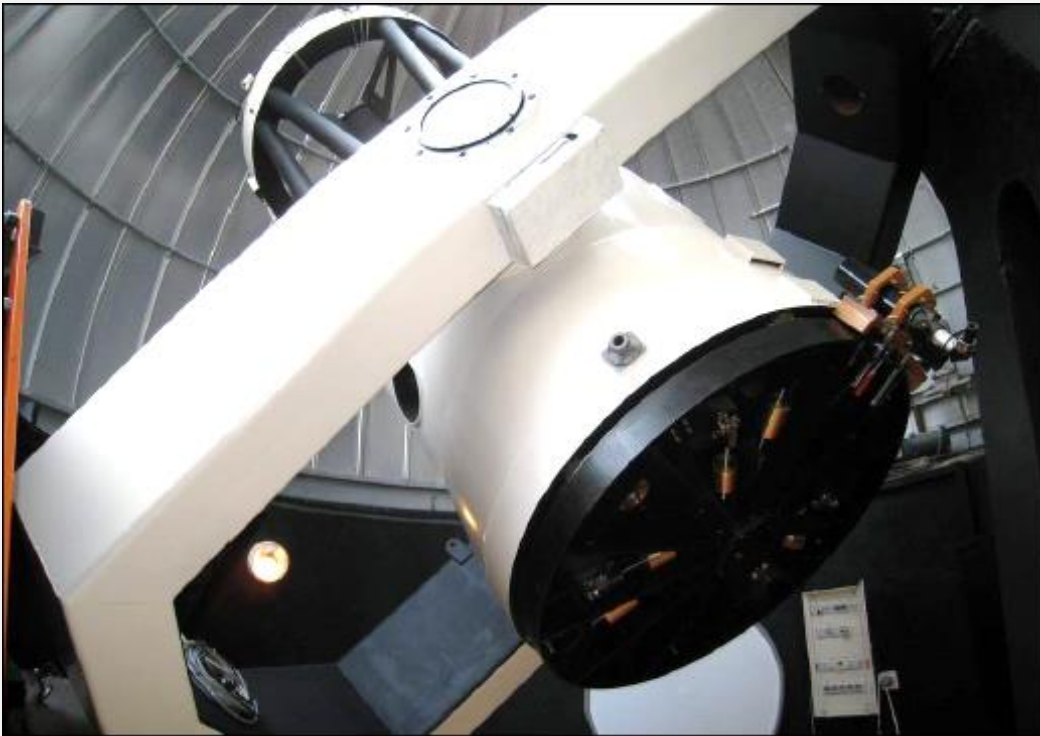
C2PU telescopes, altitude = 1280 m



Twin 1-m telescopes – *Omicron & Epsilon*, Plateau de Calern, Observatoire de la Côte d'Azur



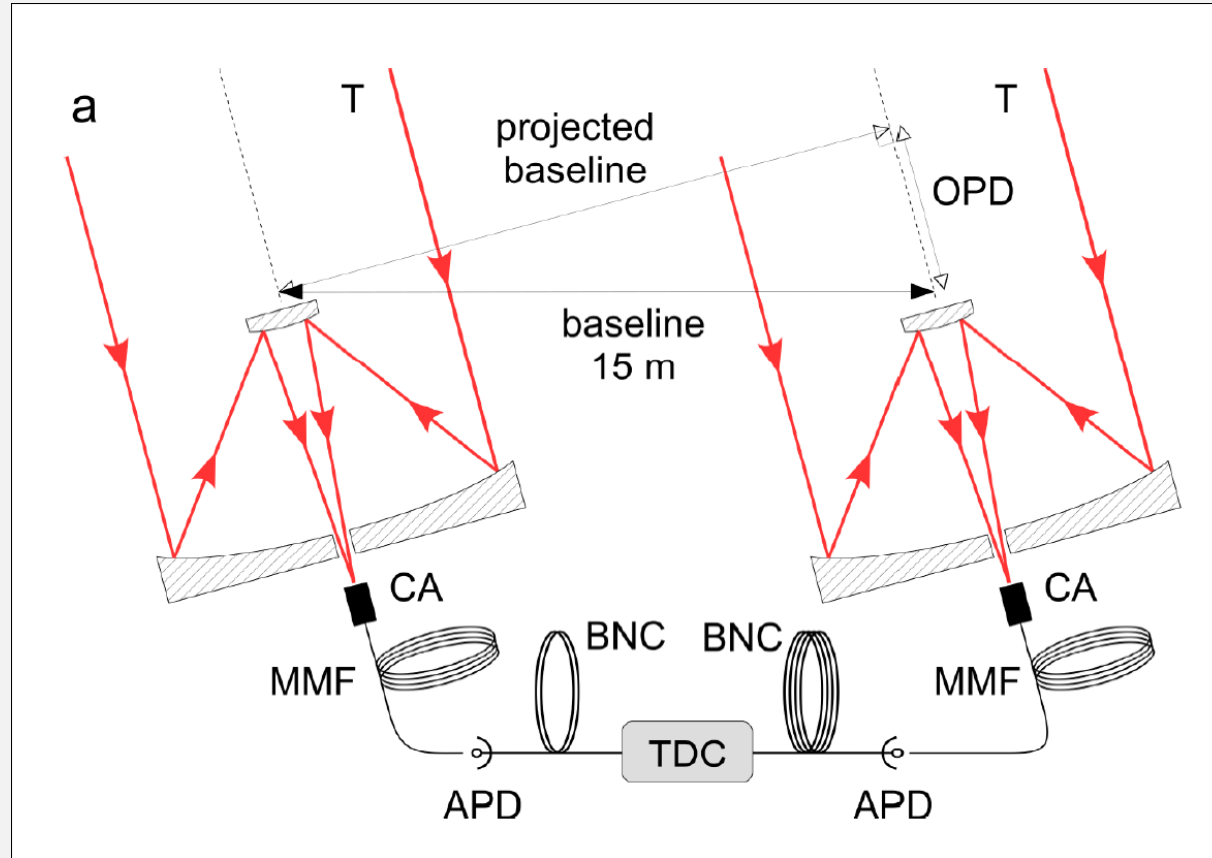
Setup at telescopes on Plateau de Calern



I2C Consortium –
Intensity Interferometry at Calern

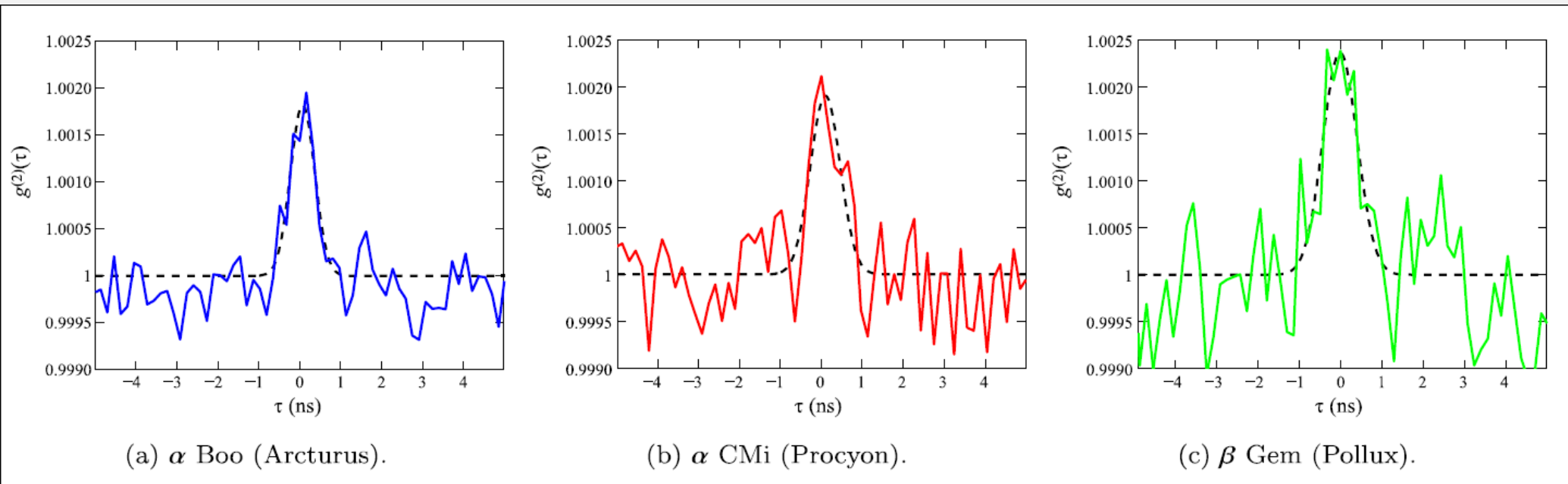
Institut de Physique de Nice (INPHYNI),
Université Côte d'Azur & CNRS

Measuring stellar intensity correlations between 1-m telescopes on Plateau de Calern



Starlight is collected by two 1-m telescopes and fed into multimode optical fibers (MMF) to an avalanche photodiode (APD), followed by a time-to-digital converter (TDC).

Photon bunching (intensity correlations) measured on one 1-m telescope

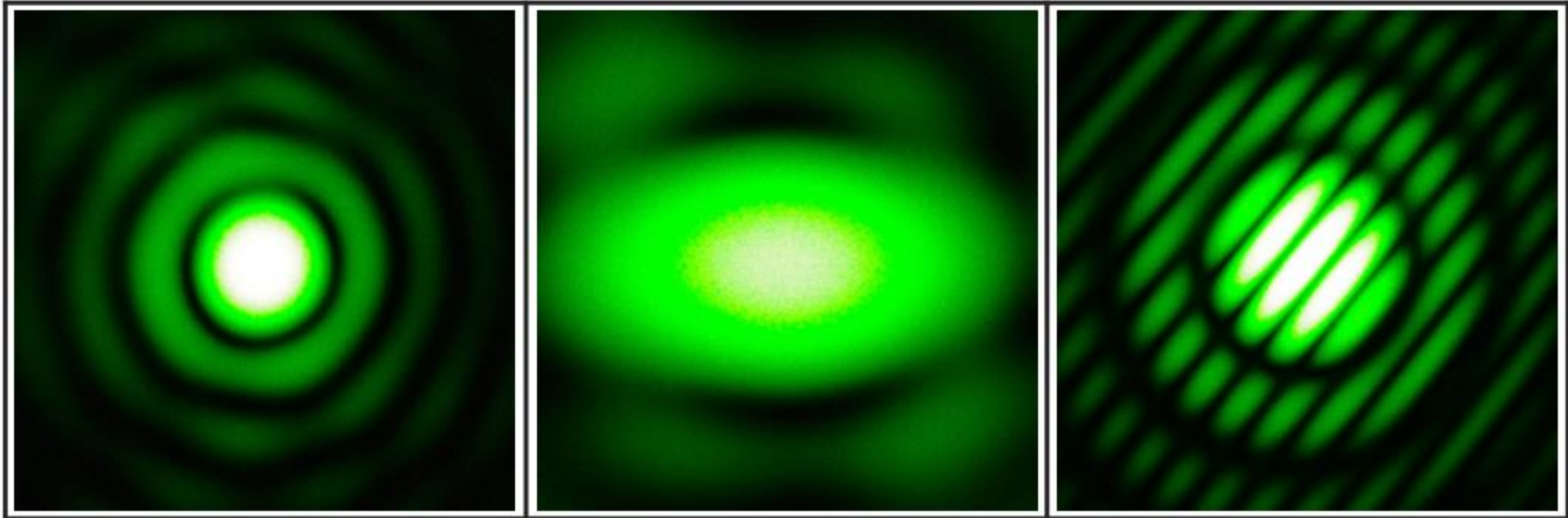


Temporal intensity correlation measured for three different stars. Gaussian fits are dashed.

Laboratory simulations

End-to-end operation of intensity interferometry in the laboratory: artificial stars; telescope array; photon-counting detectors; reconstructed images.

Artificial stars in laboratory intensity interferometer



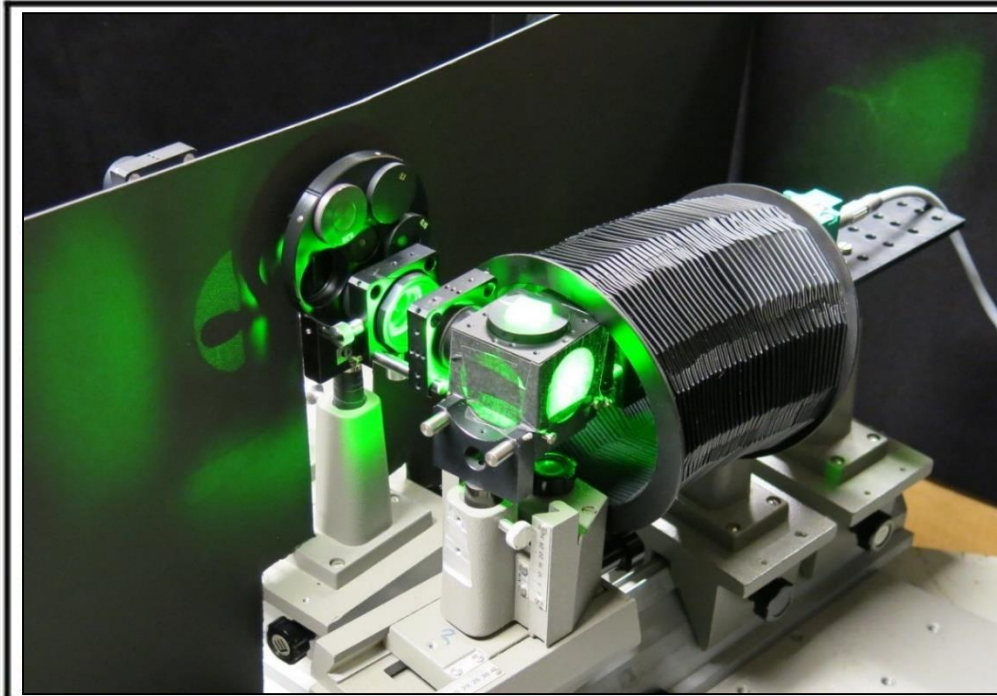
Diffraction patterns with laser light show the [squared] Fourier transforms of some artificial 'stars'. Circular single star; elliptic small single star; binary with equal components. Image widths correspond to ~70 cm in the telescope plane and such baselines are required to retrieve these patterns.

(D.Dravins, T.Lagadec, P.Nuñez, *Astron.Astrophys.* **580**, A99, 2015)

How to make an artificial star ?

S/N in intensity interferometry depends not only on instrumentation but also on the source brightness temperature

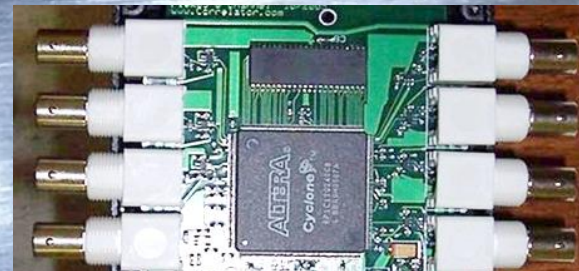
Laboratory Intensity Interferometer (Lund Observatory)



Left: Light from a 300 mW λ 532 nm laser is randomized through scattering against microscopic particles in a square-top cuvette and focused by a condenser onto artificial 'stars', being apertures in a rotatable holder. **Right:** The 'stars' are observed by an array of small telescopes, each with a photon-counting SPAD detector. 2-D coverage is achieved by rotating the asymmetric source relative to the plane of the telescopes.

(D.Dravins, T.Lagadec, P.Nuñez, *Astron.Astrophys.* **580**, A99, 2015)

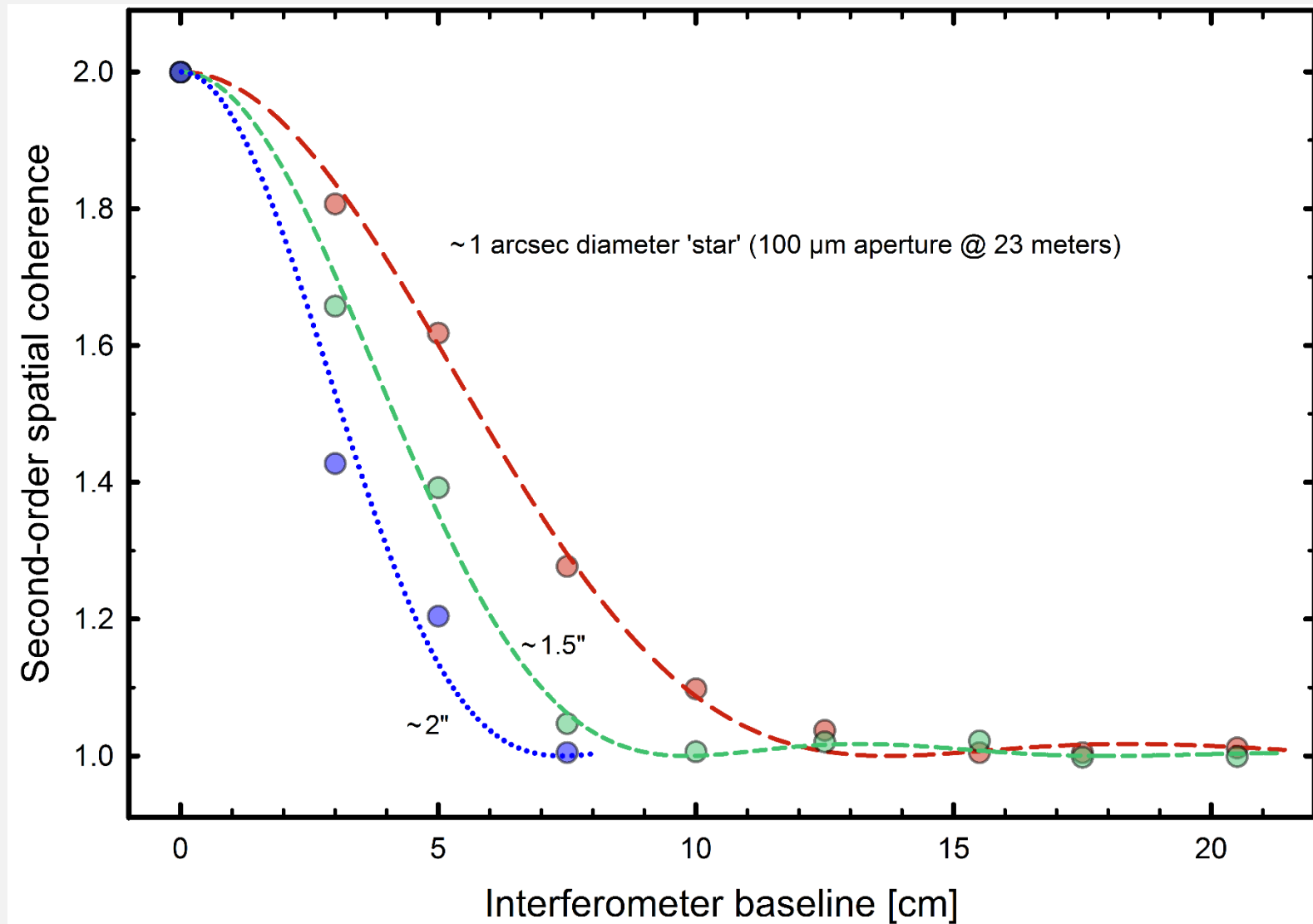
Intensity Interferometry correlator
Multi-channel, real-time, FPGA
32 channels ~20 k€



Very much more modest
computations than
in radio interferometry!

ALMA correlator
134 million processors

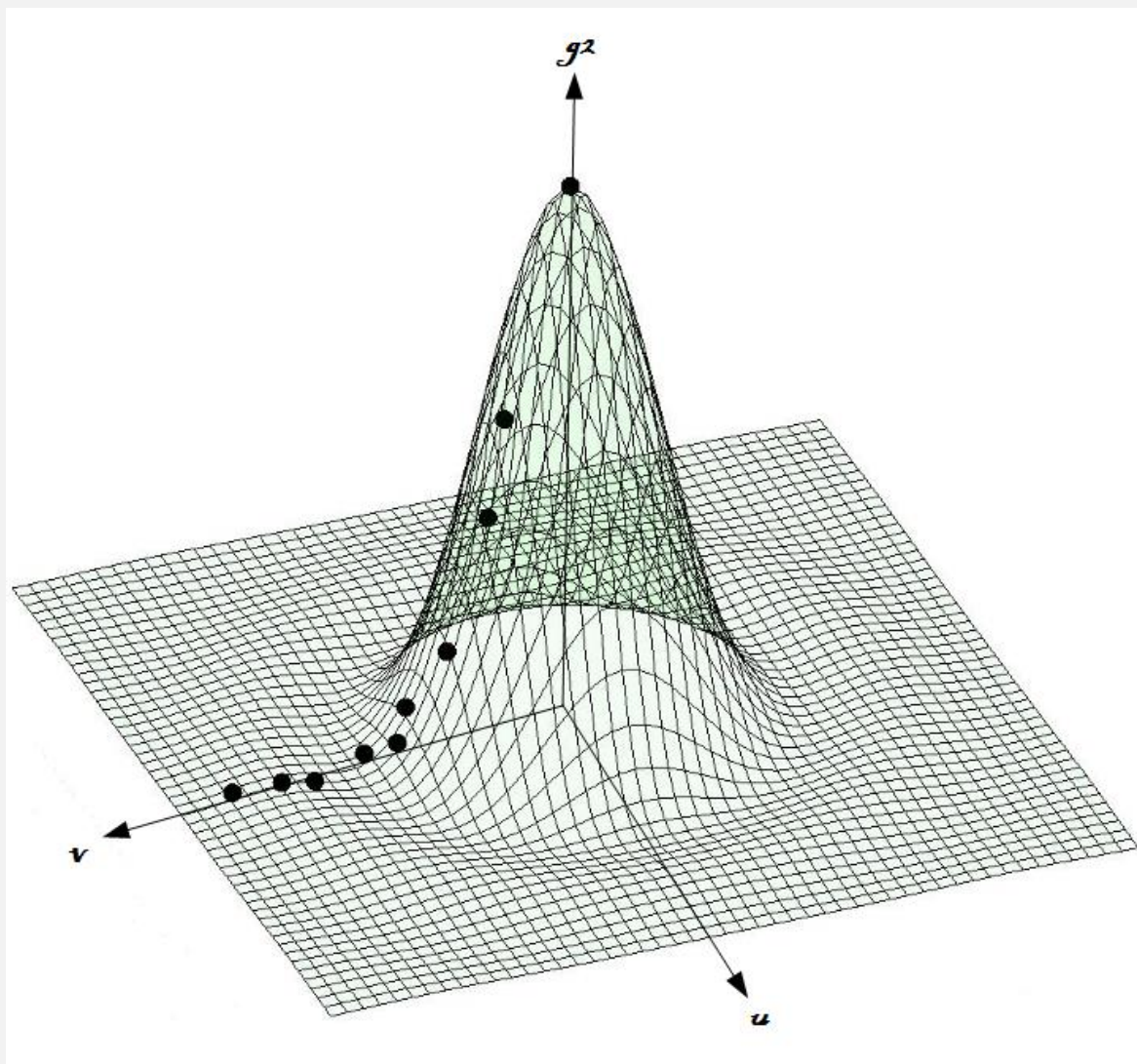
Laboratory intensity interferometry with few baselines



Second-order coherence $g(2)$ measured for artificial single stars of different angular sizes. Superposed are Airy functions for circular apertures (squared moduli of the Fourier transforms).

(D.Dravins, T.Lagadec, P.Nuñez, *Astron.Astrophys.* **580**, A99, 2015)

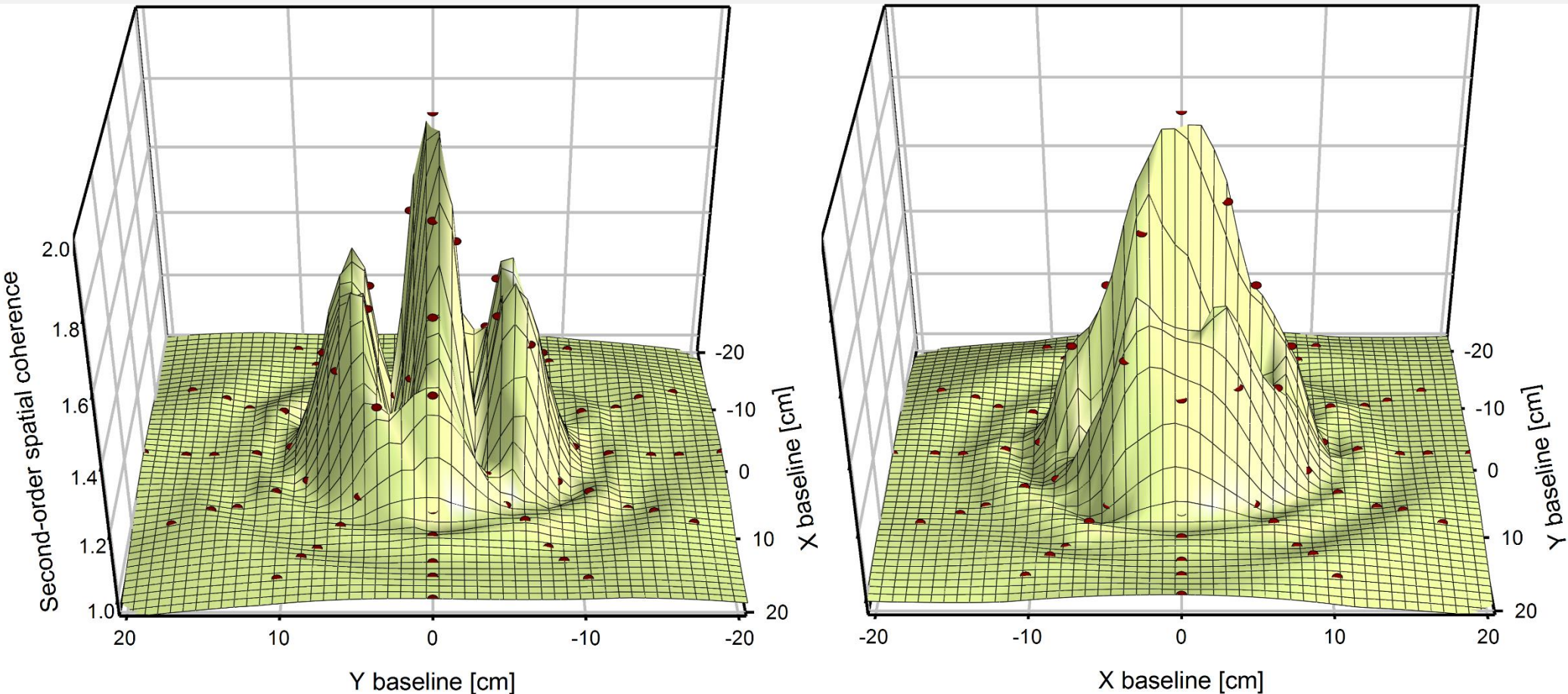
Laboratory intensity interferometry of single stars



One-dimensional coherence functions sample one particular position angle of the two-dimensional coherence surface, here a sequence of measured points on the surface for an idealized circular aperture.

(D.Dravins & T.Lagadec, Proc. SPIE **9146**, 2014)

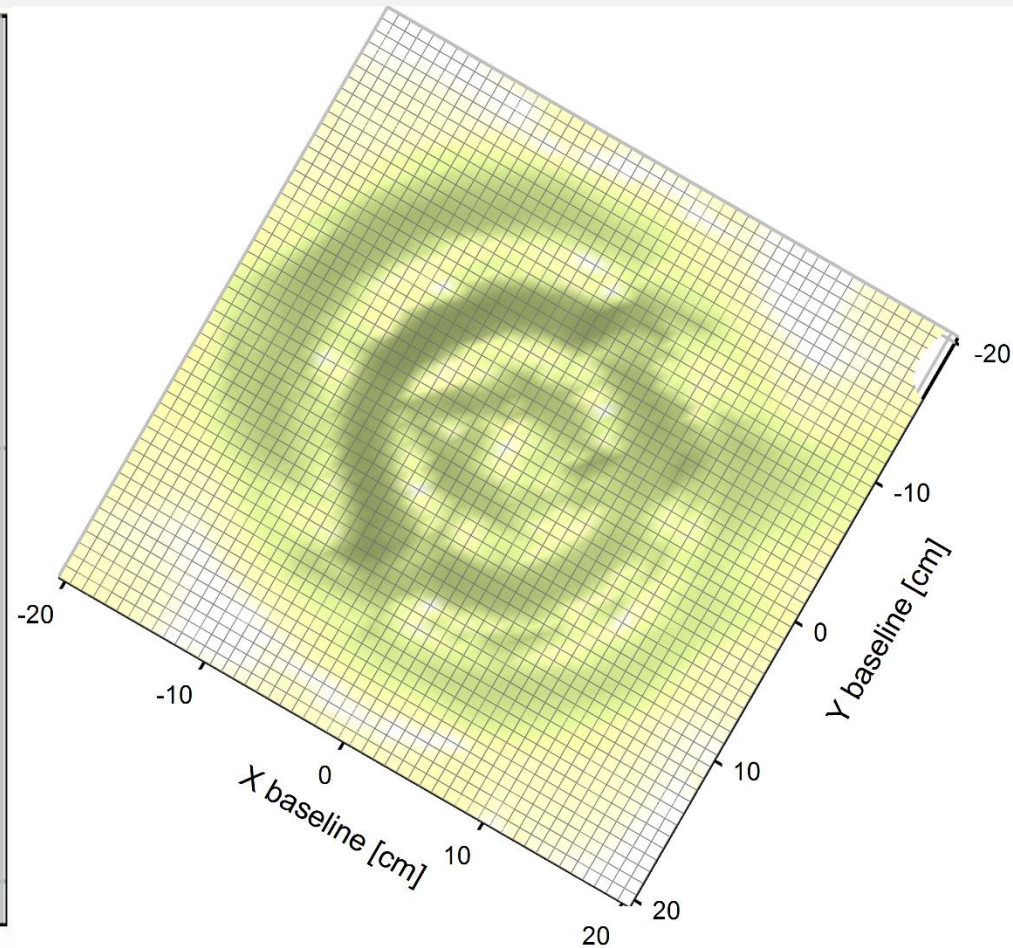
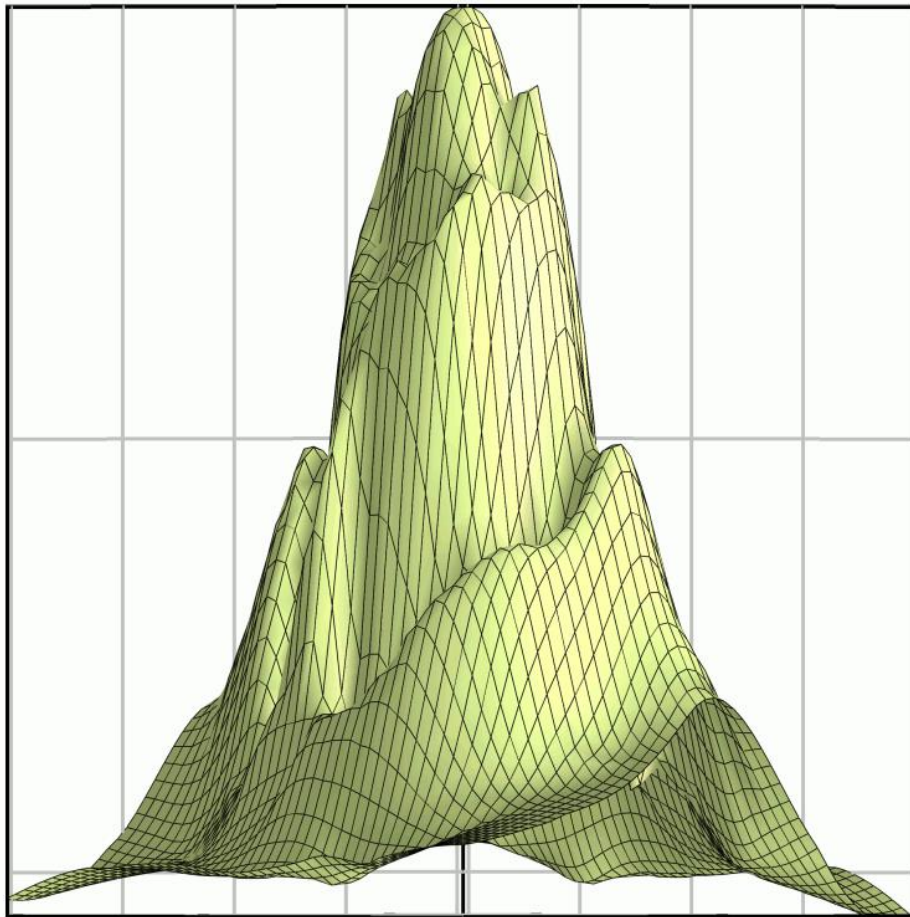
Laboratory intensity interferometry with many baselines



Second-order coherence $g(2)$ for an artificial binary star with each component of diameter ~ 1 arcsec.

This coherence surface was produced from intensity correlations measured across 60 different non-redundant baselines, illustrating how a telescope array fills in the interferometric plane. The central maxima (left) indicate the binary separation while the symmetric rings reveal the size of individual stars.

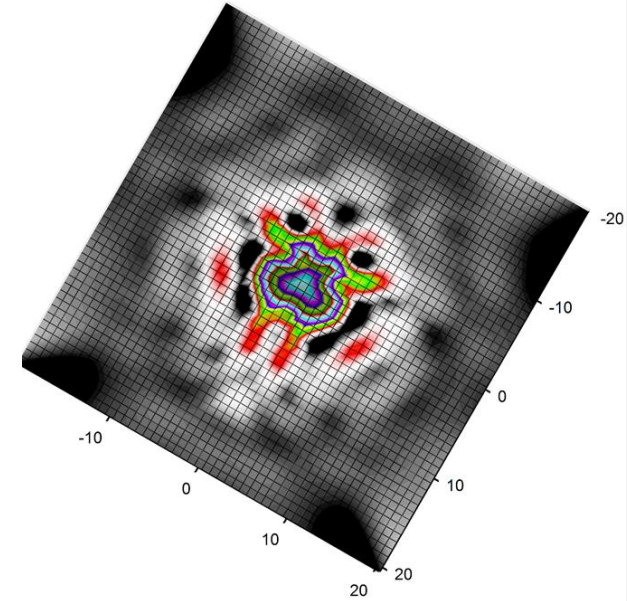
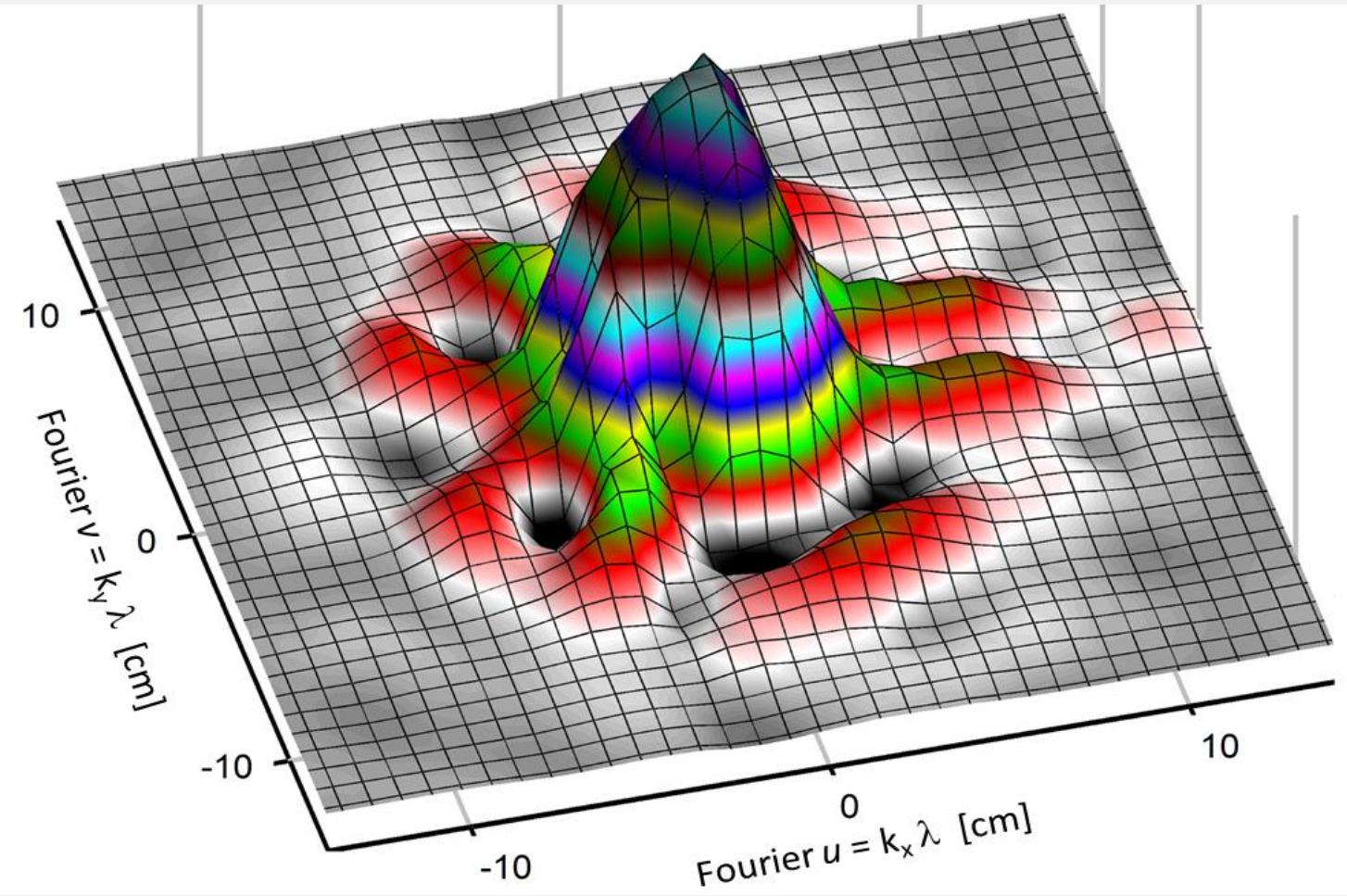
Laboratory intensity interferometry with 100 baselines



Intensity interferometry measurements with 100 different telescopic baselines. The data largely fill the interferometric (u,v) -plane of the second-order coherence $g(2)$ for an artificial star, somewhat irregular and elliptic, with angular extent just below 1 arcsecond. At right, the projection of the 3-D mesh is oriented straight down, showing [the modulus of] the source's Fourier transform ('diffraction pattern').

(D.Dravins & T.Lagadec, Proc. SPIE **9146**, 2014)

Laboratory intensity interferometry with 180 baselines



Measured second-order spatial coherence $g^{(2)}$ from intensity interferometry over 180 telescopic baselines. The source is an artificial binary star with differently large components. The structure corresponds to the pattern that would be produced by coherent light undergoing diffraction in a corresponding aperture.

(D.Dravins, T.Lagadec, P.Nuñez, *Astron.Astrophys.* **580**, A99, 2015)

Image reconstruction

Second-order coherence $g^{(2)}$

$$g^{(2)}(\tau) = 1 + |g^{(1)}(\tau)|^2$$

Does not retain phase information,
direct image reconstruction not possible.

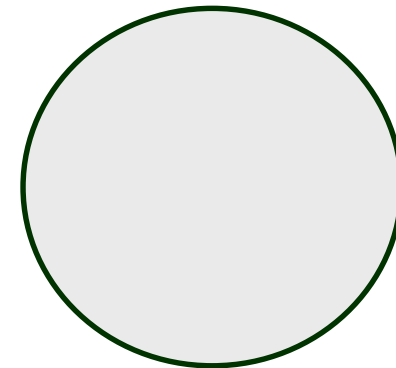
Imaging requires retrieval of
Fourier phases from amplitudes.

Feasible if dense coverage of (u,v)-plane

Image reconstruction from intensity interferometry

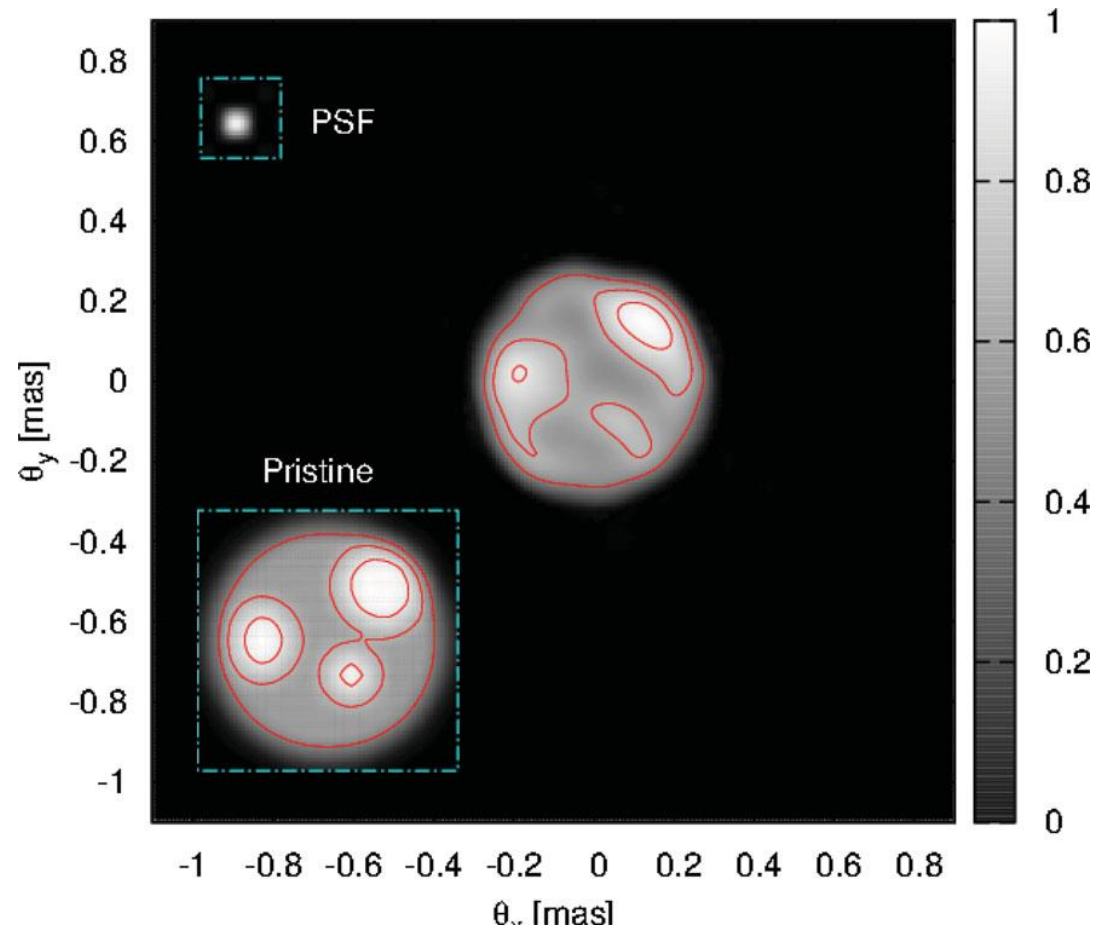


This Airy-disk diffraction pattern is immediately recognized as originating in a circular aperture, although only intensities are recorded.



Two-dimensional images can be reconstructed without phase information, provided two-dimensional coverage of the (u,v) -plane is available

Image reconstruction from intensity interferometry



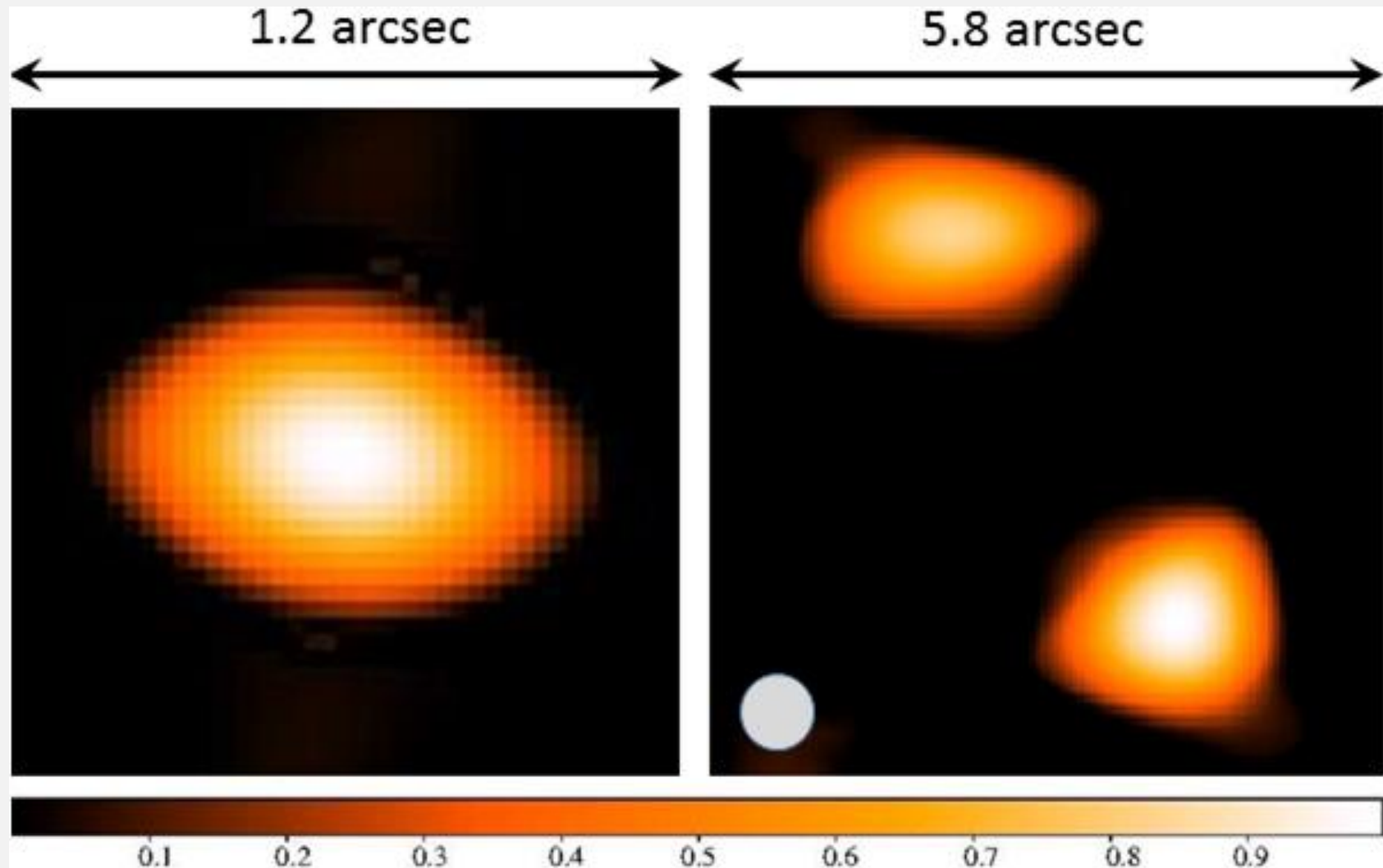
Numerical simulations of intensity-interferometry observations with a CTA-like array, with image reconstruction of a star with three hotspots

Pristine image has $T = 6000$ K; spots have 6500K (top-right and left) and 6800K.

Simulated data correspond to visual magnitude $m_v = 3$, and 10 hours of observation.

P.D.Nuñez, R.Holmes, D.Kieda, J.Rou, S.LeBohec, *Imaging submilliarcsecond stellar features with intensity interferometry using air Cherenkov telescope arrays*, MNRAS **424**, 1006 (2012)

Image reconstructions from intensity interferometry



Optical images reconstructed from intensity interferometry.
Measurements with 100 and 180 baselines, of an elliptical 'star', and a binary with brightness ratio 1:4.
(D.Dravins, T.Lagadec, P.D.Nuñez, *Nature Commun.* **6**, 6852, 2015)

1.2 arcsec

5.8 arcsec

**First diffraction-limited images
from an array of optical telescopes
with no optical connections between them**

... AS FAR AS WE ARE AWARE ...

0.1

0.2

0.3

0.4

0.5

0.6

0.7

0.8

0.9

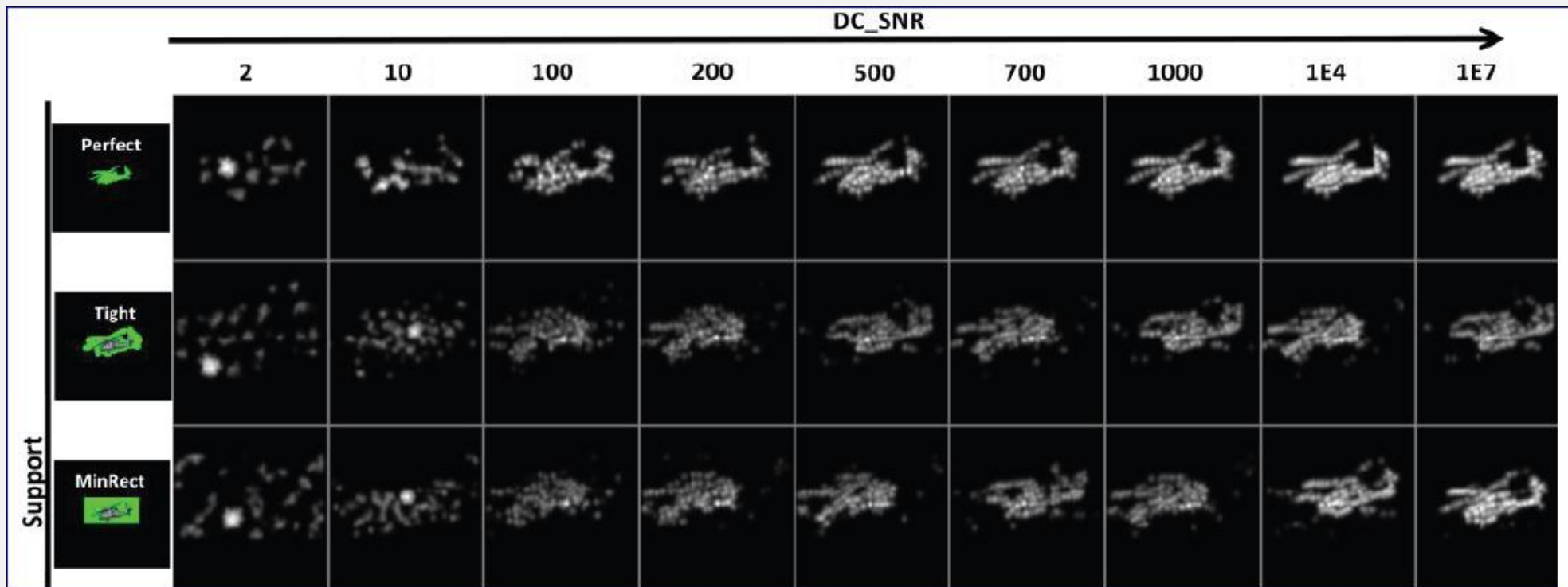
Cramér-Rao lower bound and object reconstruction performance evaluation for intensity interferometry

Jean J. Dolne^a, David R. Gerwe^b, and Peter N. Crabtree^c

^aBoeing Phantom Works, 5301 Bolsa Ave. H017-D728, Huntington Beach, CA 92647
(jean.j.dolne@boeing.com)

^bBoeing Phantom Works, 700 N. Sepulveda Blvd. S38-H320, El Segundo, CA 90245
(david.r.gerwe@boeing.com)

^cU.S. Air Force Research Laboratory, Space Vehicles Directorate,
3550 Aberdeen Ave. SE, Kirtland AFB, NM 87117



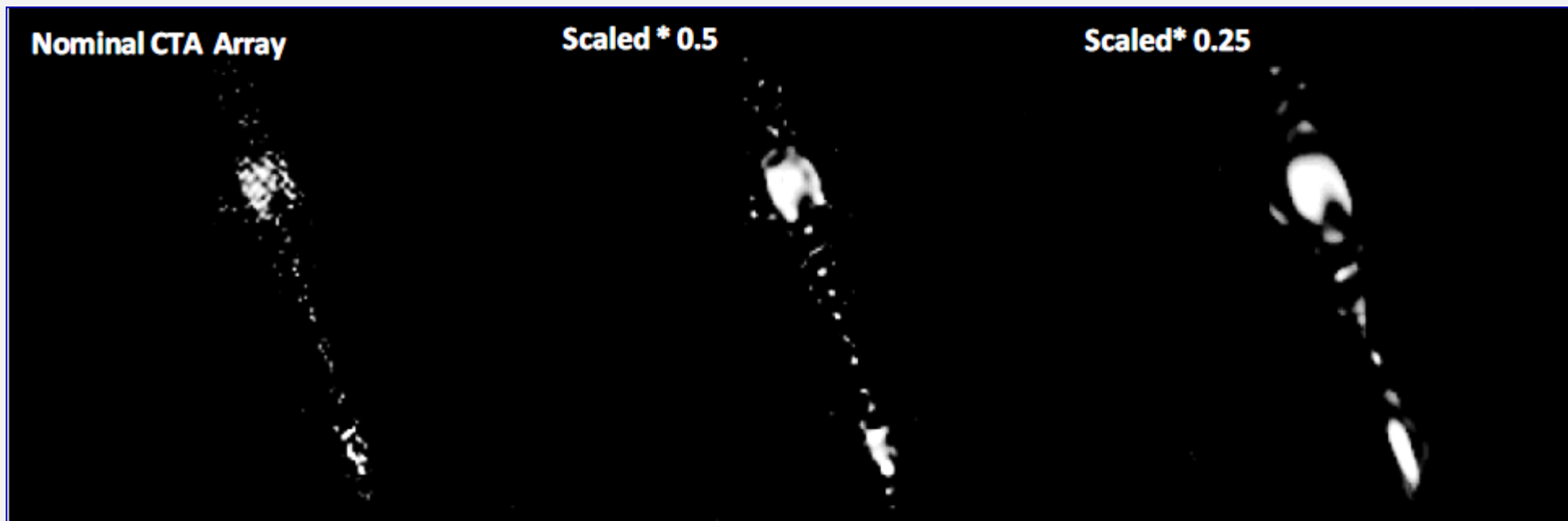


Image reconstruction of a geostationary satellite using a nominal CTA layout, and scaled versions

**Image Reconstruction from Sparse Irregular Intensity
Interferometry Measurements of Fourier Magnitude**

David R. Gerwe, J. J. Dolne

Boeing Phantomworks Space & Intelligence Systems

Peter N. Crabtree

United States Air Force Research Labs

Richard B. Holmes, Brandoch Calef

Boeing Laser and Technical Services

S/N in intensity interferometry

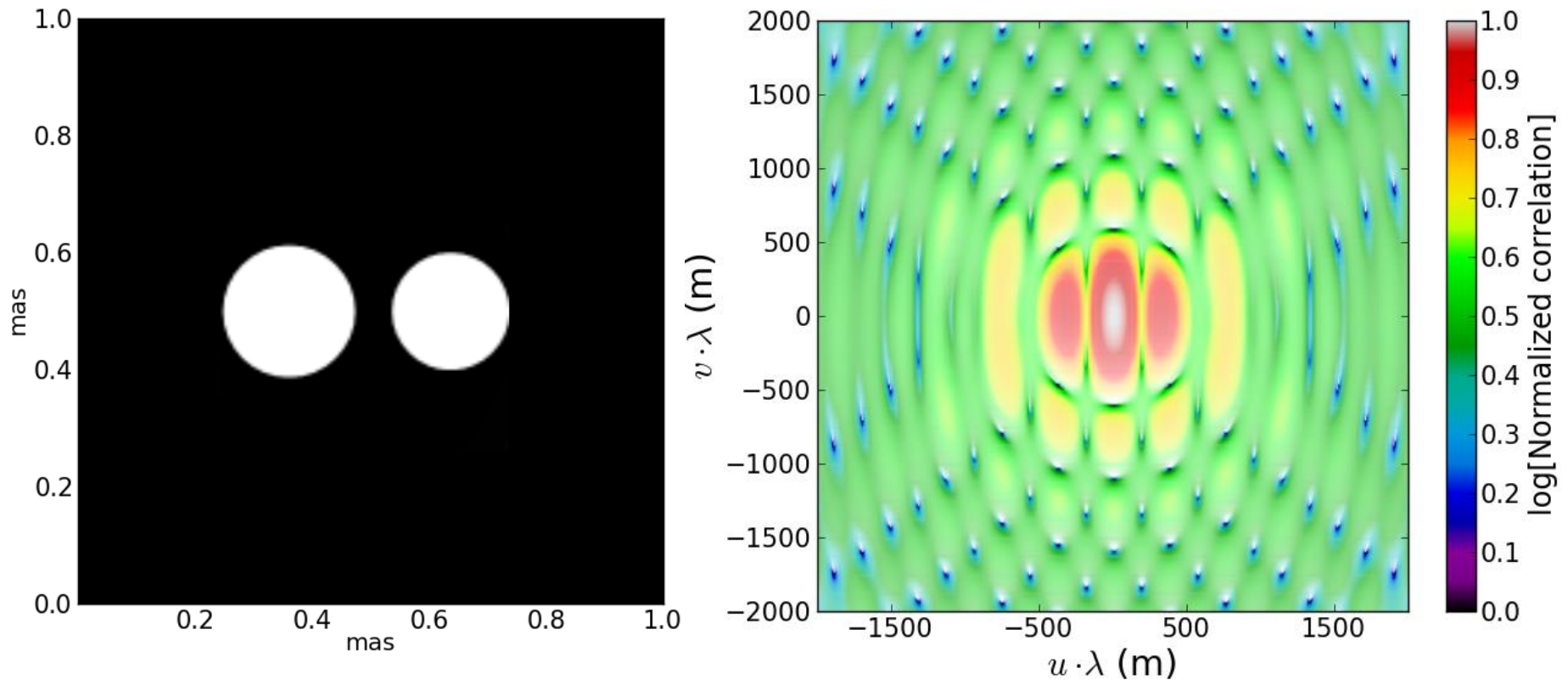
PROPORTIONAL TO:

- ★ **Telescope areas (geometric mean)**
- ★ **Detector quantum efficiency**
- ★ **Square root of integration time**
- ★ **Square root of electronic bandwidth**
- ★ **Photon flux per optical frequency bandwidth**

INDEPENDENT OF:

- ★ **Width of optical passband**

Simulated observations in intensity interferometry



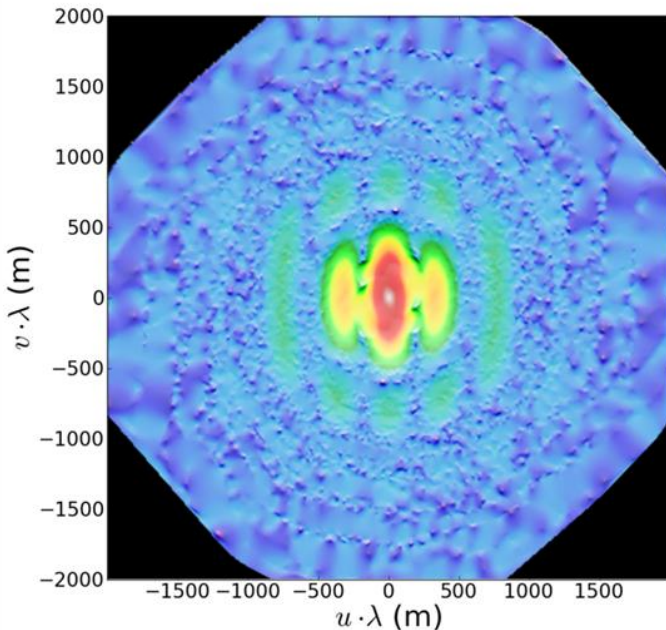
Squared visibility from a close binary star.

Left: Pristine image; Right: Logarithm of magnitude of Fourier transform

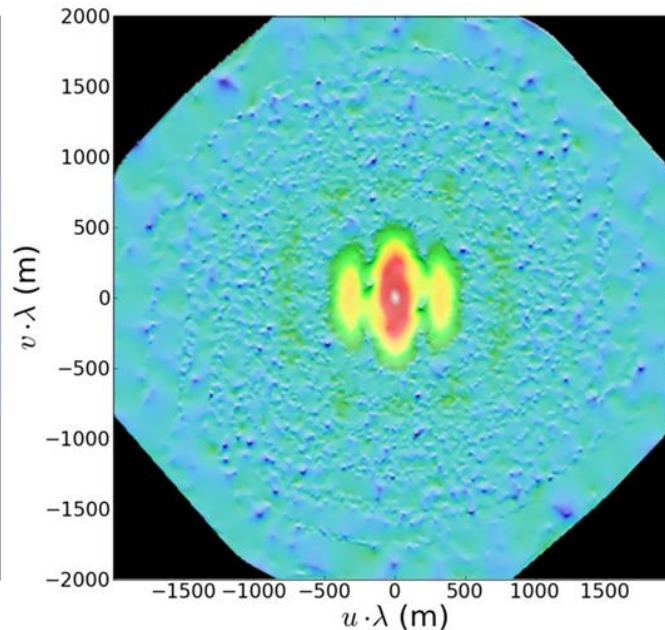
Simulated observations in intensity interferometry

Limiting magnitude for CTA with foreseen instrumentation

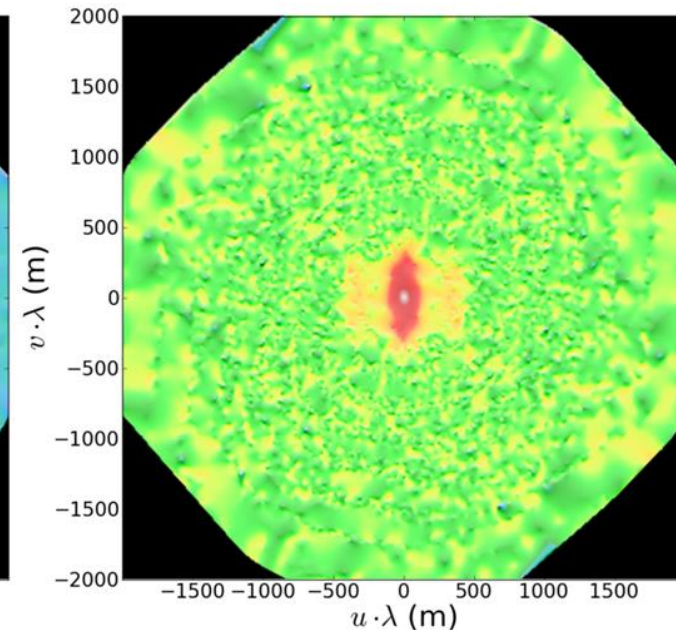
$m_v = 3$



$m_v = 5$



$m_v = 7$



Simulated observations of binary stars of visual magnitudes 3, 5, and 7.

Total integration time: 20 hours; λ 500 nm, time resolution 1 ns, quantum efficiency = 70%

Array: CTA D

D.Dravins, S.LeBohec, H.Jensen, P.D.Nuñez:

Stellar Intensity Interferometry: Prospects for sub-milliarcsecond optical imaging, New Astron. Rev. **56**, 143 (2012)

Limits to time resolution ?

Isochronous telescopes ?

**Parabolic or Schmidt better than
Davies-Cotton for $\Delta t < \text{few ns}$**

Cherenkov telescopes are usually Davies–Cotton or parabolic

In a Davies–Cotton layout, all reflector facets have same focal length f , arranged on a sphere of radius f .

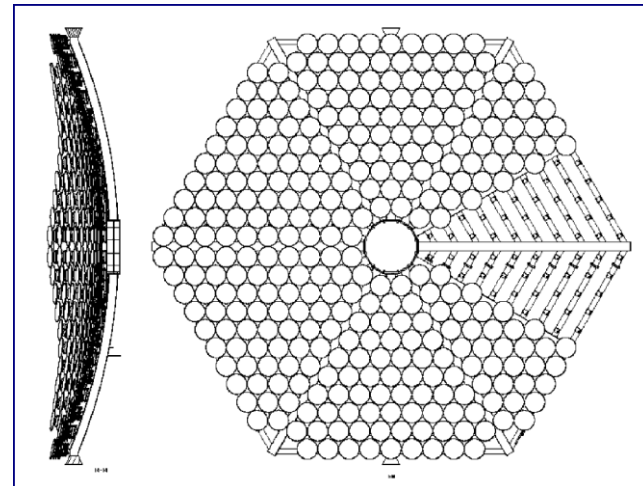
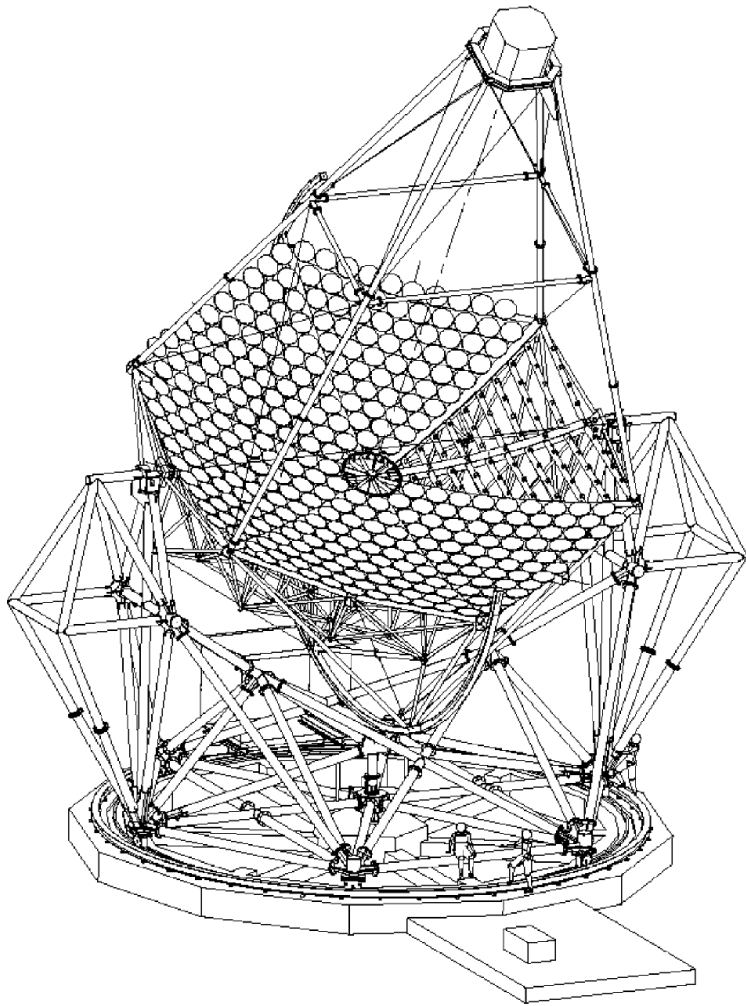
In a parabolic layout, mirrors are arranged on a paraboloid, and the focal length of the (usually spherical) mirror facets varies with the distance from the optical axis.

Both have significant aberrations off the optical axis, the parabolic slightly worse than Davies–Cotton.

Time dispersion introduced by the reflector should not exceed the intrinsic spread of the Cherenkov wavefront of a few ns.

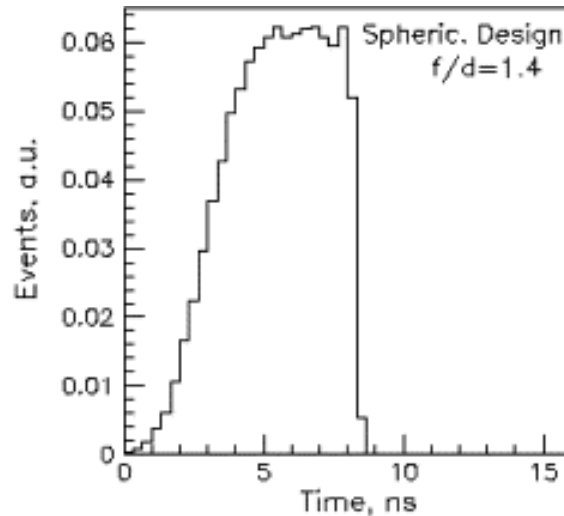
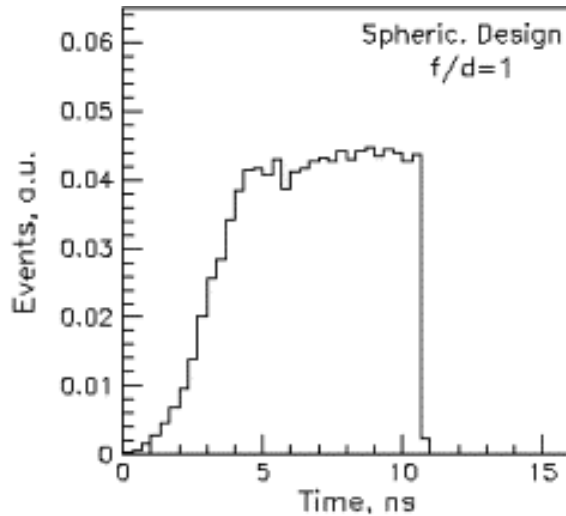
Parabolic reflectors are isochronal – apart from minute effects caused by individual mirror facets being spherical rather than parabolic.

Davies–Cotton layout causes a spread of photon arrival times at the camera; a plane incident wavefront results in photons spread over $\Delta t \approx 5$ ns, with an rms width ≈ 1.4 ns.



The optical system of the H.E.S.S. imaging atmospheric Cherenkov telescopes. Part I: Layout and components of the system
K.Bernlöhr, O.Carrol, R.Cornils, S.Elfaheem P.Espigat, S.Gillessen, G.Heinzelmann, G.Hermann, W.Hofmann, D.Horns. I.Jung, R.Kankanyan, A.Katona, B.Khelifi, H.Krawczynski, M.Panter, M.Punch, S.Rayner, G.Rowell, M.Tluczykont, R.van Staa
Astropart.Phys. **20**, 111 (2003)

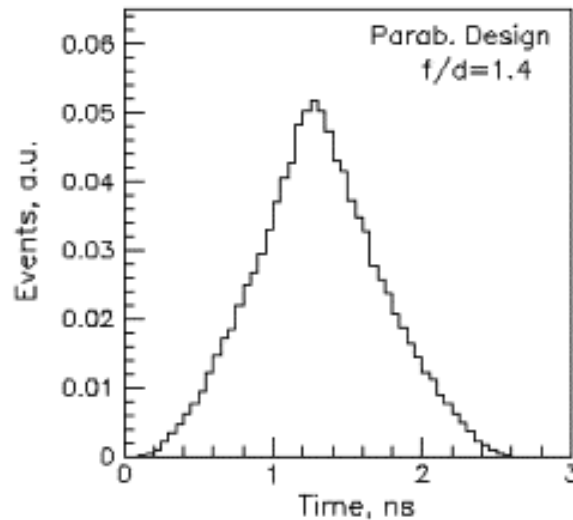
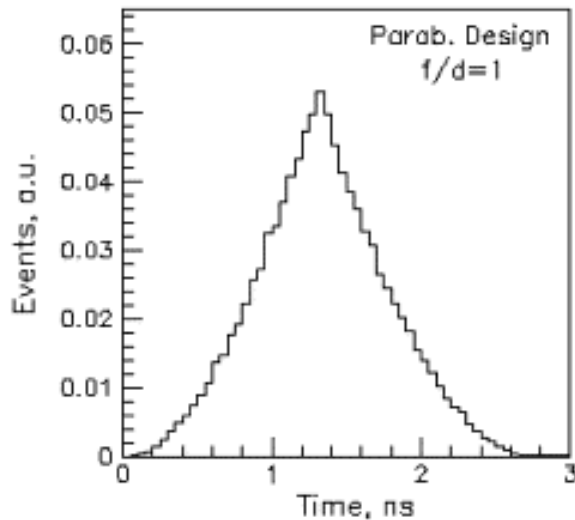
INTRINSIC TIME SPREAD IN 20 m \emptyset CHERENKOV TELESCOPES



Top: Spherical (Davies–Cotton)

A spherical reflector substantially widens the photon pulse.

At detecting 10 GeV γ -showers, the pulse width on the spherical telescope's focal plane may reach 15–20 ns instead of the inherent 5–8 ns.

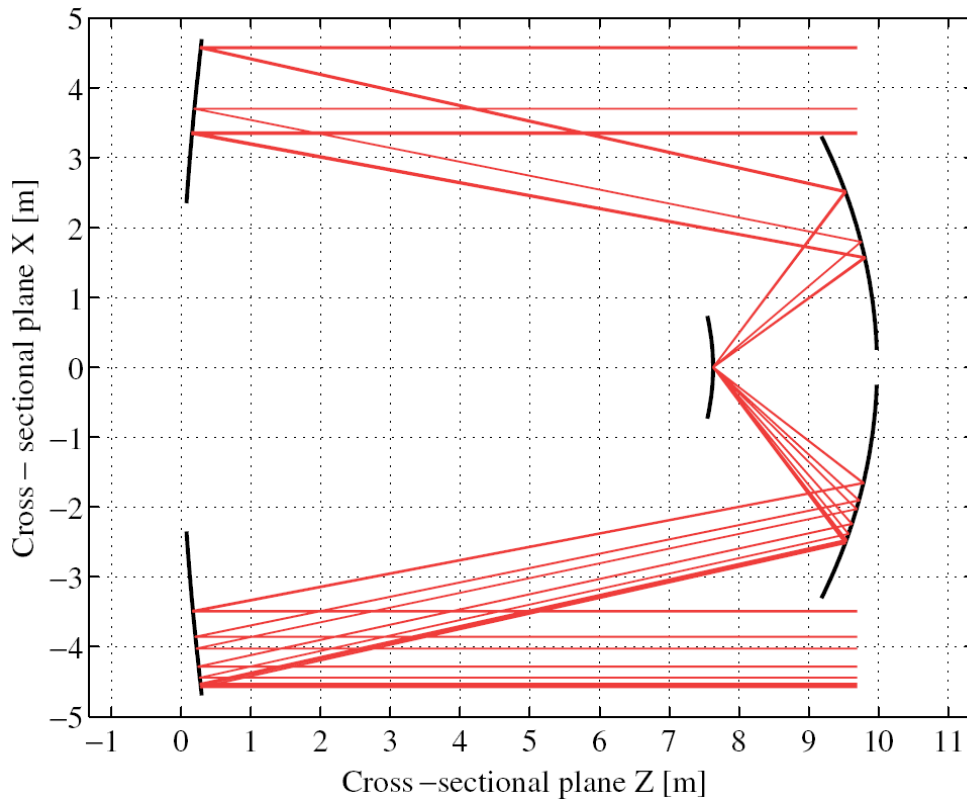


Angles of incidence = 2°

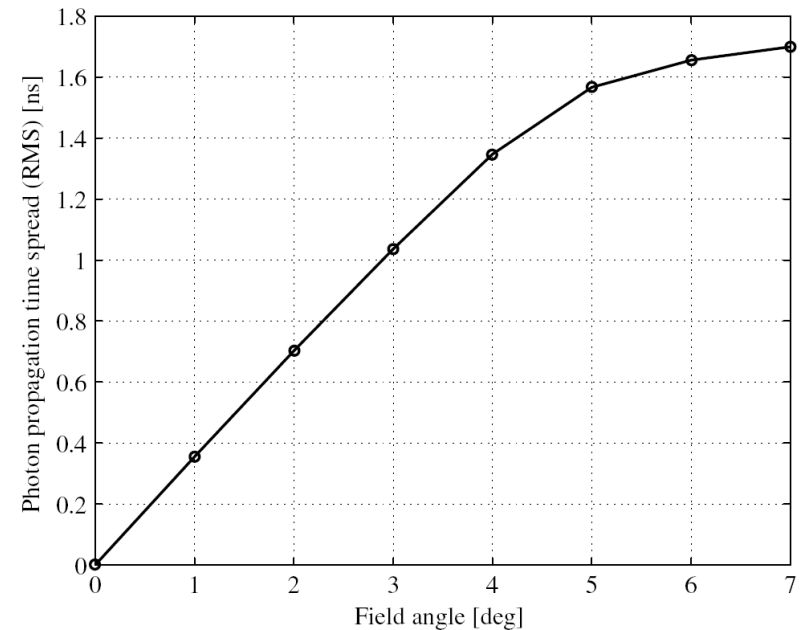
Bottom: Parabolic

**Performance of a 20 m diameter Cherenkov imaging telescope
A.Akhperjanian & V.Sahakian
Astropart.Phys. 21, 149 (2004)**

Schwarzschild-Couder two-mirror IACT telescope

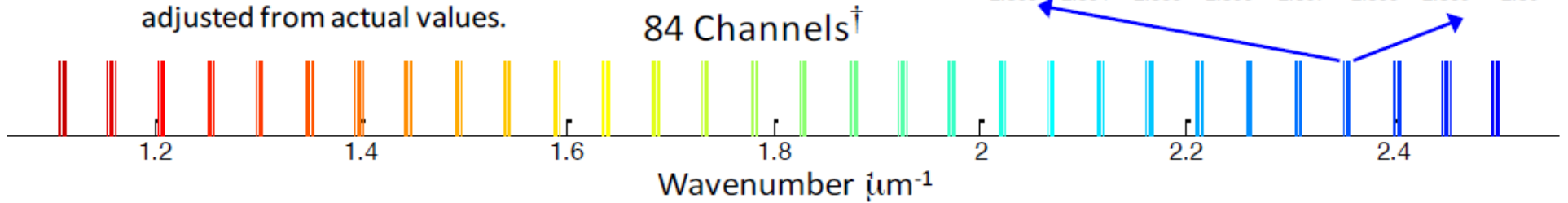


RMS spread in arrival time of rays at focal plane as a function of field angle.
Design is isochronous on optical axis.



Multiple spectral channels?

†For clarity of display the number of channels and their widths has been adjusted from actual values.



S/N improves by measurements in multiple spectral intervals

Image Reconstruction from Sparse Irregular Intensity Interferometry Measurements of Fourier Magnitude

David R. Gerwe, J. J. Dolne

Boeing Phantomworks Space & Intelligence Systems

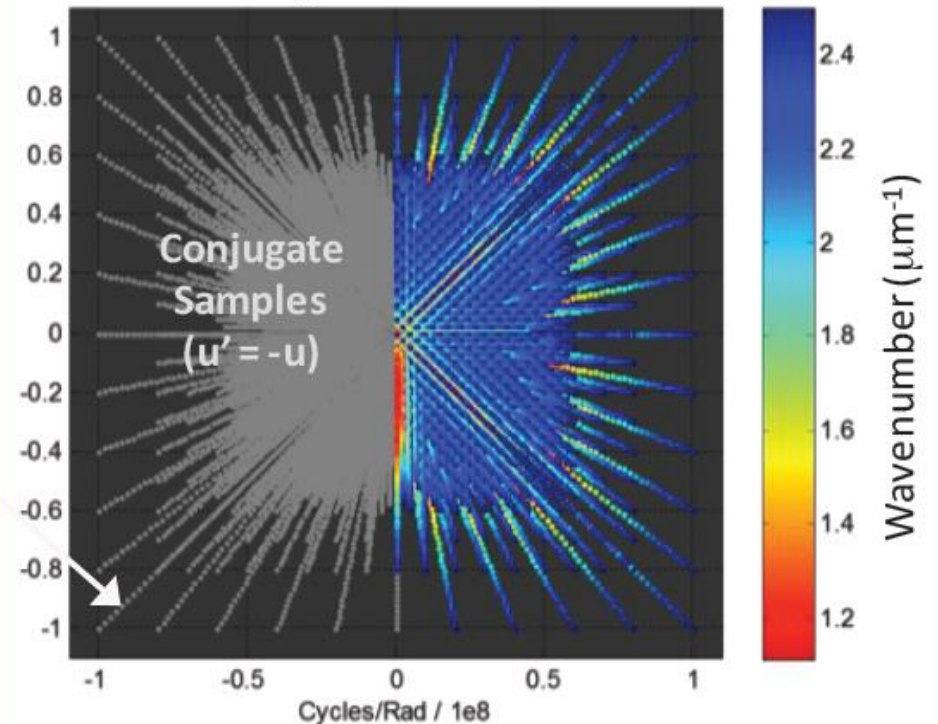
Peter N. Crabtree

United States Air Force Research Labs

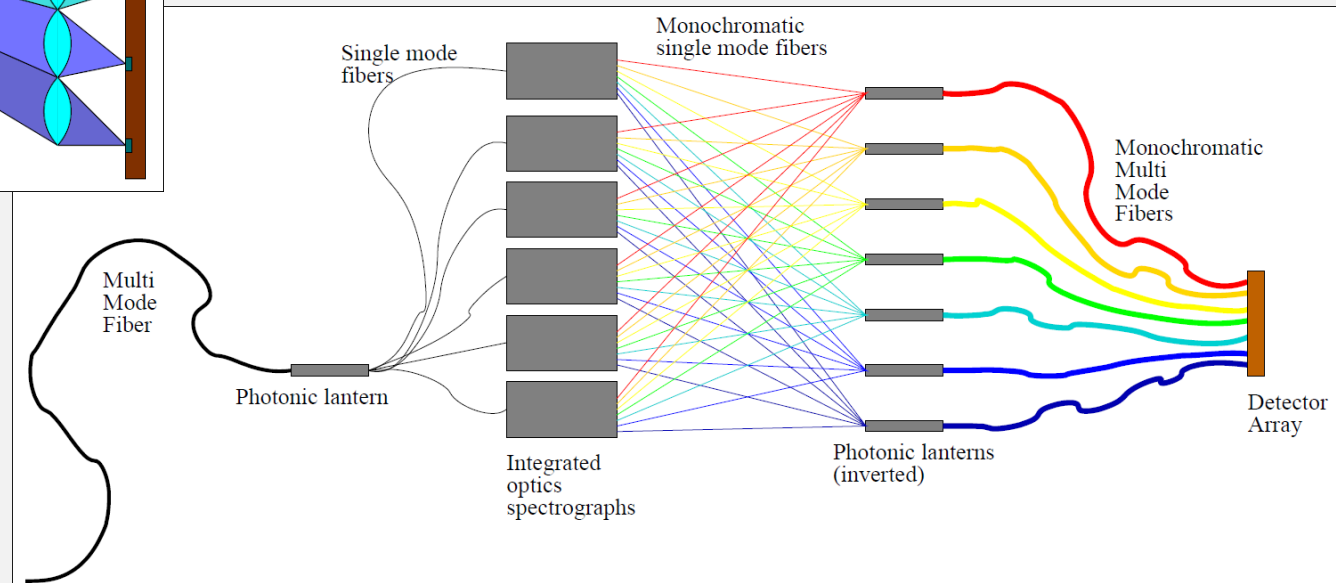
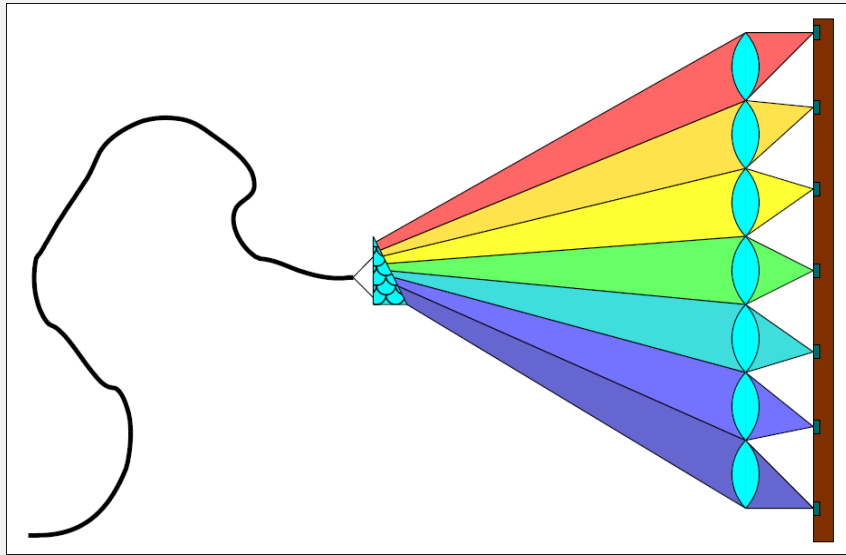
Richard B. Holmes, Brandoch Calef

Boeing Laser and Technical Services

UV Sample Locations



Multiple spectral channels?



Left: Output from a multimode fiber onto a prism to disperse the light

Right: Possible layout to operate between multi- and single-mode fibers

DARK OBJECTS ON BRIGHT BACKGROUND

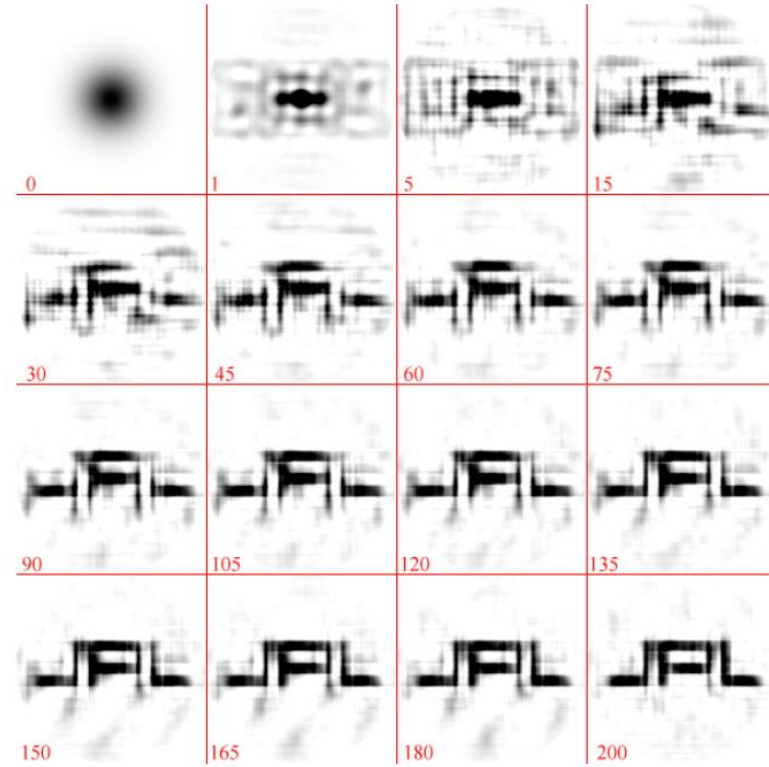
Imaging dark objects with intensity interferometry

Dmitry V. Strekalov,* Igor Kulikov, and Nan Yu

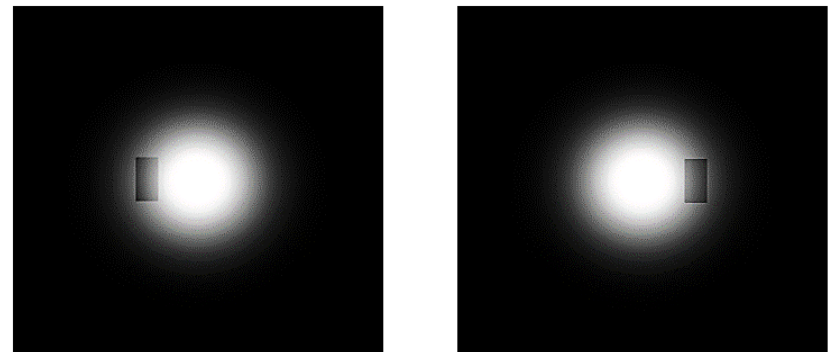
*Jet Propulsion Laboratory, California Institute of Technology, 4800 Oak Grove Drive,
Pasadena, California 91109-8099, USA*

[*Dmitry.V.Strekalov@jpl.nasa.gov](mailto:Dmitry.V.Strekalov@jpl.nasa.gov)

Abstract: We have developed a technique for imaging dark, i.e. non-radiating, objects by intensity interferometry measurements using a thermal light source in the background. This technique is based on encoding the dark object's profile into the spatial coherence of such light. We demonstrate the image recovery using an adaptive error-minimizing Gerchberg-Saxton algorithm in case of a completely opaque object, and outline the steps for imaging purely refractive objects.

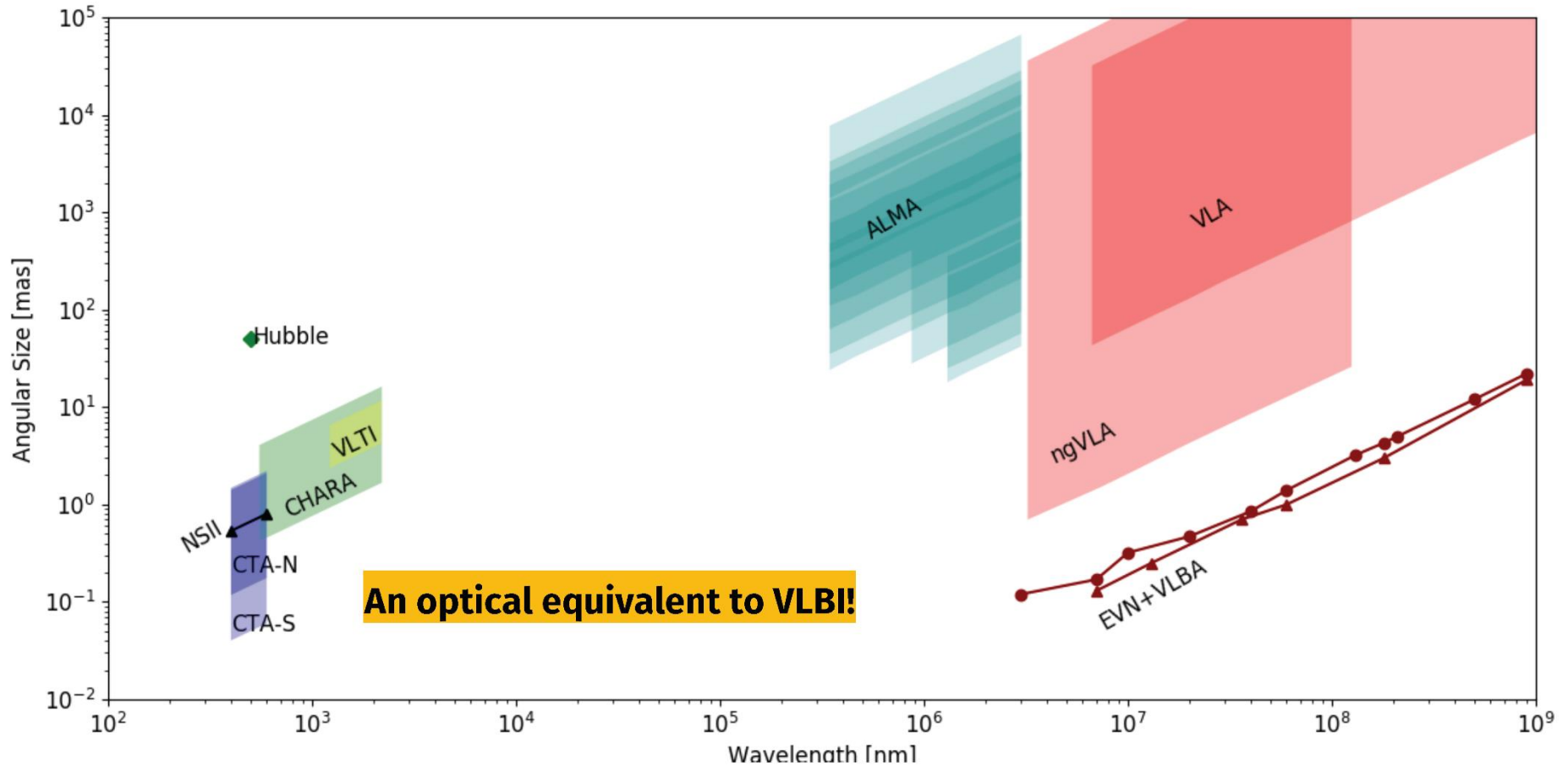


Results of simple image recovery algorithm



Gaussian source with rectangle, reconstructed by Gerchberg-Saxton algorithm

CTA Potential



(Michael Daniel, CfA Center for Astrophysics & VERITAS, Fred Lawrence Whipple Observatory)

Cherenkov Telescope Array as an Intensity Interferometer

Expected resolution for assumed exoplanet transit across the disk of Sirius



Stellar diameter = 1.7 solar

Distance = 2.6 pc

Angular diameter = 6 mas

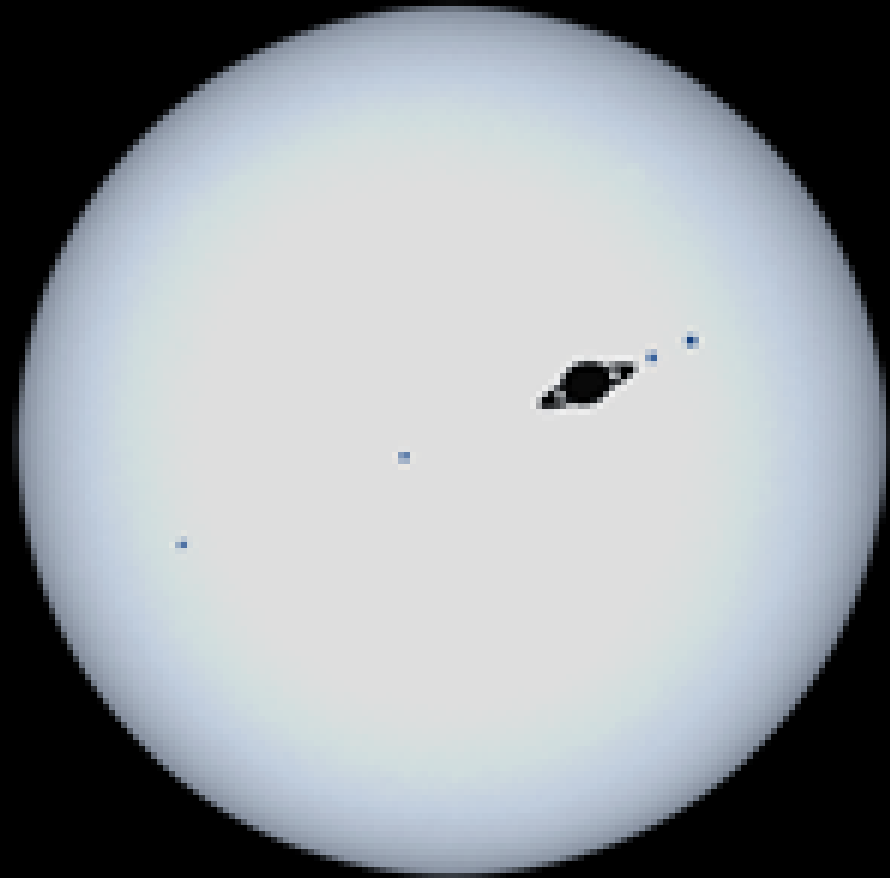
Assumed Jupiter-size planet with rings;

four Earth-size moons;

equatorial diameter = 350 μ as.

CTA array spanning 2 km;

Resolution 50 μ as at λ 400 nm provides more than 100 pixels across the stellar diameter



(D.Dravins, T.Lagadec, P.D.Nuñez, *Astron.Astrophys.* **580**, A99, 2015)

Cherenkov Telescope Array as an Intensity Interferometer

Expected resolution for assumed exoplanet transit across the disk of Sirius



Stellar diameter = 1.7 solar

Distance = 2.6 pc

Angular diameter = 6 mas

Assumed Jupiter-size planet with rings;

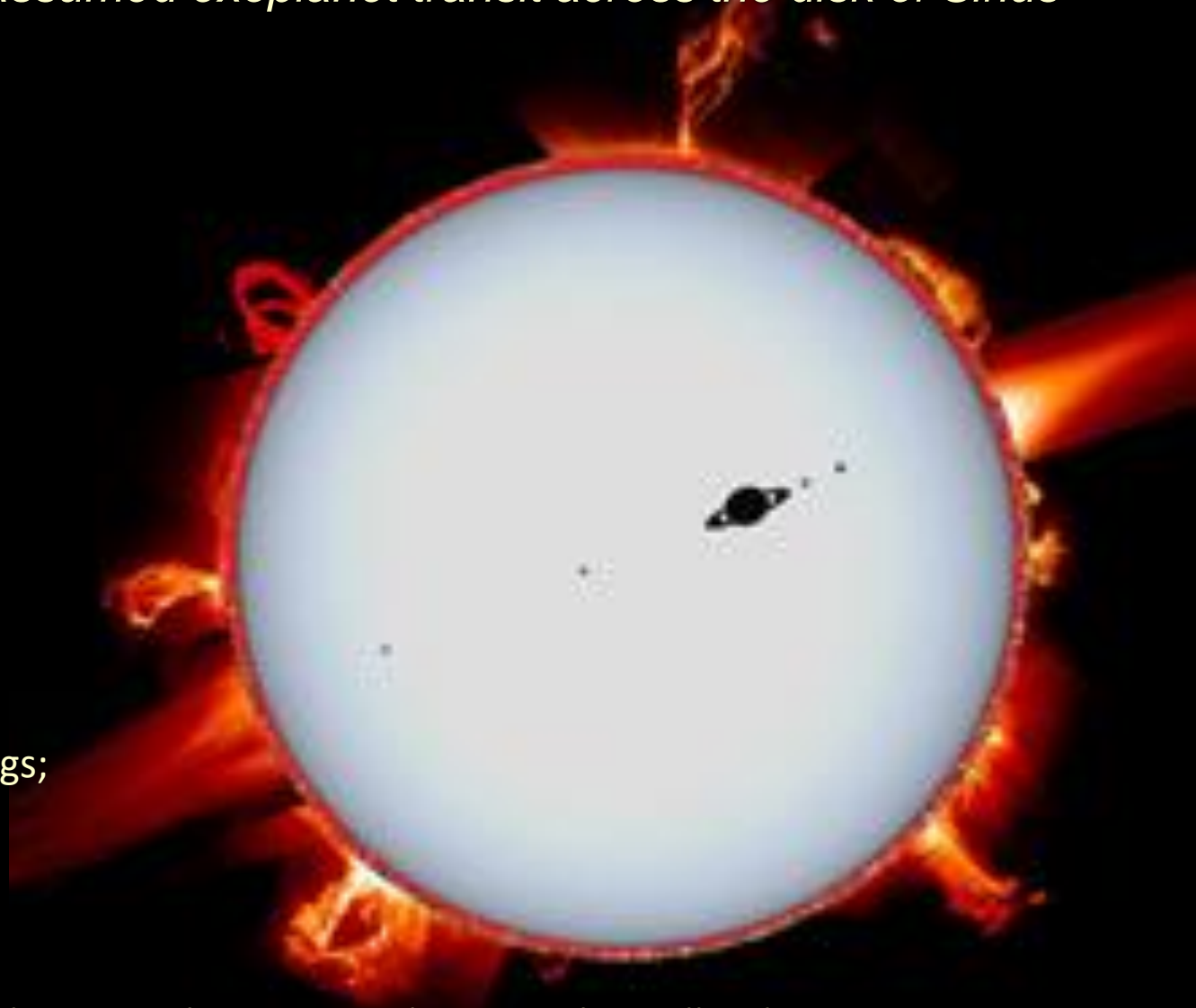
four Earth-size moons;

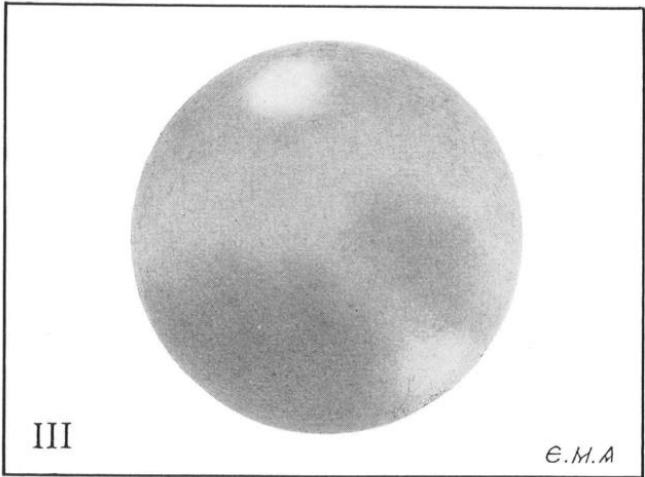
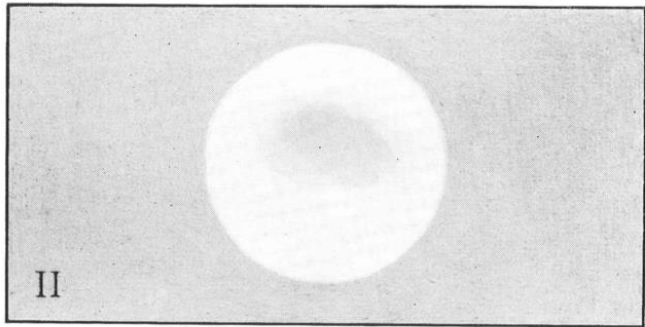
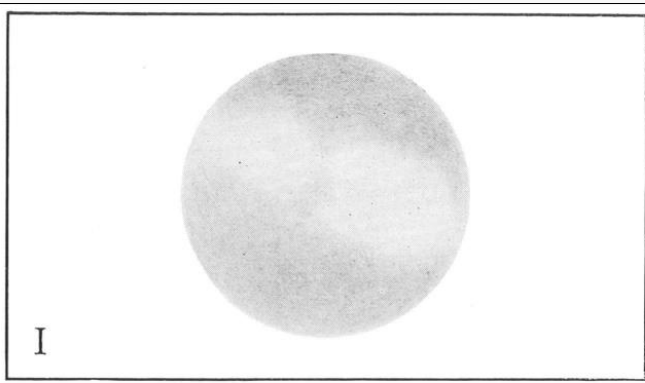
equatorial diameter = 350 μ as.

CTA array spanning 2 km;

Resolution 50 μ as at λ 400 nm provides more than 100 pixels across the stellar diameter

(D.Dravins, T.Lagadec, P.D.Nuñez, *Astron.Astrophys.* **580**, A99, 2015)





THE FIRST THREE LARGE SATELLITES OF JUPITER IN TRANSIT

Upper—Satellite I, Antoniadi's observations, completed by details discovered by Barnard.

Middle—Satellite II, as seen by Antoniadi Sept. 28, 1927.

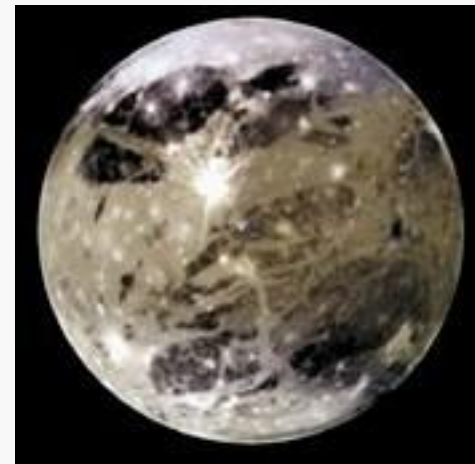
Lower—Satellite III, as seen by Antoniadi, with whitish southern spot seen by Barnard.



Io



Europa



Ganymede

JUPITER'S MOONS

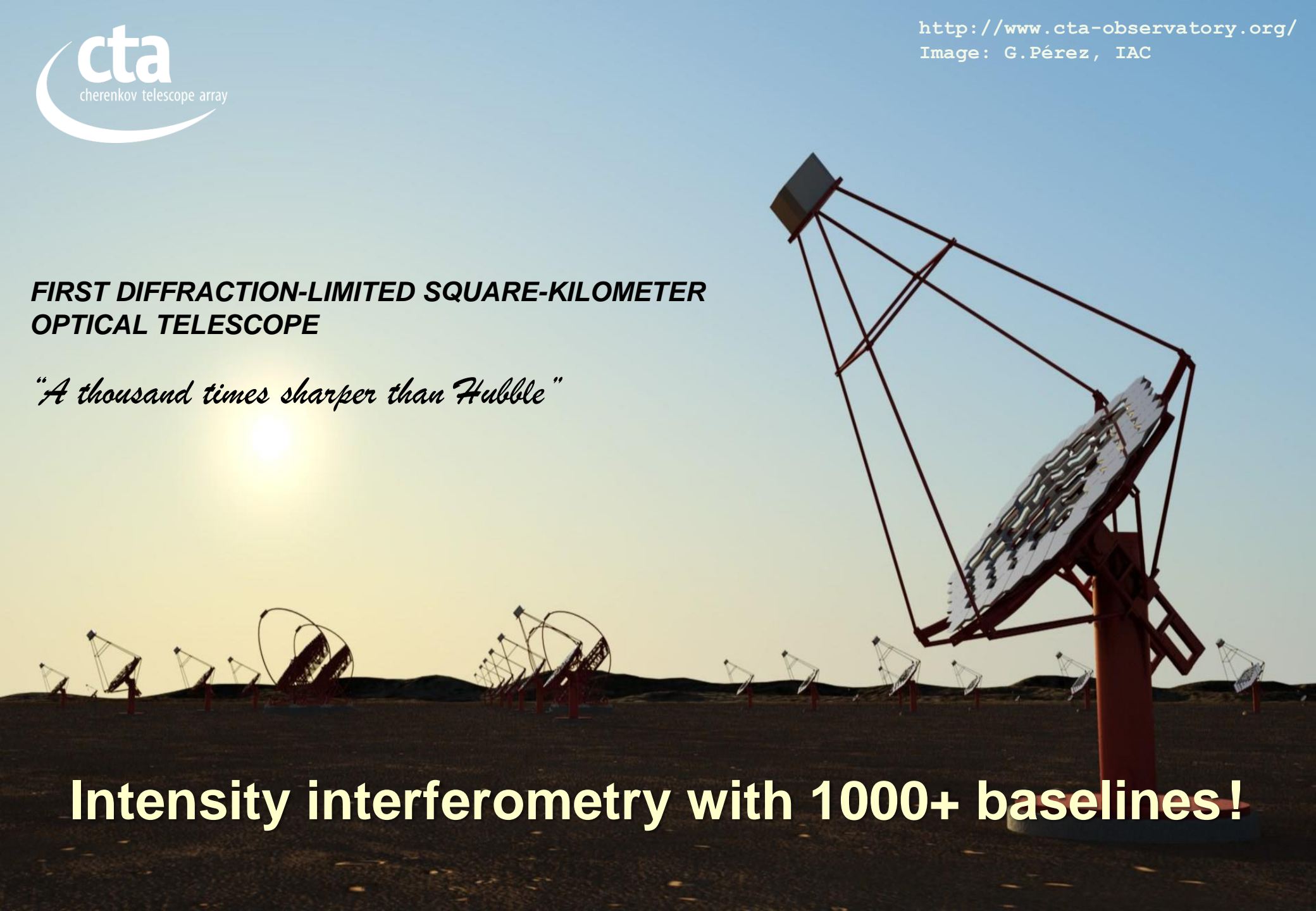
(E.-M. Antoniadi: "On the markings of the satellites of Jupiter in Transit", J.Roy.Astron.Soc. Canada **33**, 273: 1939)

(NASA/JPL/Galileo)

**FIRST DIFFRACTION-LIMITED SQUARE-KILOMETER
OPTICAL TELESCOPE**

"A thousand times sharper than Hubble"

Intensity interferometry with 1000+ baselines!



THE
END